Electronic Supplementary Material (ESI) for Organic & Biomolecular Chemistry.

How are 1,2,3-Triazoles accommodated in secondary structures? A case study on helical peptaibols.

Khoubaib Ben Haj Salah, Sanjit Das, Nicolas Ruiz, Vanessa Andreu, Jean Martinez, Emmanuel Wenger, Muriel Amblard, Claude Didierjean Baptiste Legrand,* and Nicolas Inguimbert*

Table of Contents

Abbreviations S2
Experimental procedure for the SPPS of Alamethicin F50/5 and analogs S2
Experimental conditions for LC-MS, for Analytical HPLC and for Semi-preparative HPLC purification S2
Cytotoxicity assay on KB cells S2
Antibacterial assay on *Bascillus subtilis* S3
Peptaibols sequences, yields and LC/MS S3
AlamethicinF50/5 **4a** and analogues **4b**-**j** S3-S12
Bergofungin D **5a** and analogues **5b**-**f** S13-S18
Circular Dichroism S19
Figure S1: Impact of the triazole group position in the sequence of the alamethicin on the molar ellipticity at 220 nm of the helical analogues **4b**-**g**. S19
Crystallization and crystal structure determination S20
Table S2-1. Selected crystallographic data for **4g, 4h, 5a, 5b**, **5d** and **5f.** S20
Analysis of the Alm analogues crystal structures S21
Table S2-2: ϕ and ψ dihedral angles values (°) for **4a** (PDB: 1AMT), **4g** and **4h**. S21
Table S2-3: Alamethicin **4a**(PDB 1AMT) and analogues **4g** and **4h** intramolecular hydrogen bonds. S22
Figure S2-1: Superimposition of the crystal structures of Alm and its analogues **4g-h** S23
Figure S2-2: Parts of the crystal of packings of **4g** and **4h** S24
Analysis of the BergD and analogues crystal structures S25
Figure S2-3: Structure-based sequence alignment of peptaibols which belong to the Bergofungin D subfamily SF2 S25
Figure S2-4: Superimposition of the crystal structures of bergofungin D **5a** and its analogues **5b**, **5d** and **5f**. S26
Table S2-4: Characteristic ϕ and ψ dihedral angles values (°) for **5a** (PDB: 1AMT), **5b**, **5d** and **5f**. S27
Table S2-5: Bergofungin D **5a** and analogues **5b**, **5c** and **5f** intramolecular hydrogen bonds. S28
Figure S2-5: Surperimposition of the U[YTz]Xaa with their corresponding parts in the native sequence of Alm **4a** and bergD **5a**. S29
Figure S2-6. Comparison of induced conformation and dihedral angles arround triazoles. S30
Table S2-6: Characteristic ϕ and ψ dihedral angles values (°)adjacent to the triazole core for **4g**, **4h**, **5a**, **5b**, **5d** and **5f** and in the α-helical coiled coil GCN4 (PDB : 1U9F, 2AG3, 1U9H). S30
NMR and molecular modeling studies S30
NMR experiments. S30
Structure calculations. S30
Figure S3-1: ^{1}H NMR spectra of **4a-e** in CD_3OH at 298 K S31
Figure S3-2: ^{1}H NMR spectra of **4f-j** in CD_3OH at 298 K S32
Figure S3-3: ^{1}H NMR spectra of **5a-f** in CD_3OH at 298 K S33
Table S4: ^{1}H, ^{13}C and ^{15}N NMR chemical shifts for **4a-j** and **5a-f** in CD_3OH at 298 K. S34-49
Table S5: Variation of the chemical shifts in the peptides **4b-j** and **5a-f** upon incorporation of 1,2,3-triazole. S50-55
Table S6: $^{3}J(HNH_\alpha)$ coupling constants of the Alamethicin and Bergofungin analogues in CD_3OH at 298K. S55-56
Assessment of the helical structure of the alamethicin analogues: NOE correlations. S56
Table S7-1: Expected backbone NOE correlations around the 1,2,3 triazole in helical secondary structures based on the crystal structure of modified GCN4-pLI coiled coils (pdbID: 1U9F). S56
Table S8-1: Root mean square deviations (rmsd, Å) of the 15 lowest energy NMR structures of **4a**, **4c**, **4g**, **4h**, **5a**, **5d**, **5e** and **5f**. S57
References S57
Author Contributions S57

Experimental Procedures

Abbreviations: DIC, N,N'-diisopropylcarbodiimide; Oxyma pure, Ethyl cyanoglyoxylate-2-oxime; DCM, Dichloromethane; DMF, N,N'-dimethylformamide; c-Hex, Cyclohexane; DIEA, Diisopropylethylamine; Ac_2O, Acetic anhydride;TFA,Trifluoroacetic acid; TIS, Triisopropylsilane; FA, formic acid; ACN, Acetonitrile; HPLC, High-performance liquid chromatography; LC-MS, liquid chromatography mass spectrometry; ELSD, evaporative light scattering detector; SPPS, solid phase peptide synthesis.

SPPS of Alamethicin F50/5 and analogues: Solid-phase peptide synthesis was run on an automated microwave peptide synthesizer (CEM liberty one, Orsay, France) using Fmoc/O-tbutyl chemistry. All Fmoc-protected amino acids, DIC, Oxyma, 2-chlorotrityl chloride resin preloaded with phenylalaninol (loading 0.67 mmol/g or 0.36 mmol/g) were purchased from Iris Biotech (Germany). DCM, DMF, cHex, DIEA, Ac_2O, TFA, TIS, FA, ACN and piperidine for peptide synthesis were obtained from Aldrich (USA).). FmocAib[ψTz]Xaa dipeptide were obtained according to previously reported procedure.[1]

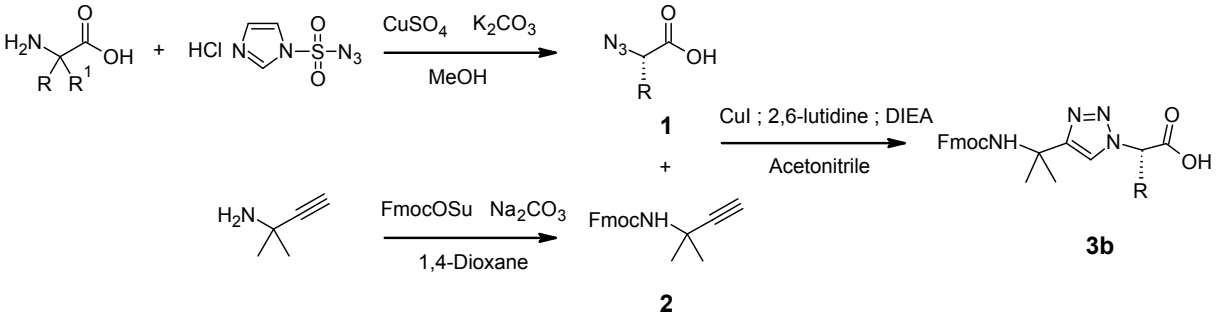

Scheme S1: Synthesis of compunds **3b**.

SPPS was performed at a 0.10 mmol scale with DIC/Oxyma as coupling reagent and 20% piperidine in DMF for Fmoc deprotection. After transfer to the reaction vessel the resin was swelled for 1 h in 10 mL of DMF the elongation was carried automatically using a 5-fold excess of protected amino acids and coupling reagent. The mixture was irradiated in a microwave cavity at 70 °C for 20 min. Fmoc deprotection was achieved using 20% piperidine in DMF (7 mL for 30s at 33 °C and 7 mL for 3min at 70 °C). The N-terminal acetylation was accomplished in 10 min using 10 ml of Ac_2O/DIEA/DMF 1:2:7 (v/v) under microwave irriadiation at a final temperature of 70°C. After completion of the automatic synthesis the peptidyl-resin was washed twice with 10 mL of DCM. Cleavage and deprotection of the peptide was performed by treating the peptidyl-resin with 10 mL of TFA/DCM/H_2O/TIPS 4.7:4.7:4:2 (v/v) for 60 min. After resins' filtration, the filtrate was concentrated and co-evaporated with cyclohexane. The peptide was precipitated with ice-cold diethyl ether, recovered by centrifugation and washed with cold diethyl ether. After purification by semi-preparative HPLC and concentration of the fraction containing the peptide of interest the remaining solution is dried freeze to afford a white powder.

LCMS: LC-MS analyses were carried out using a Thermo Fisher Scientific LC-MS device, Accela HPLC coupled to a LCQ Fleet fitted with an electrospray ionisation source and a 3D ion-trap analyser. The analysis was performed with a Phenomenex Kinetex C-18 column (100 x 300 mm) using gradient mixture of water with 0.1 % AF (buffer A) and ACN with 0.1 % AF (buffer B). Standard conditions were a flow rate of 0.5 ml/min eluting with 10% B to 100% B 30 min and 10%B for 7 min. Standard conditions were applied to all LC-MS analysis unless otherwise stated. As expected the pseudo molecular ion $[M+H]^+$ and high intensity doubly charged ions $[M+2H]^{2+}$ were observed for all the compounds with masses bellow 2000 Da. In some cases, as previously reported, in source cleavage of the labile Aib_{13}-Pro_{14} bond led to y_7 and b_{13} diagnostic ions.[2]

Analytical HPLC: The HPLC analysis was conducted on a Waters 2695 HPLC system with a Grace Vydac 218MS 5 µM C-18 column (250 x 4.6 mm) and an ELSD-detector using a gradient mixture of water with 0.1% FA (Buffer A) and ACN with 0.1% FA (Buffer B).

Semi-preparative HPLC purification: Semi-preparative purification of peptides was performed using a Waters 1525 chromatography system fitted with a Waters 2487 tunable absorbance detector with detection at 214 nm and 254 nm. Purification was performed by eluting solvents A (water) with 0.1 % TFA and B (ACN) with 0.1 % TFA on a Grace Vydac 218MS510 C-18 column (250 x 10 mm 5um) at 3 ml/min.

Cytotoxicity assay on KB cells: KB cells (human oral epidermoid carcinoma ATCC CCL 17, American Type Culture Collection, Rockville, MD) were cultivated in BME (Basal Medium Eagle) supplemented with 5% (*v/v*) fetal calf serum, 1% (*v/v*) glutamine 200 mM and 1% (*v/v*) streptomycin (10 mg/ml) / penicillin (10000 U) (all *Sigma-Aldrich*). Cells were cultivated in plastic flasks (*Greiner Bio One*, F-Courtaboeuf) at 37°C in a 5% CO_2 enriched atmosphere. After an incubation period of 48 h, trypsinized cells were suspended as a 200,000 cells/ml suspension in supplemented BME and 50 µl were put in each well of 96-well microplates (*Nunclon Delta Surface*, *Thermo Scientific Nunc*). After an incubation of 48h, 50 µl of peptaibol samples were added to the initial 50-µl cell suspension. Peptaibols samples were tested in well as a final 5% (*v/v*) methanolic solution in supplemented BME with concentrations ranging from 3 to 400 µg/ml. A final 5%

(*v/v*) methanolic solution in supplemented BME was used as solvent control. After 76 h of incubation, the cell viability was evaluated by the colorimetric MTT (3-(4,5-dimethylthiazol-2-yl)-2,5-diphenyltetrazolium bromide, *Sigma-Aldrich*) bioassay.[3,4] All the *in vitro* assays were done in technical and biological triplicates.

Antibacterial assay on *Bascillus subtilis*:
Broth assay was performed to compare peptaibols activity at one concentration, 50µg/ml, which is ten-fold higher than the IC50 determined previously for alamethicin. Bacillus subtilis strain (CIP 103406) was grown and maintained on LB broth and Tryptic soy agar at 28°C.[5] An exponential growth phase culture in LB broth (after 6 hours incubation in a fresh medium) was diluted to $1x10^4$ CFU/ml. 20 µl of peptaibols solution in DMSO (5 mg/ml) were first diluted with 980 µl broth in sterile eppendorf tubes. These diluted solutions (100 µg/ml) were then added in 96-well microplate containing 100 µl Bacillus subtilis solution. A positive control was setup with broth and Bacillus subtilis solution complemented with 1% DMSO and a negative control with broth alone. All peptaibols were tested in triplicate. Microplates were mixed and incubated at 28°C overnight. Optical density (OD) was taken at 600 nm with negative control as blank.
Inhibitory percentage was determined using following formula: $I = [1-(ODp/OD_0)]*100$
Where ODp is OD obtained with peptaibols solution and OD_0 is OD of positive control.

Peptaibols sequences, yields and LC/MS

AlamethicinF50/5 4a and analogues 4b-j:

Ac-Aib-Pro-Aib-Ala-Aib-Ala-Gln-Aib-Val-Aib-Gly-Leu-Aib-Pro-Val-Aib-Aib-Gln-Gln-Phol (**4a**)

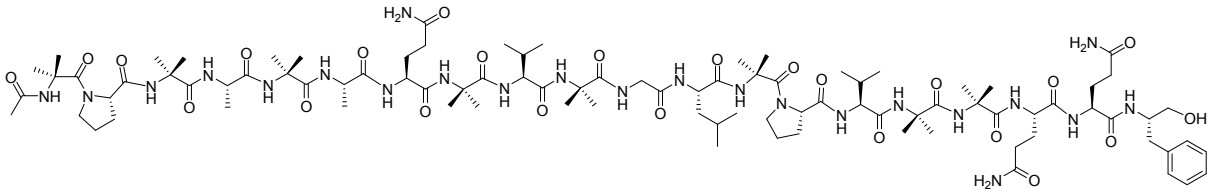

Crude peptide (~210 mg, 100% yield) was purified by semi-preparative HPLC using a linear gradient from 50% to 100% B in A over 35 min with a flow rate of 3 mL/min to yield alamethicin F-50/5 (89 mg, 45% yield, >98% purity). ESI-MS: Calculated for $C_{92}H_{152}N_{23}O_{24}$: $[M+H]^+$ m/z 1963.14 ; $[M+Na+H]^{2+}$ m/z 993.06 ; $[M+3H]^{3+}$ m/z 655.05 ; b_{13} ion $[C_{55}H_{93}N_{14}O_{15}]^+$ m/z 1189.69 ; y_7 ion $[C_{37}H_{60}N_9O_9]^+$ m/z 774.45 ; found m/z: 1963.41 ; 993.27 ; 655.21 ; 1189.33 ; 774.39.

Analytical HPLC-ELSD: gradient: 0.9 ml/min flow rate from 10% B to 100% B over 50 min

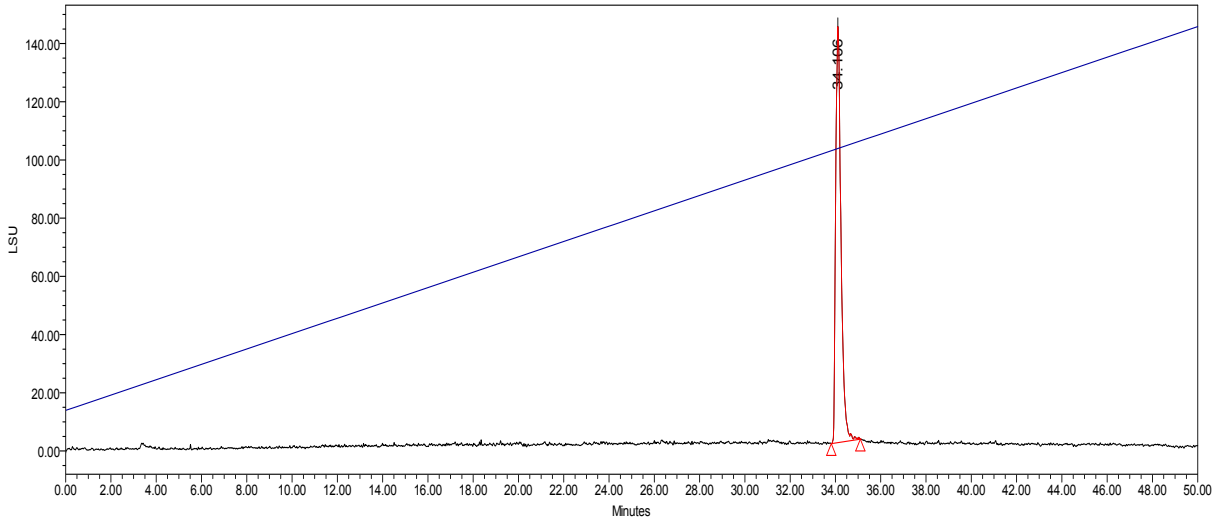

ESI-MS:

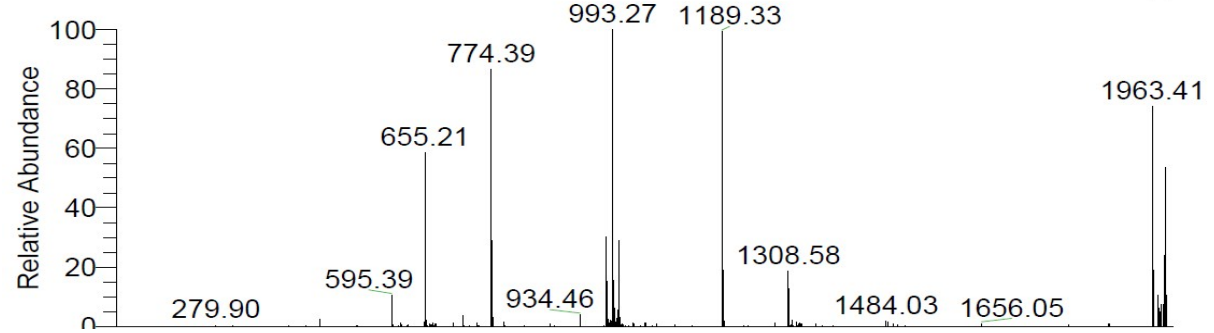

Ac-Aib-Pro-Aib$_{[\psi Tz]}$Ala-Aib-Ala-Gln-Aib-Val-Aib-Gly-Leu-Aib-Pro-Val-Aib-Aib-Gln-Gln-Phol **(4b)**

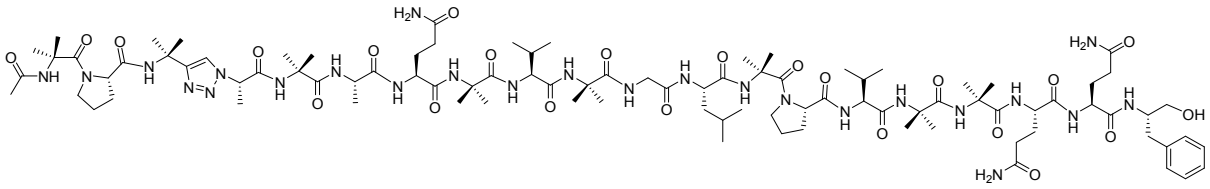

Crude peptide (~210 mg, 100% yield) was purified by semi-preparative HPLC using a linear gradient from 30% to 70% B in A over 40 min with a flow rate of 3 mL/min to yield compound **4b** (56 mg, 28% yield, >98% purity). ESI-MS: Calculated for $C_{93}H_{151}N_{25}O_{23}$: $[M+H]^+$ m/z 1987.14 ; $[M+2H]^{2+}$ m/z 994.07 ; $[M+3H]^{3+}$ m/z 663.05 ; b_{13} ion $[C_{56}H_{93}N_{16}O_{14}]^+$ m/z 1213.70 ; y_7 ion $[C_{37}H_{60}N_9O_9]^+$ m/z 774.45 ; found m/z: 1987.24 ; 993.80 ; 662.95 ; 1213.00 ; 774.39.

Analytical HPLC-ELSD: gradient: 0.9 ml/min flow rate from 10% B to 100% B over 50 min

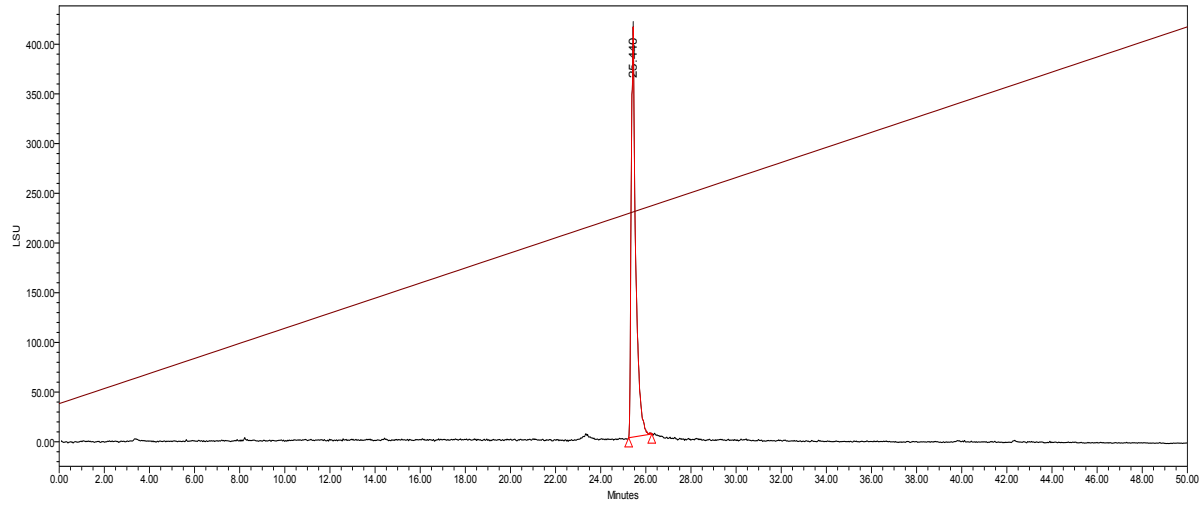

ESI-MS:

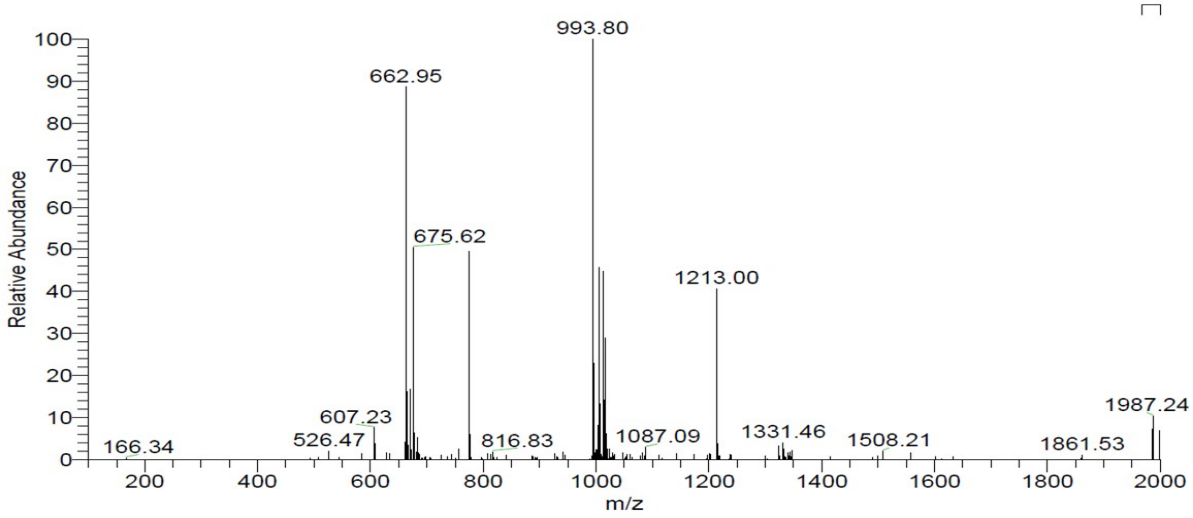

Ac-Aib-Pro-Aib-Ala-Aib$_{[\Psi Tz]}$Ala-Gln-Aib-Val-Aib-Gly-Leu-Aib-Pro-Val-Aib-Aib-Gln-Gln-Phol **(4c)**

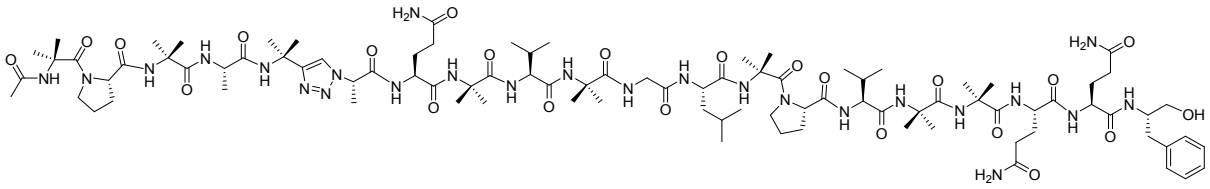

Crude peptide was (~210 mg, 100% yield) purified by semi-preparative HPLC using a linear gradient from 30% to 70% B in A over 40 min with a flow rate of 3 mL/min to yield compound **4c** (68 mg, 34% yield, >95% purity). ESI-MS: Calculated for $C_{93}H_{151}N_{25}O_{23}$: $[M+H]^+$ m/z 1987.14 ; $[M+2H]^{2+}$ m/z 994.07 ; $[M+3H]^{3+}$ m/z 663.05 ; found m/z: 1987.21 ; 994.18 ; 662.79.

Analytical HPLC-ELSD: gradient: 0.9 ml/min flow rate from 10% B to 100% B over 50 min

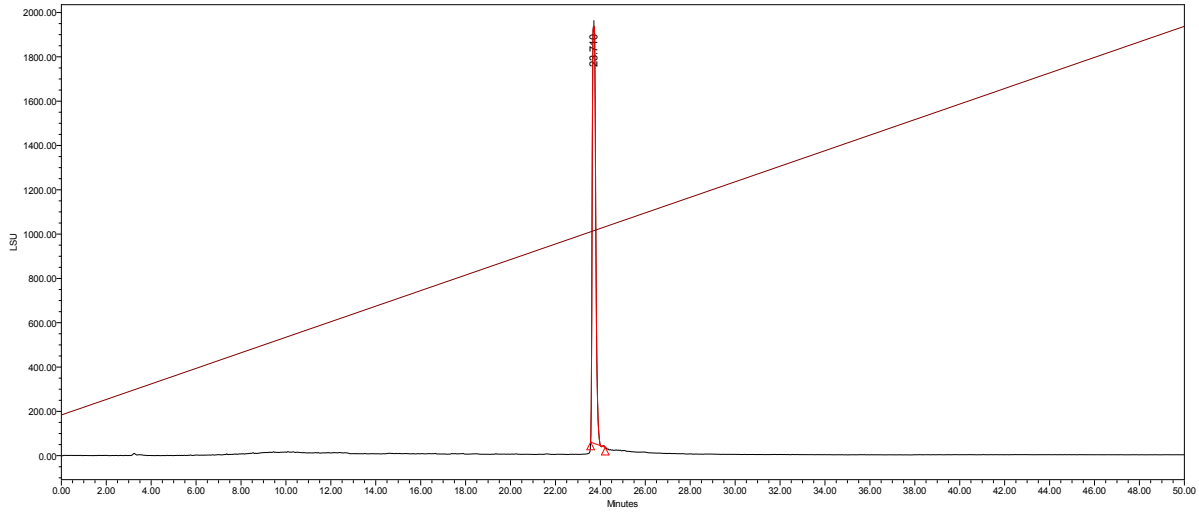

ESI-MS:

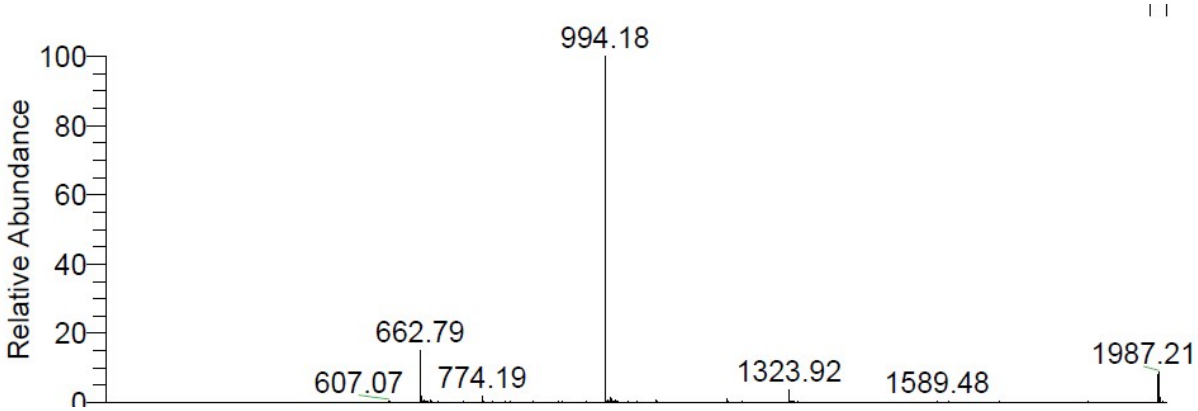

Ac-Aib-Pro-Aib-Ala-Aib-Ala-Gln-Aib$_{[\psi Tz]}$Val-Aib-Gly-Leu-Aib-Pro-Val-Aib-Aib-Gln-Gln-Phol **(4d)**

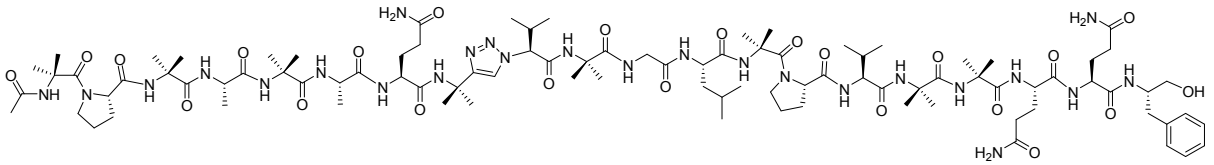

Crude peptide (~220 mg, 100% yield) was purified by semi-preparative HPLC using a linear gradient from 30% to 70% B in A over 40 min with a flow rate of 3 mL/min to yield compound **4d** (40 mg, 20% yield, >95% purity). ESI-MS: Calculated for $C_{93}H_{151}N_{25}O_{23}$: $[M+H]^+$ m/z 1987.14 ; $[M+2H]^{2+}$; $[M+3H]^{3+}$ m/z 663.05 ; b_{13} ion $[C_{56}H_{93}N_{16}O_{14}]^+$ m/z 1213.70 ; y_7 ion $[C_{37}H_{60}N_9O_9]^+$ m/z 774.45 ; found m/z: 1987.04 ; 662.75 ; 1213.17 ; 774.16.

Analytical HPLC-ELSD: gradient: 0.9 ml/min flow rate from 10% B to 100% B over 50 min

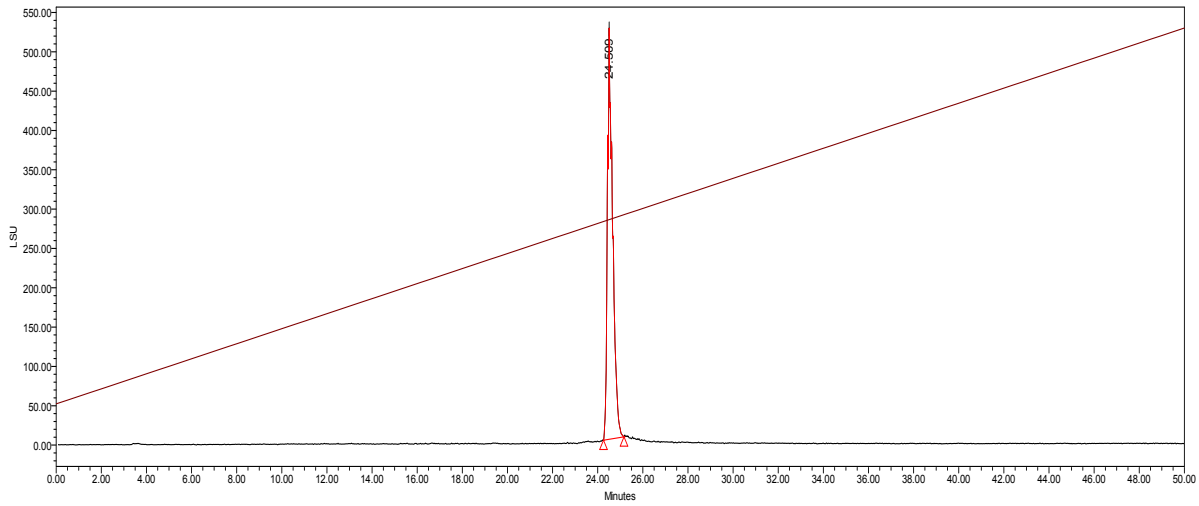

ESI-MS:

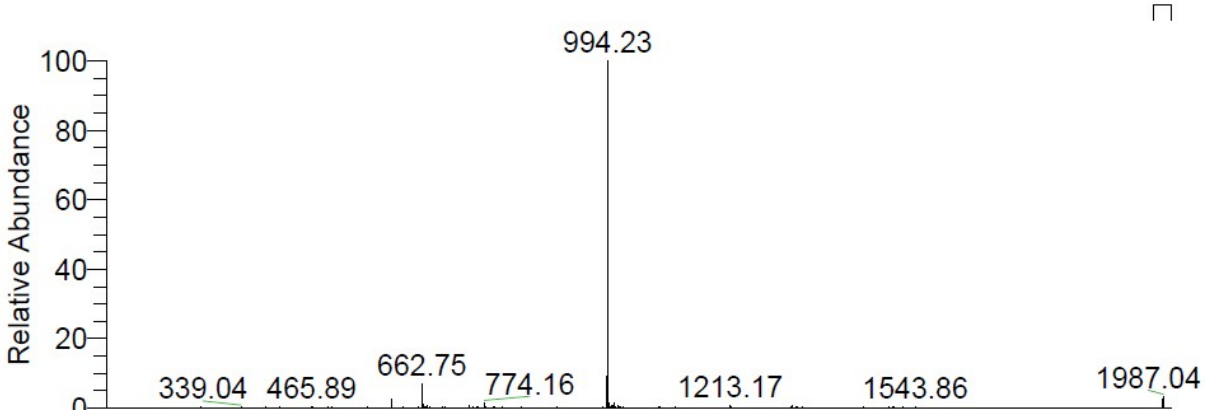

Ac-Aib-Pro-Aib-Ala-Aib-Ala-Gln-Aib-Val-Aib$_{[\psi Tz]}$Gly-Leu-Aib-Pro-Val-Aib-Aib-Gln-Gln-Phol **(4e)**

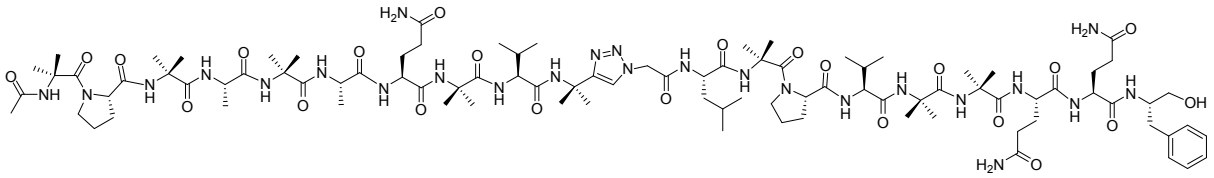

Crude peptide (~220 mg, 100% yield) was purified by semi-preparative HPLC using a linear gradient from 30% to 70% B in A over 40 min with a flow rate of 3 mL/min to yield compound **4e** (83 mg, 42% yield, >95% purity). ESI-MS: Calculated for $C_{93}H_{151}N_{25}O_{23}$: $[M+H]^+$ m/z 1987.14 ; $[M+2H]^{2+}$ m/z 994.07 ; found m/z: 1987.30 ; 994.36.

Analytical HPLC-ELSD: gradient: 0.9 ml/min flow rate from 10% B to 100% B over 50 min

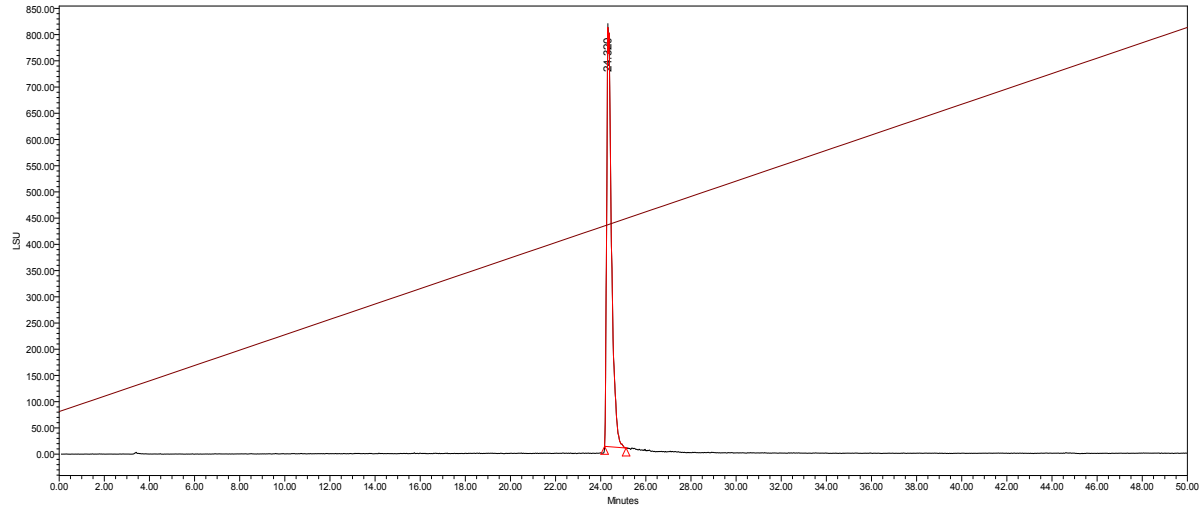

ESI-MS:

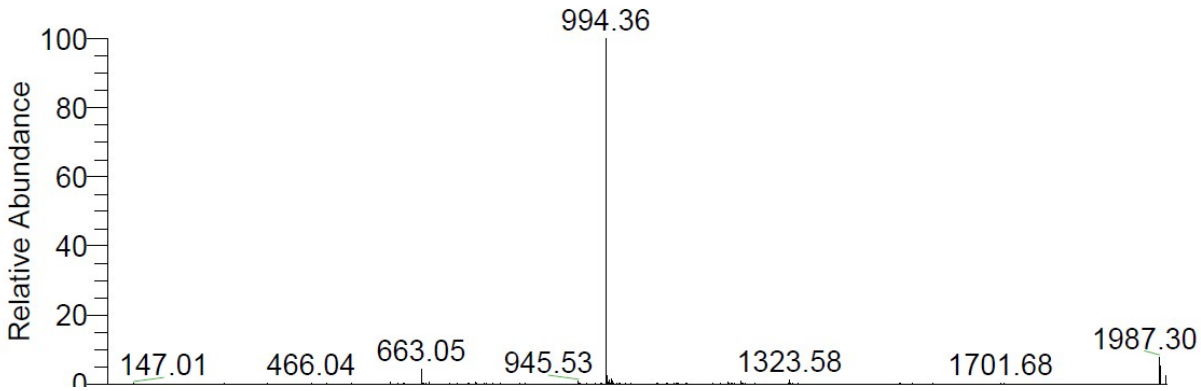

Ac-Aib-Pro-Aib-Ala-Aib-Ala-Gln-Aib-Val-Aib-Gly-Leu-Aib-Pro-Val-Aib$_{[\psi Tz]}$Aib-Gln-Gln-Phol **(4f)**

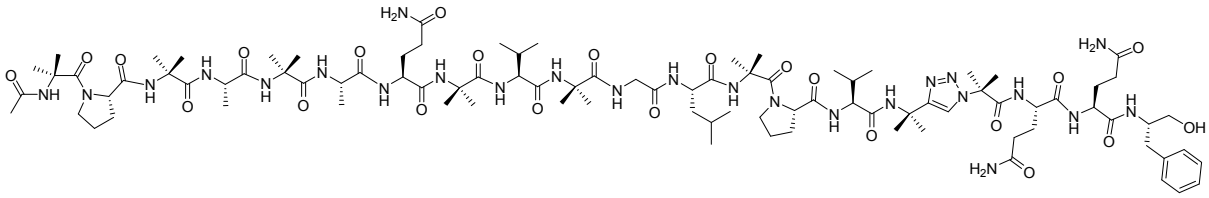

Crude peptide yield (~200 mg, 100% yield) was purified by semi-preparative HPLC using a linear gradient from 30% to 70% B in A over 40 min with a flow rate of 3 mL/min to yield compound **4f** (89 mg, 45% yield, >95% purity). ESI-MS: Calculated for $C_{93}H_{151}N_{25}O_{23}$: $[M+H]^+$ m/z 1987.14 ; $[M+2H]^{2+}$ m/z 994.07 ; $[M+3H]^{3+}$ m/z 663.05 ; b_{13} ion $[C_{55}H_{93}N_{14}O_{15}]^+$ m/z 1189.69 ; y_7 ion $[C_{38}H_{60}N_{11}O_8]^+$ m/z 798.46 ; found m/z: 1987.11 ; 993.84 ; 662.98 ; 1189.07 ; 798.29.

Analytical HPLC-ELSD: gradient: 0.9 ml/min flow rate from 10% B to 100% B over 50 min

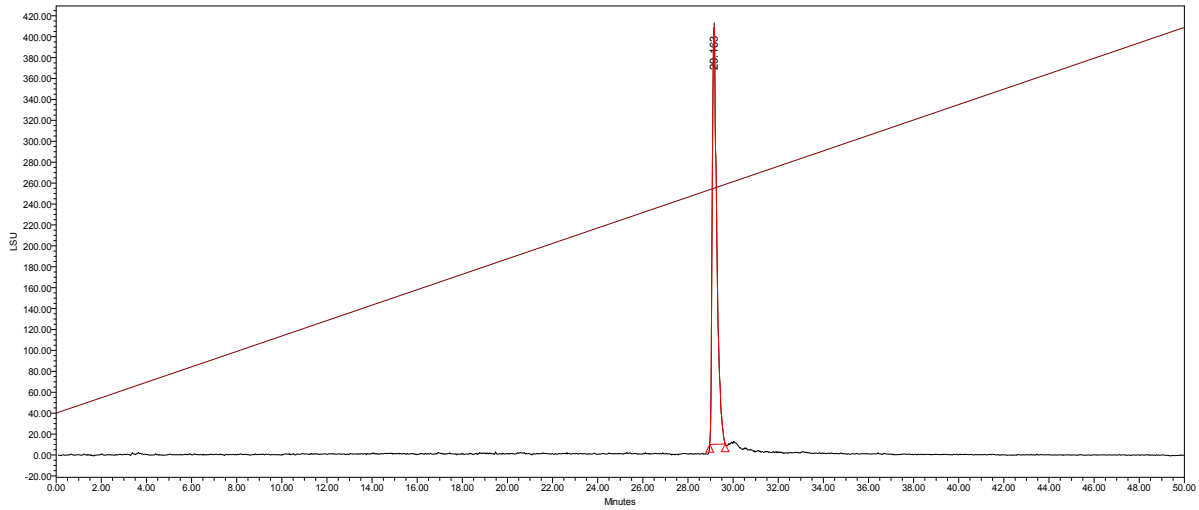

ESI-MS:

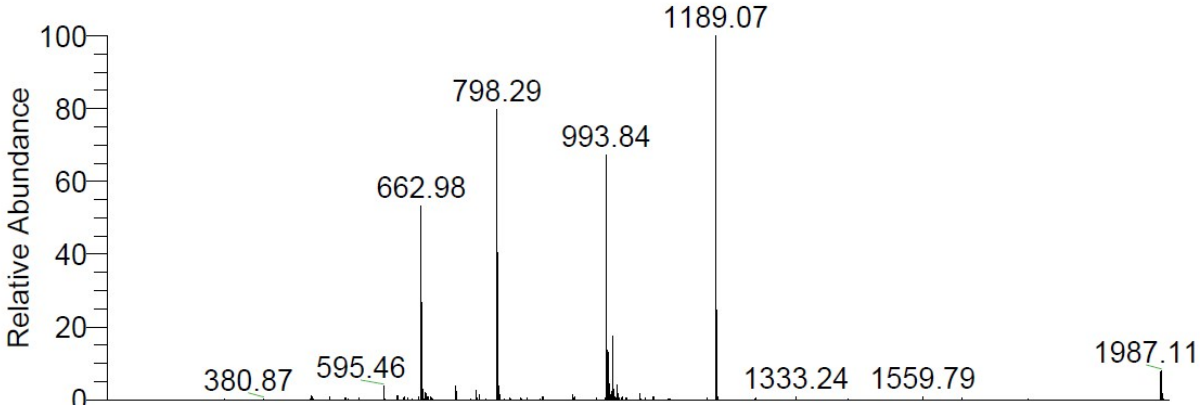

Ac-Aib-Pro-Aib-Ala-Aib-Ala-Gln-Aib-Val-Aib-Gly-Leu-Aib-Pro-Val-Aib-Aib$_{[\Psi Tz]}$Gln-Gln-Phol **(4g)**

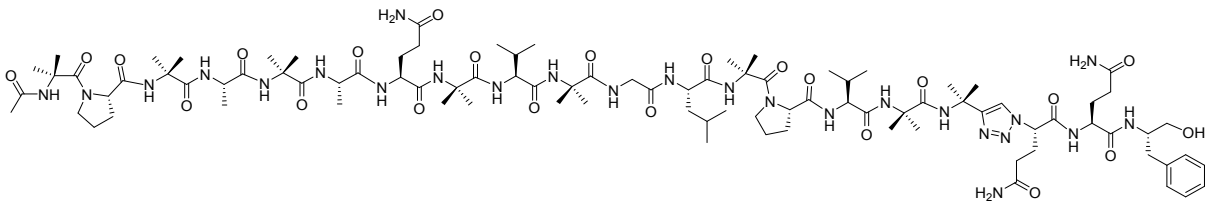

Crude peptide (~200 mg, 100% yield) was purified by semi-preparative HPLC using a linear gradient from 30% to 70% B in A over 40 min with a flow rate of 3 mL/min to yield compound **4g** (56 mg, 28% yield, >95% purity). ESI-MS: Calculated for $C_{93}H_{151}N_{25}O_{23}$: $[M+H]^+$ m/z 1987.14 ; $[M+2H]^{2+}$ m/z 994.07 ; $[M+3H]^{3+}$ m/z 663.05 ; b_{13} ion $[C_{55}H_{93}N_{14}O_{15}]^+$ m/z 1189.69 ; y_7 ion $[C_{38}H_{60}N_{11}O_8]^+$ m/z 798.46 ; found m/z: 1987.59 ; 994.08 ; 663.02 ; 1189.37 ; 798.52.

Analytical HPLC-ELSD: gradient: 0.9 ml/min flow rate from 10% B to 100% B over 50 min

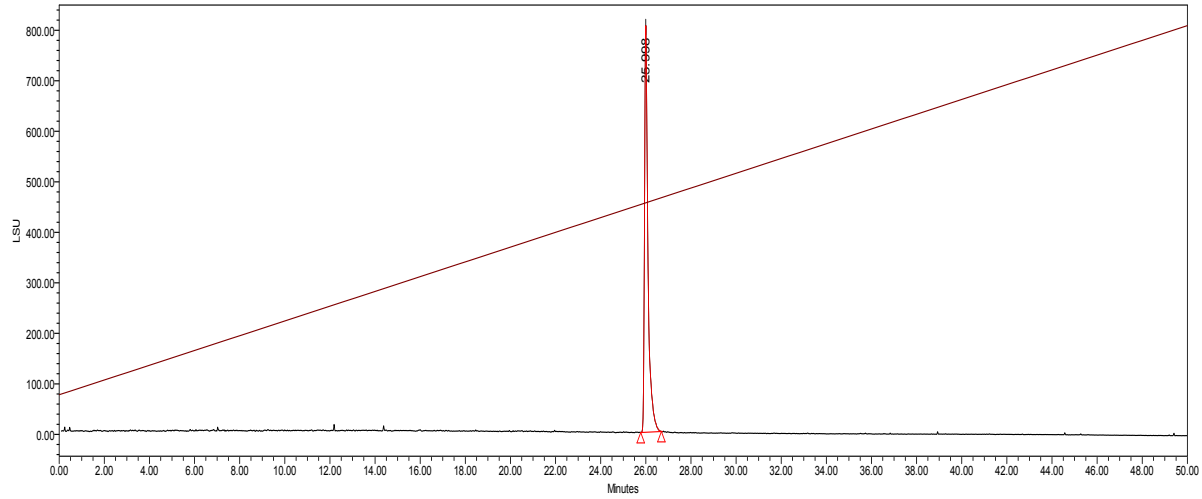

ESI-MS:

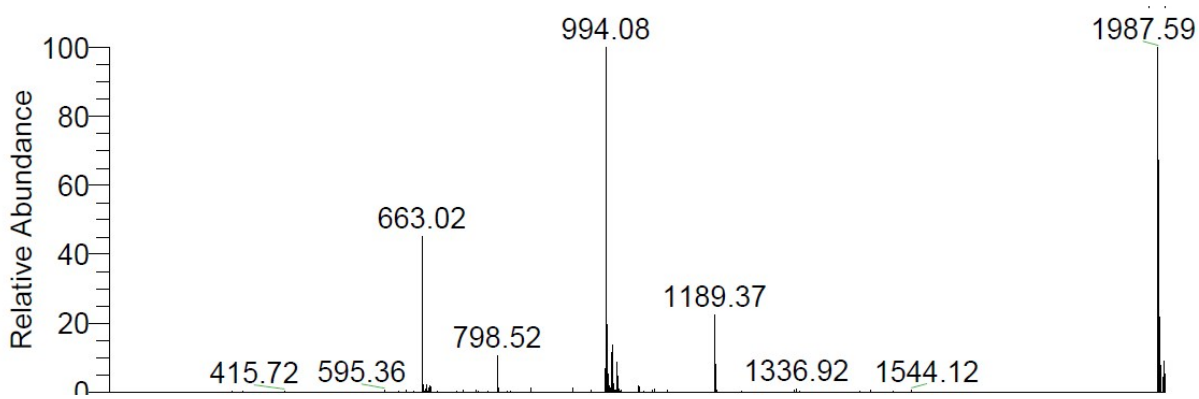

Ac-Aib-Pro-Aib-Ala-Aib-Ala-Gln-Aib-Val-Aib-Gly-Leu-Aib$_{[\psi Tz]}$Aib-Val-Aib-Aib-Gln-Gln-Phol (**4h**)

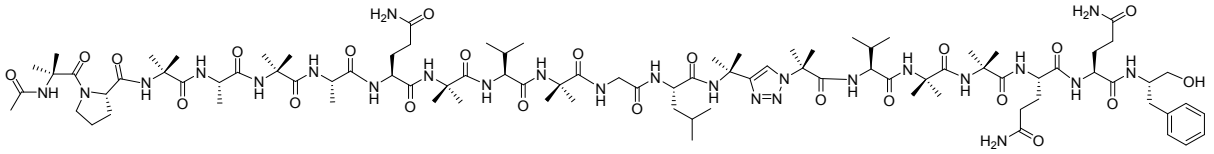

Crude peptide (~200 mg, 100% yield) was purified by semi-preparative HPLC using a linear gradient from 40% to 80% B in A over 40 min with a flow rate of 3 mL/min to yield compound **4h** (95 mg, 48% yield, >95% purity). ESI-MS: Calculated for $C_{92}H_{151}N_{25}O_{23}$ $[M+H]^+$ m/z 1975.15 ; $[M+2H]^{2+}$ m/z 987.58 ; $[M+3H]^{3+}$ m/z 659.05 ; found m/z: 1975.17 ; 988.31 ; 658.94.

Analytical HPLC-ELSD: gradient: 0.9 ml/min flow rate from 10% B to 100% B over 50 min

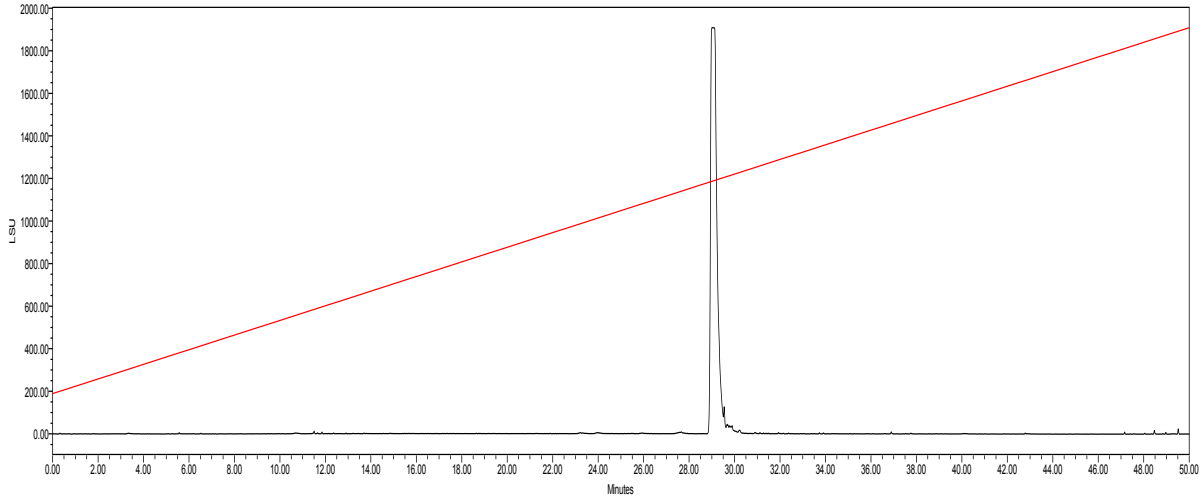

ESI-MS:

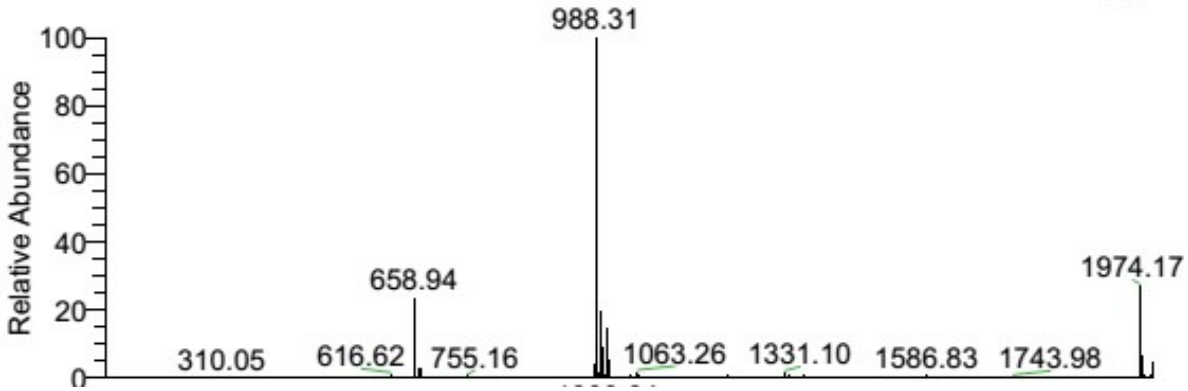

Ac-Aib-Pro-Aib$_{[\psi Tz]}$Ala-Aib$_{[\psi Tz]}$Ala-Gln-Aib$_{[\psi Tz]}$Val-Aib$_{[\psi Tz]}$Gly-Leu-Aib-Pro-Val-Aib$_{[\psi Tz]}$Aib-Gln-Gln-Phol **(4i)**

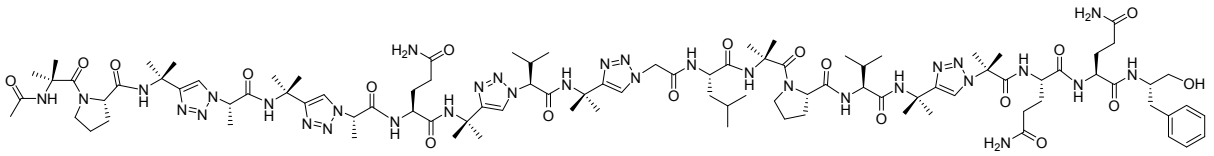

Crude peptide (~230 mg, 100% yield) was purified by semi-preparative HPLC using a linear gradient from 30% to 70% B in A over 40 min with a flow rate of 3 mL/min to yield compound **4i** (77 mg, 37% yield, >95% purity). ESI-MS: Calculated for $C_{97}H_{151}N_{33}O_{19}$ $[M+Na]^+$ m/z 2105.17, found 2105.20.

Analytical HPLC-ELSD: gradient: 0.9 ml/min flow rate from 10% B to 100% B over 50 min

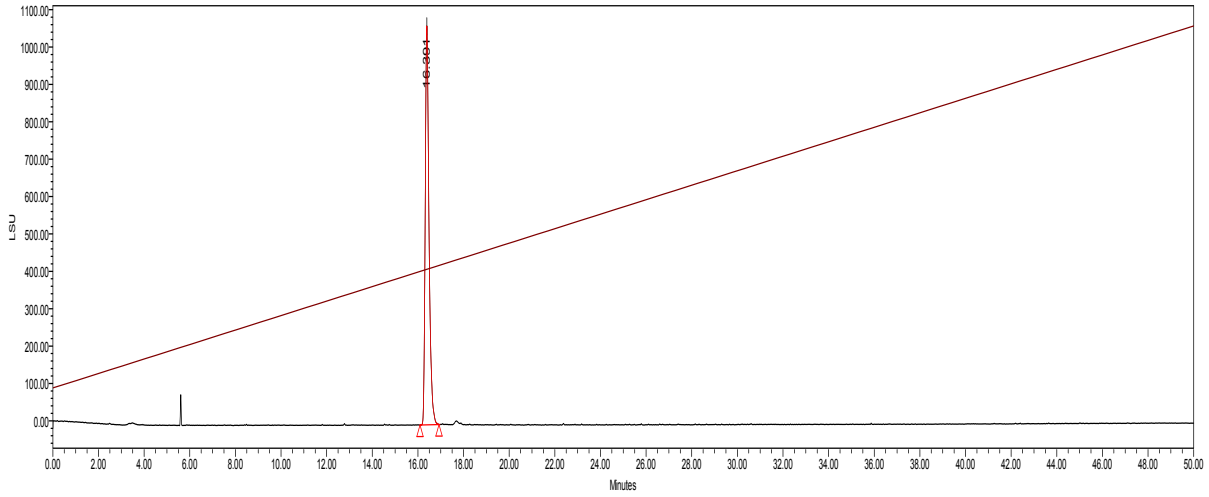

ESI-MS:

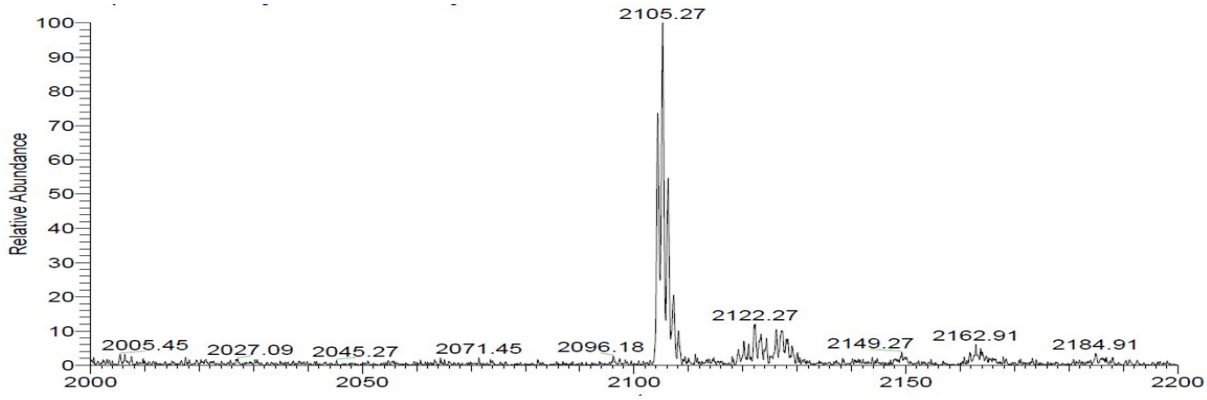

Ac-Aib-Pro-Aib$_{[\psi Tz]}$Ala-Aib$_{[\psi Tz]}$Ala-Gln-Aib$_{[\psi Tz]}$Val-Aib$_{[\psi Tz]}$Gly-Leu-Aib-Pro-Val-Aib-Aib$_{[\psi Tz]}$Gln-Gln-Phol **(4j)**

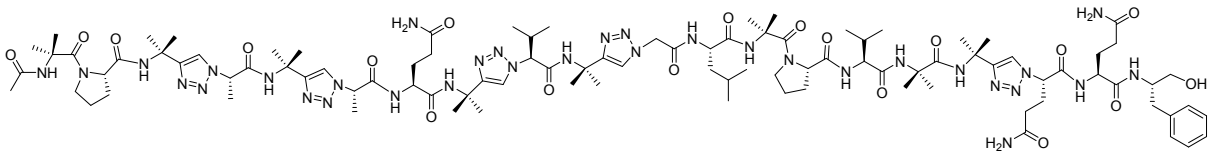

The crude peptide was purified by semi-preparative HPLC using a linear gradient from 30% to 70% B in A over 40 min with a flow rate of 3 mL/min to yield compound **4j** (80 mg, 38% yield, >95% purity). ESI-MS: $C_{97}H_{151}N_{33}NaO_{19}$ Calculated for $C_{97}H_{151}N_{33}O_{19}$: $[M+Na]^+$ m/z 2105.17 ; $[M+H]^+$ m/z 2083.19, found 2103.20 ; 2081.

Analytical HPLC-ELSD: gradient: 0.9 ml/min flow rate from 10% B to 100% B over 50 min

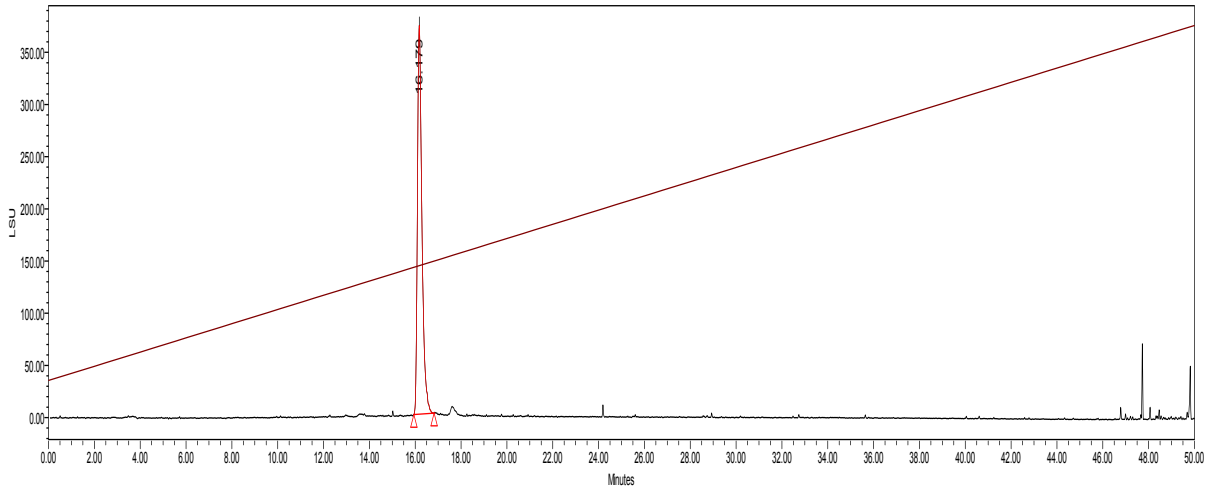

ESI-MS:

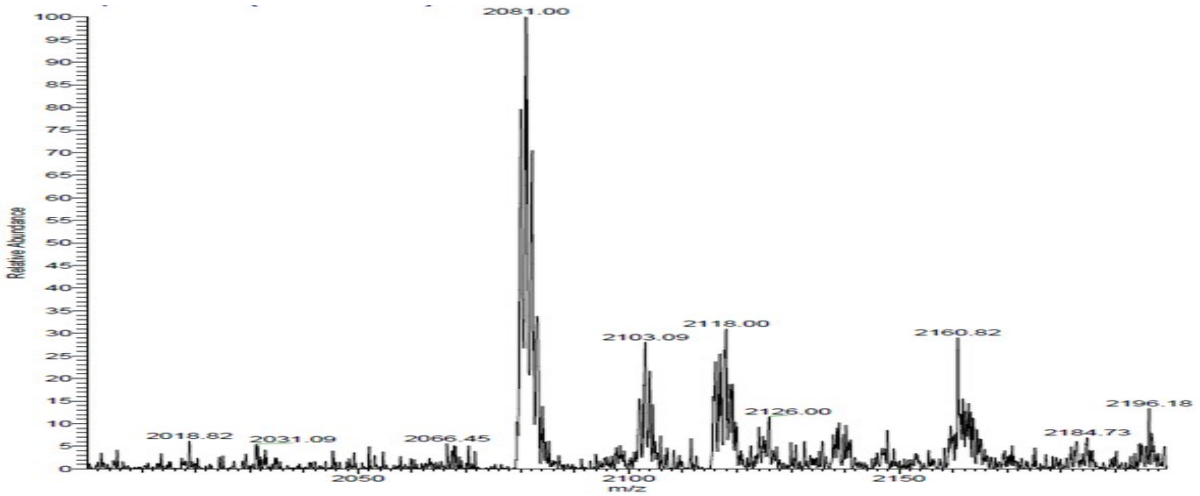

Bergofungin D 5a and analogues 5b-f:

Ac-Val-Aib-Aib-Val-Gly-Leu-Aib-Aib-Hyp-Gln-Aib-Hyp-Aib-Phol (**5a**)

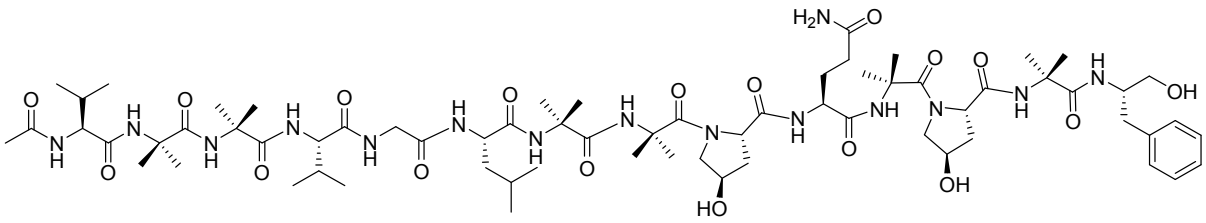

The crude peptide was purified by semi-preparative HPLC using a linear gradient from 40% to 70% B in A over 30 min with a flow rate of 3 mL/min to yield the Bergofungin D (90 mg, 63% yield, >95% purity). ESI-MS: $C_{68}H_{111}N_{15}O_{18}$ [M+H+]; calculated 1426.82, found 1425.8. ESI-MS: Calculated for $C_{68}H_{111}N_{15}O_{18}$ $[M+H]^+$ m/z 1426.82 ; $[M+2H]^{2+}$ m/z 713.92 ; found m/z: 1425.87 ; 714.03.

Analytical HPLC-ELSD gradient: 0.9 ml/min flow rate from 10% B to 100% B over 50 min

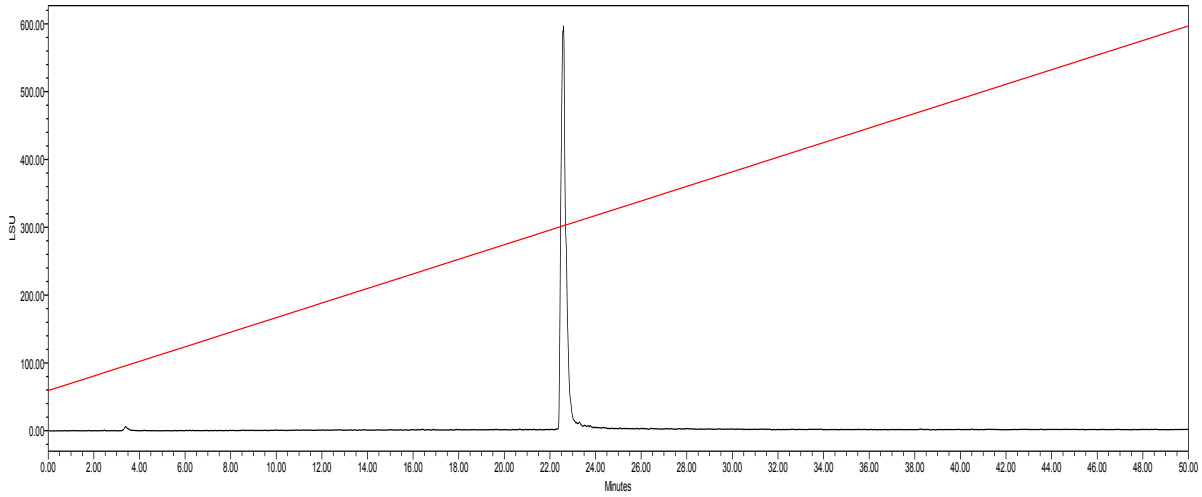

ESI-MS:

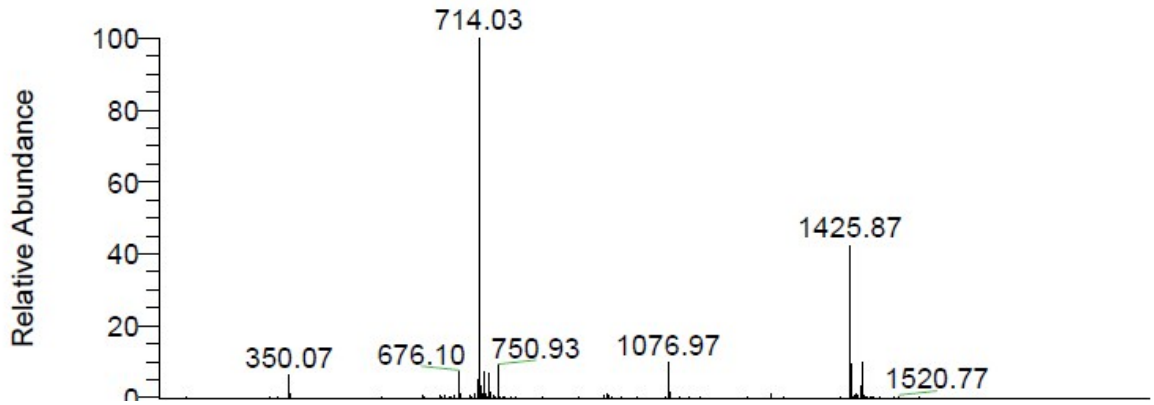

Ac-Val-Aib$_{[\Psi Tz]}$Aib-Val-Gly-Leu-Aib-Aib-Hyp-Gln-Aib-Hyp-Aib-Phol (**5b**)

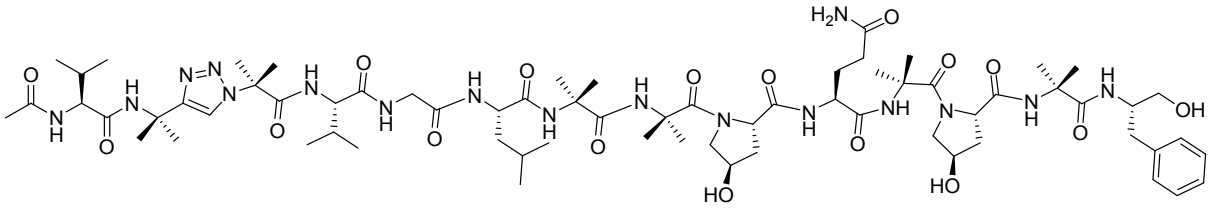

The crude peptide was purified by semi-preparative HPLC using a linear gradient from 30% to 65% B in A over 30 min with a flow rate of 3 mL/min to yield compound **5b** (90 mg, 56% yield, >95% purity). ESI-MS: $C_{68}H_{112}N_{15}O_{18}$ [M+H+]; calculated 1450.8, found 1449.8. Calculated for $C_{69}H_{111}N_{17}O_{17}$ $[M+H]^+$ m/z 1450.84 ; $[M+2H]^{2+}$ m/z 725.93 ; found m/z: 1449.89 ; 725.84.

Analytical HPLC-ELSD: gradient: 0.9 ml/min flow rate from 10% B to 100% B over 50 min

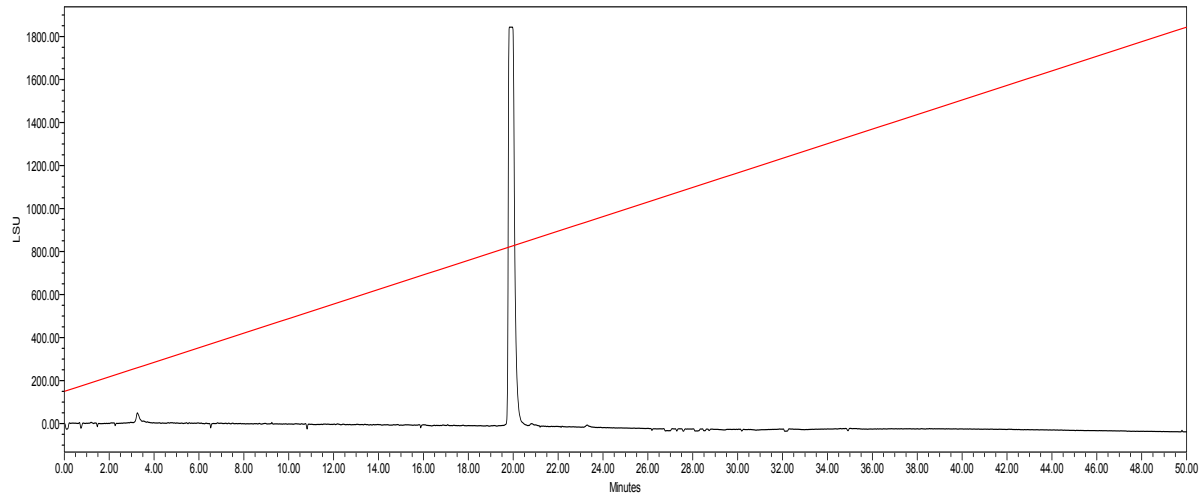

ESI-MS:

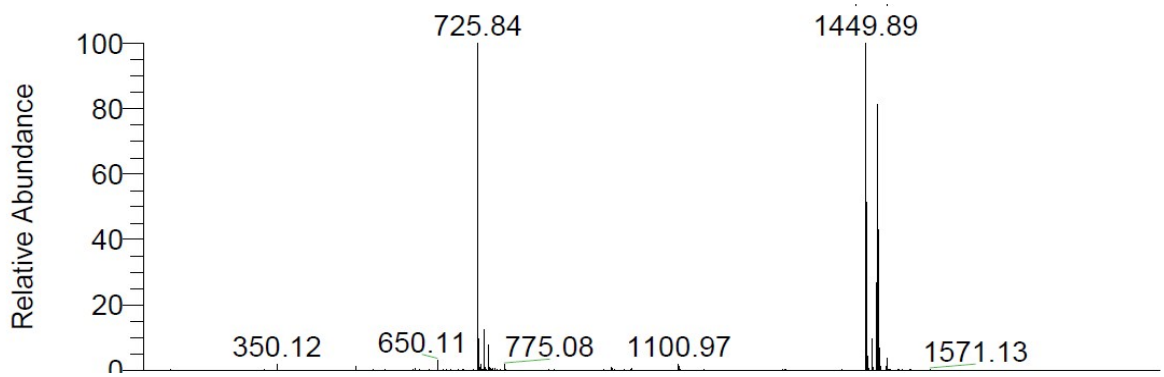

Ac-Val-Aib-Aib$_{[\psi Tz]}$Val-Gly-Leu-Aib-Aib-Hyp-Gln-Aib-Hyp-Aib-Phol (**5c**)

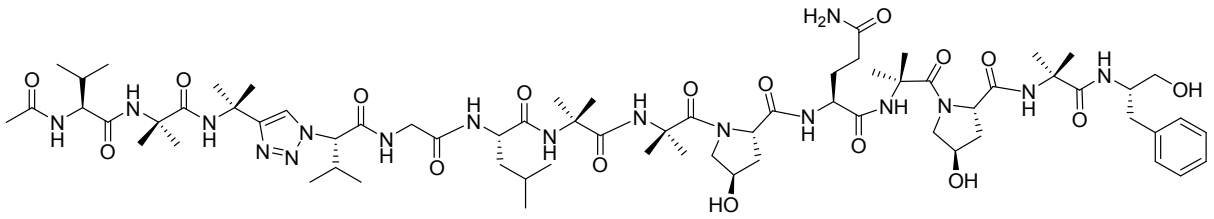

The crude peptide was dissolved in ~4 ml of ACN/H_2O and purified by semi-preparative HPLC using a linear gradient from 30% to 65% B in A over 30 min with a flow rate of 3 mL/min to yield compound **5c** (50 mg, 34% yield, >95% purity). ESI-MS: Calculated for $C_{69}H_{111}N_{17}O_{17}$ $[M+H]^+$ m/z 1450.84 ; $[M+2H]^{2+}$ m/z 725.93 ; found m/z: 1450.38 ; 7256.14.

Analytical HPLC-ELSD: gradient: 0.9 ml/min flow rate from 10% B to 100% B over 50 min

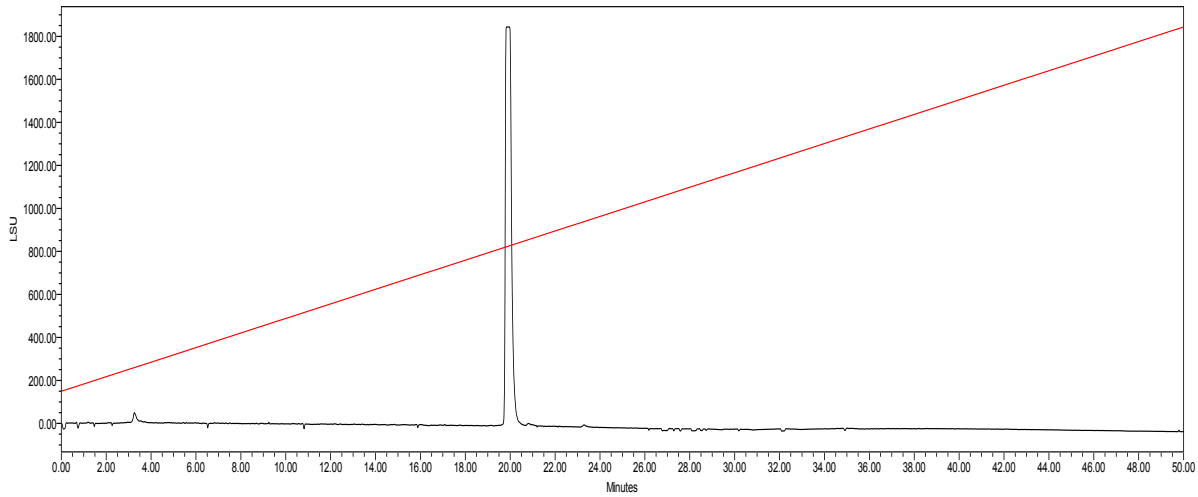

ESI-MS:

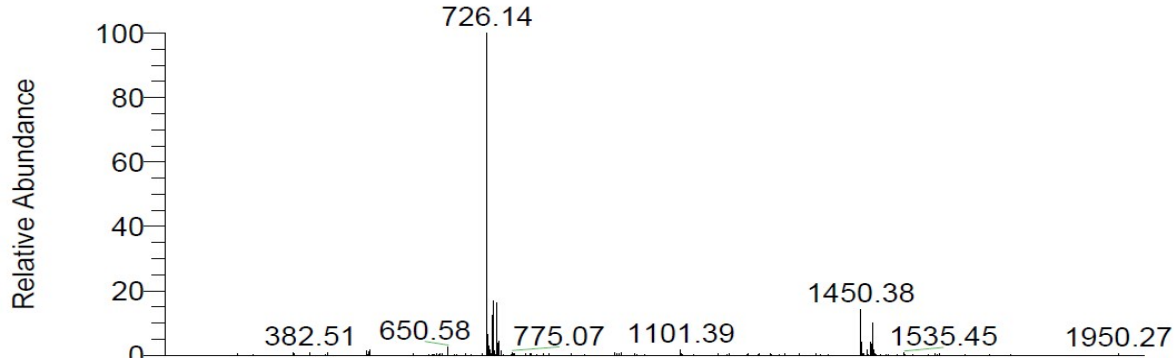

Ac-Val-Aib-Aib-Val-Gly-Leu-Aib$_{[\psi Tz]}$Aib-Hyp-Gln-Aib-Hyp-Aib-Phol (**5d**)

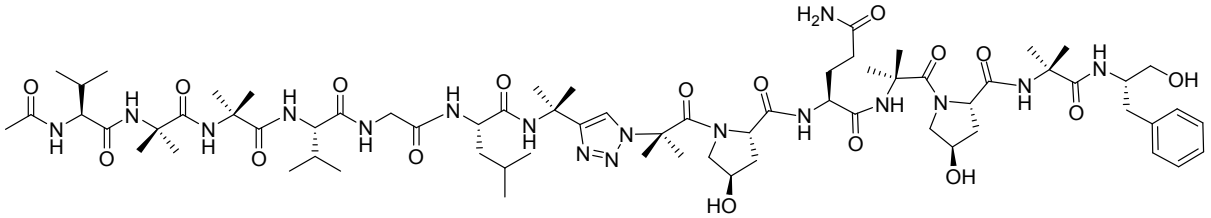

The crude peptide was purified by semi-preparative HPLC using a linear gradient from 30% to 65% B in A over 30 min with a flow rate of 3 mL/min to yield compound **5d** (80 mg, 55% yield, >95% purity). ESI-MS: Calculated for $C_{69}H_{111}N_{17}O_{17}$ $[M+H]^+$ m/z 1450.84 ; $[M+2H]^{2+}$ m/z 725.93 ; found m/z: 1450.02 ; 726.11.

Analytical HPLC-ELSD: gradient: 0.9 ml/min flow rate from 10% B to 100% B over 50 min

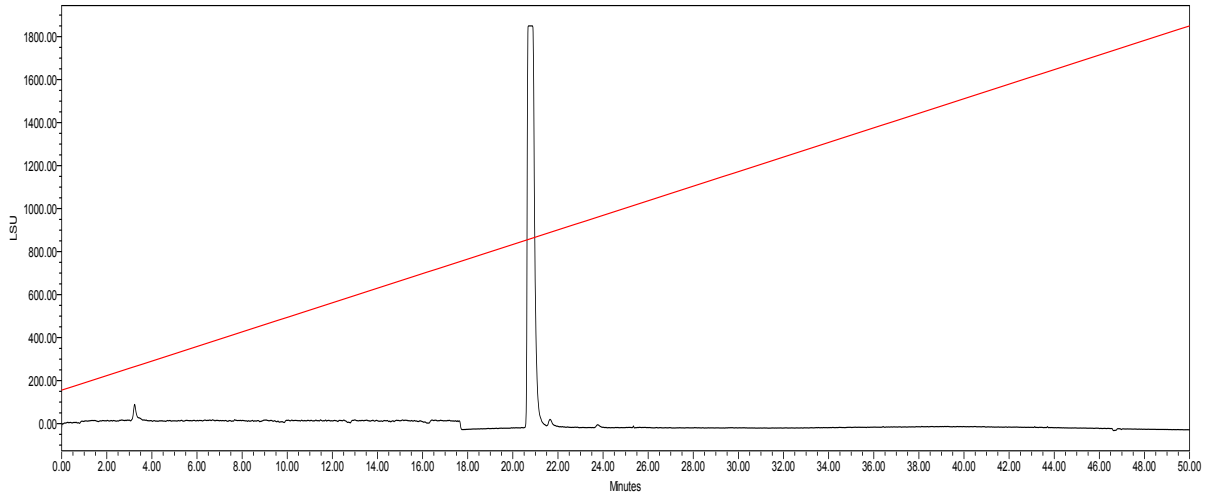

ESI-MS:

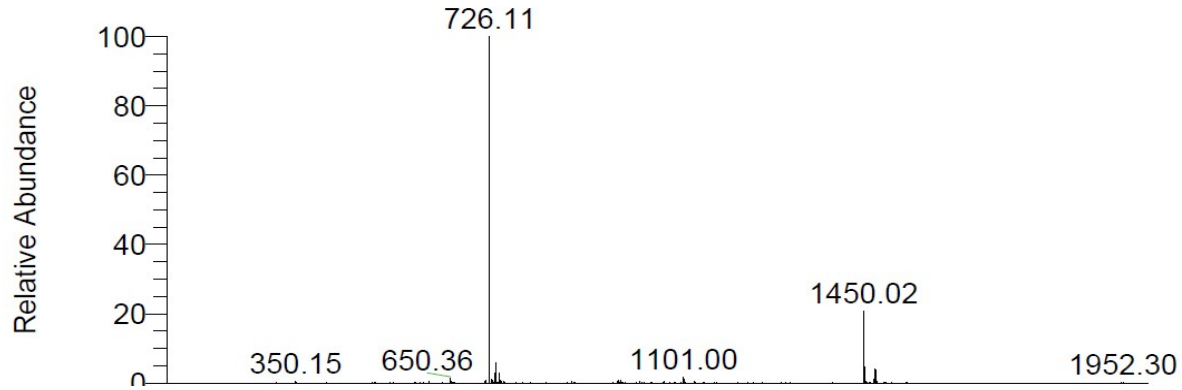

Ac-Val-Aib$_{[\Psi Tz]}$Aib-Val-Gly-Leu-Aib$_{[\Psi Tz]}$Aib-Hyp-Gln-Aib-Hyp-Aib-Phol (**5e**)

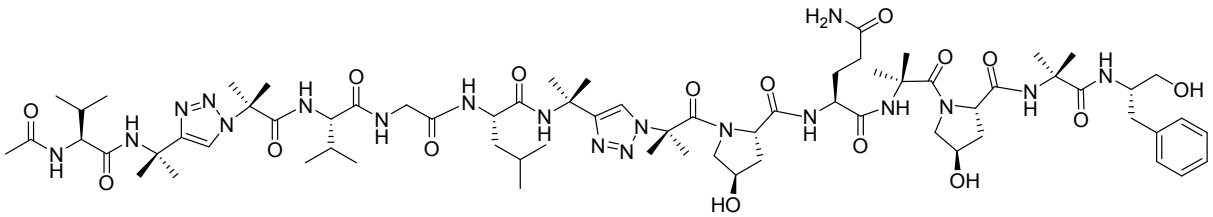

The crude peptide was purified by semi-preparative HPLC using a linear gradient from 30% to 65% B in A over 30 min with a flow rate of 3 mL/min to yield the compound **5e** (80 mg, 54% yield, >95% purity). Calculated for $C_{70}H_{111}N_{19}O_{16}$ $[M+H]^+$ m/z 1474.85 ; $[M+2H]^{2+}$ m/z 737.93 ; found m/z: 1474.00 ; 737.85.

Analytical HPLC-ELSD: gradient: 0.9 ml/min flow rate from 10% B to 100% B over 50 min

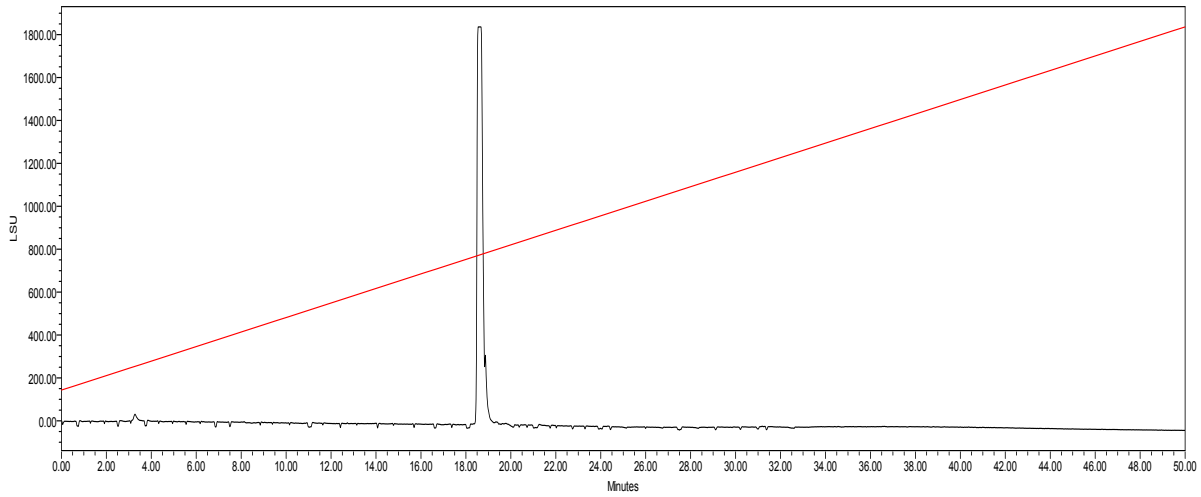

ESI-MS:

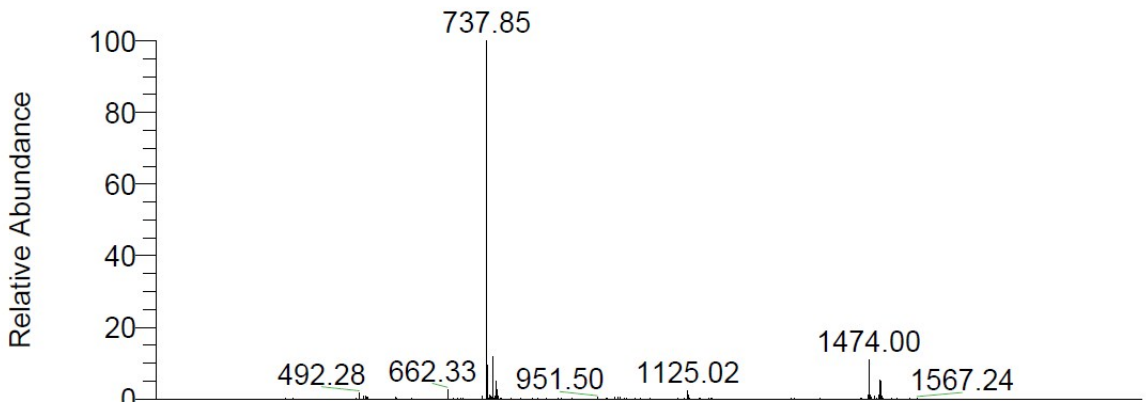

Ac-Val-Aib-Aib$_{[\Psi Tz]}$Val-Gly-Leu-Aib$_{[\Psi Tz]}$Aib-Hyp-Gln-Aib-Hyp-Aib-Phol (**5f**)

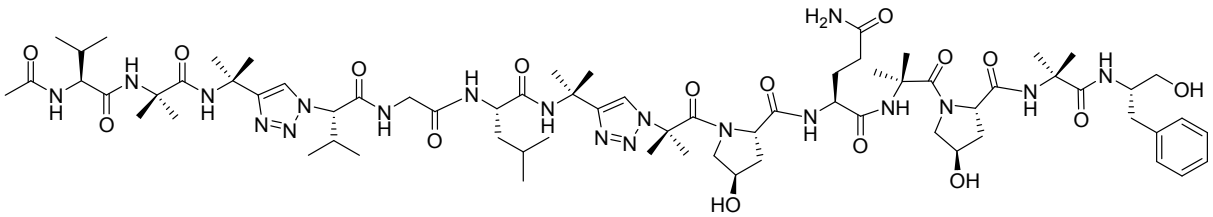

The crude peptide was purified by semi-preparative HPLC using a linear gradient from 30% to 65% B in A over 30 min with a flow rate of 3 mL/min to yield compound **5f** (80 mg, 54% yield, >95% purity). ESI-MS: Calculated for $C_{70}H_{111}N_{19}O_{16}$ $[M+H]^+$ m/z 1474.85 ; $[M+2H]^{2+}$ m/z 737.93 ; found m/z: 1474.66 ; 737.17.

Analytical HPLC-ELSD: gradient: 0.9 ml/min flow rate from 10% B to 100% B over 50 min

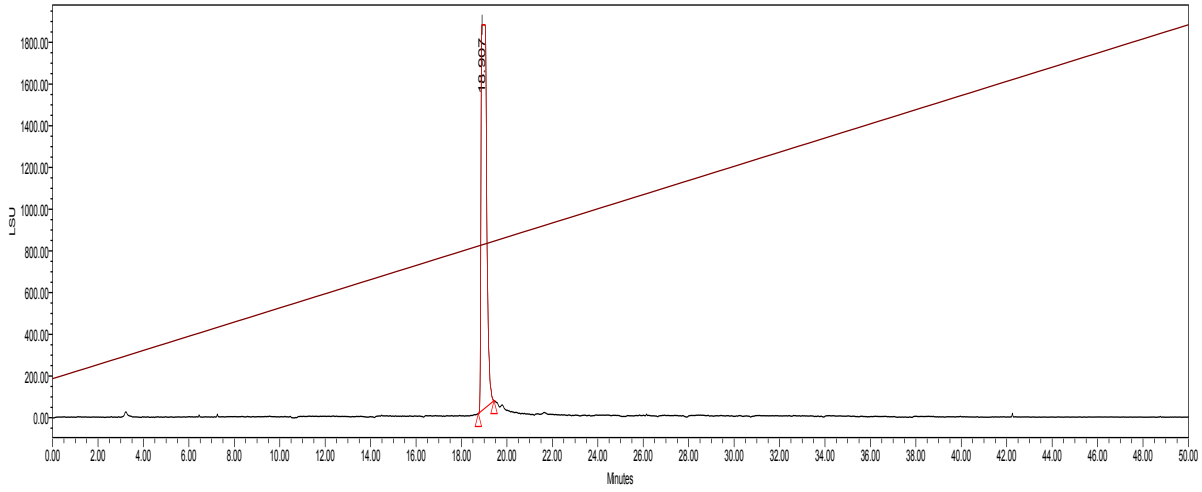

ESI-MS:

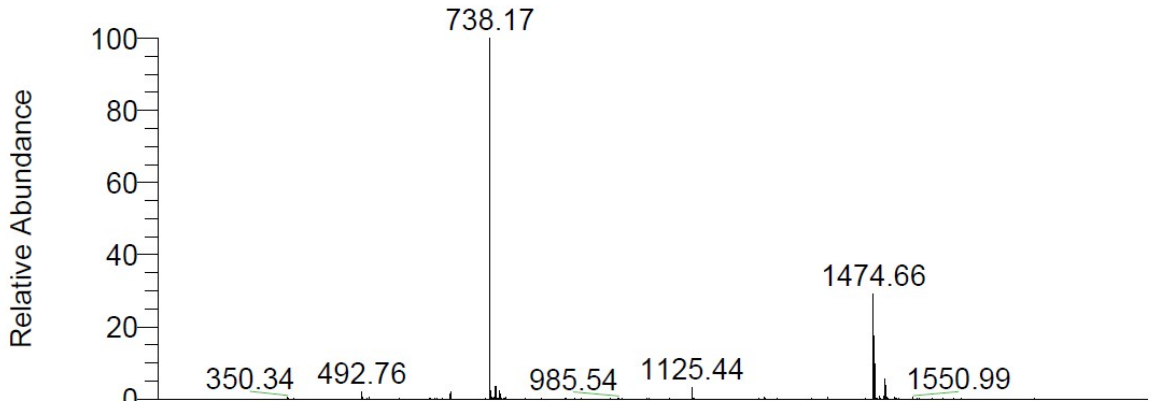

Circular Dichroism

Circular dichroism (CD) experiments were carried out using a Jasco J815 spectropolarimeter. The spectra were obtained in MeOH using a 1 mm path length CD cuvette, at 20 °C, over a wavelength range of 190-260 nm. Continuous scanning mode was used, with a response of 1.0 s with 0.2 nm steps and a bandwidth of 2 nm. The signal to noise ratio was improved by acquiring each spectrum over an average of two scans. Baseline was corrected by substracting the background from the sample spectrum. The samples were dissolved in a spectrophotometric grade MeOH at 100-200 µm.

Figure S1: Impact of the triazole group position in the sequence of the alamethicin on the molar ellipticity at 220 nm of the helical analogues **4b-g**. The non helical compounds **4i** and **4j** including multiple triazoles and the compound **4h** with the Pro14Aib mutation were not considered.

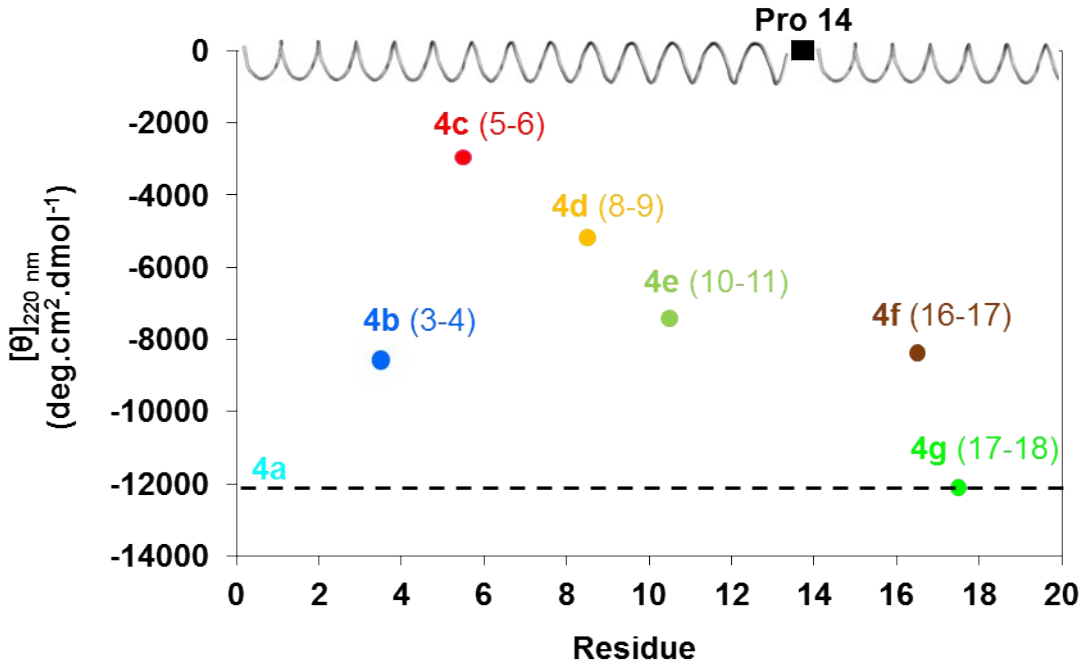

We noticed a close relationship between the position of the Tz substitutions and the helicity of Alm analogues. Indeed, the first 12 residues of Alm adopt a well defined helix while the residues after Pro^{14} are less organized. Hence, Tz substitution located in the middle of this main helix induced a drop of the global helicity.

Crystallization and crystal structure determination

The compounds were dissolved in spectroscopic grade solvents (**4g** : 2,5 mg in 0.4 mL acetonitrile ; **4h** : 3 mg in 0.8 mL acetonitrile ; **5a**, **5b** and **5d** : 1 mg in 0.3 mL acetonitrile ; **5f** : 1 mg in 0.3 mL acetonitrile/octan-1ol (99:1 v/v)). The solution was heated to reflux and allowed to cool in closed vials. Obtained crystals exhibited prismatic habit.

X-ray data for **4g**, **4h**, **5a**, **5b** and **5d** were collected at 100K with an Rigaku Oxford Diffraction Xcalibur 2 diffractometer equipped with a copper microsource (λ = 1.5418 Å). Diffraction data were processed using CrysAlis RED (Oxford Diffraction, 2003). X-ray data for **5f** were collected at the synchrotron ESRF (Grenoble, France) on beamline FIP (BM30A) dedicated to macromolecular biocrystallography.[6] The beamline wavelength was 0.920021Å and the crystal-detector distance 100 mm. In these conditions the resolution was 0.85Å in the corner of the detector. The diffraction data were processed with XDS.[7] The precision of the unit cell parameters were estimated according the conclusions of the article of Dauter and Wlodawer on the accuracy of unit-cell parameters in protein crystallography.[8] The structures were solved by direct methods with SIR2004[9] or SHELXT[10] or SHELXD[11] or SUPERFLIP.[12] The crystallographic refinements were conducted using SHELXL-97.[13] In the refinement of **4g** and **5b**, contributions of disordered solvent molecules were tentatively attenuated from the diffraction data with PLATON using the SQUEEZE procedure.[14] Selected crystallographic data are provided in the table S2-1.

CCDC 1559843 (**4g**), 1559860 (**4h**), 1559864 (**5a**), 1559865 (**5b**), 1559866 (**5d**) and 1559867 (**5f**) contain the supplementary crystallographic data for this paper. These data can be obtained free of charge from The Cambridge Crystallographic Data Centre via www.ccdc.cam.ac.uk/data_request/cif

Table S2-1. Selected crystallographic data for **4g**, **4h**, **5a**, **5b**, **5d** and **5f.**

Compound	**4g**	**4h**	**5a**	**5b**	**5d**	**5f**
Formula	$C_{93}H_{151}N_{21}O_{18}$	$C_{92}H_{151}N_{25}O_{23}$	$C_{68}H_{111}N_{15}O_{18}$	$C_{69}H_{111}N_{17}O_{17}$	$C_{69}H_{111}N_{17}O_{17}$	$C_{70}H_{112}N_{19}O_{166}$
Solvent	disordered	disordered	3(C_2H_3N), H_2O	C_2H_3N, disord.	H_2O	$C_8H_{18}O$, H_2O, disord.
Space group	$P2_12_12_1$	$P2_1$	P1	$P2_12_12_1$	I2	$P2_12_12$
a	9.2019(6)	12.0625(3)	9.0696(1)	10.1857(2)	24.5384(13)	29.04(2)
b	33.434(2)	35.0403(8)	21.6230(3)	17.9944(4)	8.9796(5)	33.47(2)
c	36.933(3)	31.1624(8)	23.9383(4)	46.7774(9)	40.3241(19)	10.30(1)
α	90	90	111.419(1)	90	90	90
β	90	100.906(3)	95.745(1)	90	105.026(5)	90
γ	90	90	98.514(1)	90	90	90
Volume	11362.8(14)	12933.6(6)	4261.16(11)	8573.6(3)	8581.4(8)	10011(13)
Z'(1)	1	2	2	1	1	1
Nref (measured)	44067	52911	44186	40992	34448	195568
R_{int}	0.092	0.153	0.09	0.068	0.064	0.08
Completeness	0.992	0.989	0.973	0.964	0.974	0.85
Resolution (Å)	1.1	0.8	0.87	0.87	0.87	0.85
R_1 ($F^2 > 2\sigma(F^2)$)	0.132 (5892)	0.0719 (40646)	0.0802 (20800)	0.0660 (10572)	0.0629 (9528)	0.0968 (11792)
wR_2 (all data)	0.376 (8973)	0.211 (51775)	0.216 (25113)	0.1985 (12568)	0.1651 (12909)	0.2748 (13538)
S ($F^2 > 2\sigma(F^2)$)	1.308	1.051	0.970	0.840	1.031	1.634
N_{par}	1020	2735	1958	1014	968	1053

(1) Number of oligomer chains in the asymmetric unit

Analysis of the Alm analogues crystal structures

Table S2-2: ϕ and ψ dihedral angles values (°) for **4a** (PDB entry 1AMT), **4g** and **4h.** The dihedrals values of the ϕ and ψ torsion angles adjacent to the Tz core were measured using the C^5H_{Tz} and N^2_{Tz} of the heterocycle, respectively (in bold). The angles values deviating more than 20° from those of the native Alm structures were highlighted in yellow. *d*: disordered.

	Torsion angles (°)		
Residue	**4a**	**4g**	**4h**
Aib 1	-48.6 ± 7.4	-42.1	-50.1 ± 0.2
	-45.3 ± 3.8	-49.9	-46.7 ± 1.7
Pro 2	-67.6 ± 6.9	-60.2	-63.2 ± 0.4
	-33.0 ± 2.9	-34.7	-45.0 ± 1.1
Aib 3	60.1 ± 5.2	-55.3	-53.5 ± 0.4
	-50.2 ± 0.5	-49.7	-46.0 ± 0.9
Ala 4	-60.0 ± 3.0	-71.8	-68.1 ± 0.6
	-45.5 ± 4.3	-36.2	-40.7 ± 0.8
Aib 5	-62.8 ± 9.2	-58.7	-54.6 ± 0.3
	-45.3 ± 1.7	-47.1	-47.2 ± 1.1
Ala 6	-67.9 ± 3.4	-67.3	-66.7 ± 0.9
	-36.1 ± 1.4	-38.2	-43.8 ± 0.4
Gln 7	-67.1 ± 0.8	-60.6	-59.8 ± 1.3
	-45.5 ± 2.4	-49.3	-45.0 ± 0.1
Aib 8	-57.0 ± 2.8	-58.5	-54.9 ± 0.6
	-47.0 ± 3.7	-43.4	-50.7 ± 0.5
Val 9	-67.1 ± 3.5	-62.8	-58.8 ± 0.4
	-50.6 ± 10.1	-55.7	-49.5 ± 0.3
Aib 10	-51.8 ± 10.2	-48	-55.7 ± 0.5
	-43.2 ± 8.6	-45.5	-46.4 ± 0.7
Gly 11	-75.0 ± 10.3	-72.7	-70.8 ± 1.1
	-29.2 ± 2.1	-22.5	-39.4 ± 3.8
Leu 12	-82.6 ± 6.8	-78.2	-62.9 ± 1.3
	-28.6 ± 23.7	-31.8	-42.9 ± 2.0
Aib 13	53.7 ± 4.8	-48.4	-52.0 ± 0.8
	-38.7 ± 7.1	-46.7	**-49.7 ± 0.6**
Pro 14	-70.1 ± 2.2	-59.6	**-60.0 ± 0.2**
	-28.3 ± 2.4	-24.7	-63.8 ± 0.4
Val 15	-62.3 ± 3.5	- 69.2	-61,0 ± 0.6
	-51.8 ± 9.4	-30.5	-55,2 ± 0.2
Aib 16	-52.6 ± 4.6	-73.5	-54.6 ± 1.1
	-52.9 ± 2.0	-50.6	-49.7 ± 0.1
Aib 17	-56.7 ± 6.7	-63.6	-54,7 ± 0.3
	-32.8 ± 6.4	**-19.6**	-46.7 ± 0.7
Glu 18	-77.0 ± 1.7	*d*	-77.3 ± 0.5
	-19.4 ± 13.4	*d*	-27.3 ± 1.1
Gln 19	-80.3 ± 11.7	*d*	-81.2 ± 1.4
	-32.3 ± 22.1	*d*	-28.4 ± 1.3
Fol 20	-131.5 ± 14.4	*d*	-165.5 ± 0.0
	-63.7 ± 7.47	*d*	68.6 ± 1.1

Table S2-3. Intramolecular hydrogen bonds stabilizing the helices of Alm **4a** (PDB entry 1AMT) and analogues **4g** and **4h.** Hydrogen bonds involving the N^2_{Tz} and C^5H_{Tz} atoms of the triazole were highlighted in bold. Criteria for H-Bonds are distance between donor (N-H) and acceptor (usually O) less than 3.5 Å and the angles at the donor and acceptor greater than 90°.[15, 16]

	α-Helix			3_{10} Helix				
	Distance O…HN			Distance O…HN				
	Alm **4a**	**4g**	**4h**		Alm **4a**	**4g**	**4h**	Alm **4a** Hydrogen bond network[b]
Bonded atoms	Mean value		Mean value	Bonded atoms	Mean value		Mean value	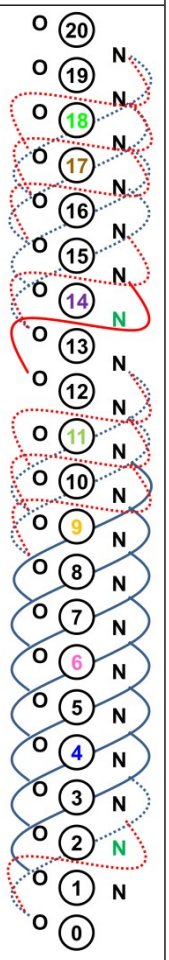
$N4_{A...}O_{Ace}$	2.44 ±0.20		2.20 ±0.01	$N3_{U.....}O_{Ace}$	2.41 ±0.21	2.42	2.69 ±0.01	
$N5_{U.....}O1_{U}$	2.26 ±0.14	2.02	2.17 ±0.01	$N4_{A.....}O1_{u}$	2.63 ±0.07	2.62	2.78 ±0.03	
$N6_{A.....}O2_{P}$	1.95 ±0.05	2.09	2.19 ±0	$N5_{U.....}O2_{P}$	2.88		2.79 ±0.02	
$N7_{Q.....}O3_{U}$	2.14 ±0.14	2.27	2.13 ±0.01	$N6_{A.....}O3_{U}$	2.95		2.75 ±0.16	
$N8_{U.....}O4_{A}$	2.10 ±0.04	2.06	2.17 ±0.01	$N7_{Q.....}O4_{A}$	2.49 ±0.07	2.74	2.92 ±0.05	
$N9_{V.....}O5_{U}$	2.25 ±0.11	2.22	2.27 ±0.01	$N8_{U.....}O5_{U}$	2.76 ±0.06	2.97	3.05 ±0.01	
$N10_{U...}O6_{A}$	1.99 ±0.03	2.05	2.12 ±0.01	$N9_{V.....}O6_{A}$	2.58 ±0		2.88 ±0.01	
$N11_{G....}O7_{Q}$	1.98 ±0.16	2.01	2.13 ±0.01	$N10_{U...}O7_{Q}$	2.86		2.94 ±0.03	
$N12_{L...}O8_{U}$	2.24 ±0.16	2.20	2.03 ±0.01	$N11_{G...}O8_{U}$	2.42 ±0.02		2.86 ±0.02	
$N13_{U}...O9_{V}$	2.26 ±0.48	2.45	2.14 ±0.01	$N12_{L...}O9_{V}$	2.35 ±0.1	2.57	2.93 ±0.01	
				$N13_{U....}O10_{U}$	2.42 ±0.37	2.65		
$C^5H_{Tz}13_{U..}O10_{U}$			**2.74 ±0.02**	**$C^5H_{Tz}13_{U..}O11_{G}$**			**2.80 ±0.01**	
$N15_{V..}O11_{G}$			2.28 ±0.01					
$N16_{U...}O12_{L}$	2.64 ±0.08		2.05 ±0.01	$N15_{V.....}O12_{L}$	2.19 ±0.09	2.17		
$N17_{U..}O13_{U}$	2.21 ±0.21	2.54	**2.51±0 N^2_{Tz}**	$N16_{U....}O13_{U}$	2.75 ±0.26	2.39		
$N18_{U...}O14_{P/U}$	2.36 ±0.34	n.d	2.45 ±0.01					
$C^5H_{Tz}17_{U..}O14_{P}$		**2.74**		**$C^5H_{Tz}17_{U..}O15_{V}$**		**2.53**		
$N19_{Q..}O15_{V}$	2.40	n.d	2.13 ±0.01	$N18_{U.....}O15_{V}$	2.43 ±0.31	n.d	2.55 ±0.02	
$N20_{Fol}O16_{U}$	2.38 ±0.04	n.d	2.18 ±0.01	$N19_{Q.....}O16_{U}$	2.14 ±0.15	n.d	2.72 ±0	

[a] Ace: acetyl ; Fol : Phenylalaninol ; U : Aib ; *n. d.*: Not defined ; For **4h** $U_{13}P_{14}$ was mutated to $U_{13[\Psi Tz]}U_{14}$. [b] Most of hydrogen bonds allowing alamethicin helix stabilization are bifurcated but i,i+4 bonds corresponding to an α-helix are on average 0.5 angström shorter than the i,i+3 bond characterizing the 3_{10} helix. Therefore alamethicin is mainly structured as an α-helix. The mean intramolecular hydrogen bonding pattern for alamethicin is represented in which residue 0 stand for the acetyl group, N atoms of proline are highlighted in green. i,i+3 H-bonds are represented by red line, i,i+4 H-bonds are represented in blue. Doted lines indicate the presence of the two types of H-Bond in different alamethicin conformers.

Figure S2-1: Superimposition of the crystal structures of Alamethicin (in cyan, PDB entry 1amt) and its analogues **4g** (in green) and **4h** (in magenta). Protons were omitted for clarity. The $Aib_{[\Psi Tz]}Xaa$ dipeptide was in yellow. The root mean square deviations (rmsd, Å) on the Cα atoms on various regions were calculated.

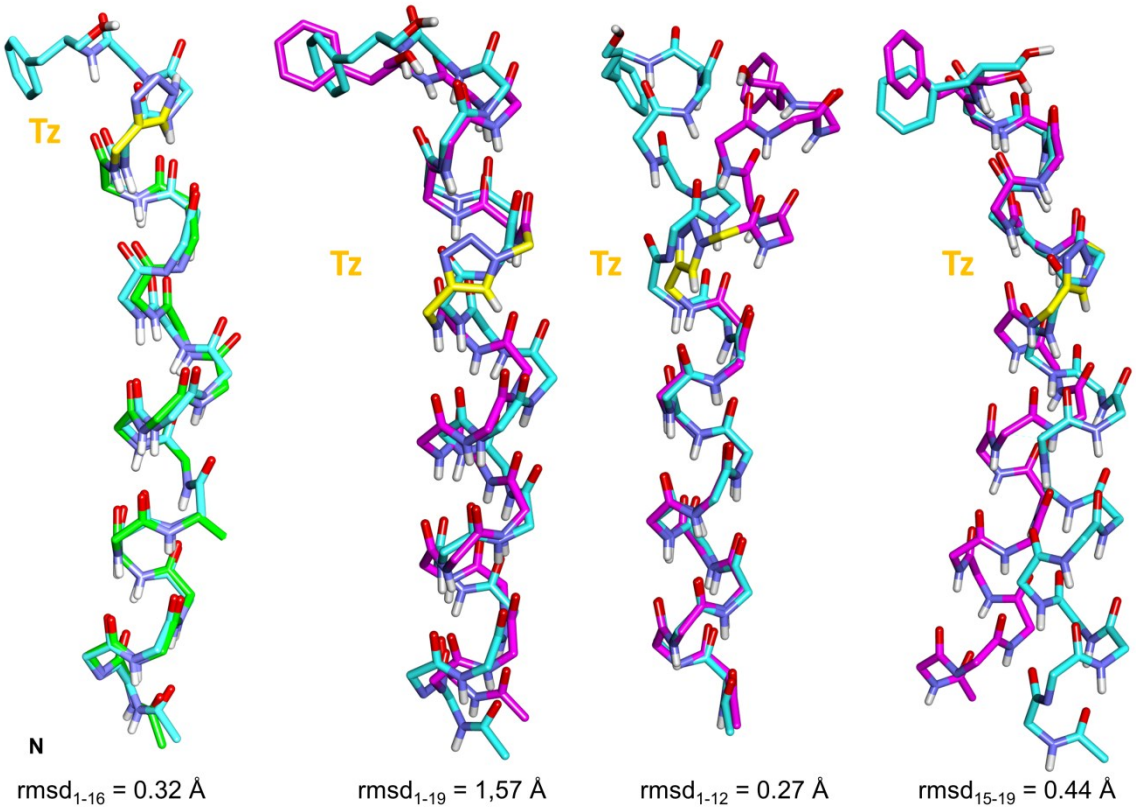

Figure S2-2: Parts of the crystal of packings of **4g** (upper panel) and **4h** (lower panel), showing solvent-accessible channels along [1 0 0] (highlighted by dashed circles). In both case, the axis of the helices and the axis of the solvent channels are perpendicular. As found in most helical peptide structures, **4h** molecules are arranged in head-to-tail mode arrangement. Surprisingly, **4g** molecules were not stacked on top of each other as usually observed in the crystal packing of helical-oligomers. The unfolded C-terminal region of **4g** hindered probably a self-assembling into columns. Intra- and Intermolecular hydrogen bonds are shown as black and orange dotted sticks, respectively. The H atoms on C atoms have been omitted for clarity.

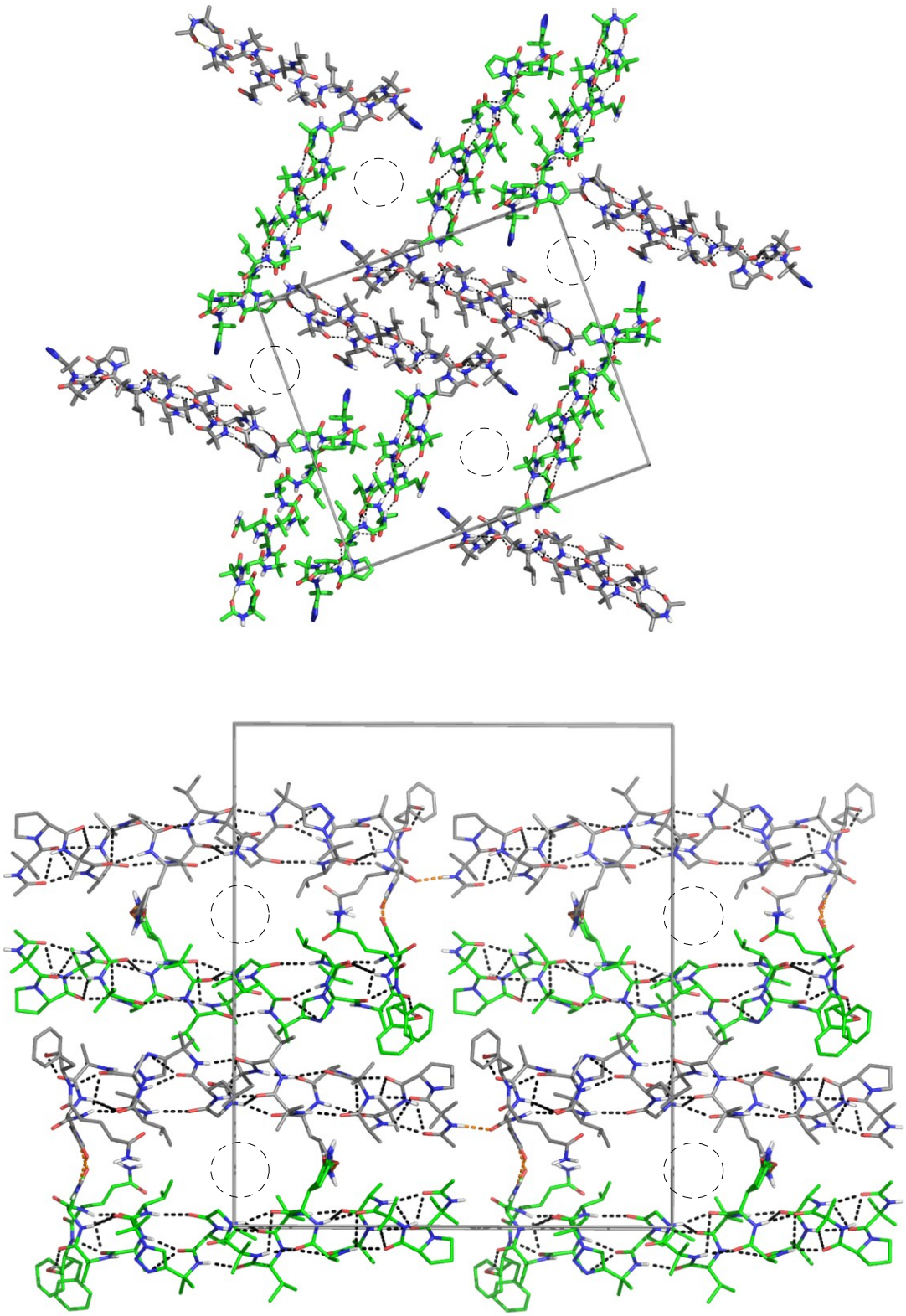

Analysis of the BergD and analogues crystal structures

Figure S2-3: Structure-based sequence alignment of peptaibols which belong to the subfamily SF2.[17] The PDB entries of Bergofungin A, Cephaibol A, Cephaibol B, Cephaibol C, Antiamoebin I and Samarosporin I are respectively 5MAS, 1OB4, 1OB6, 1OB7, 4G14 and 1JOH. Ac is acetyl, U is Aib (α-aminoisobutyryl), O is Hyp (trans-4-hydroxy-L-proline), J is Iva (D-isovaline) and Fol is a phenylalaninol residue.

Bergofungin D		Ac	V	U	U	V	G	L	U	U	O	Q	U	O	U	Fol	
Bergofungin A	Ac	V	U	U	U	V	G	L	U	U	O	Q	J	O	U	Fol	
Cephaibol A	Ac	F	U	U	U	U	G	L	J	U	O	Q	J	O	U	P	Fol
Cephaibol B	Ac	F	U	U	U	J	G	L	J	U	O	Q	J	O	U	P	Fol
Cephaibol C	Ac	F	U	U	U	U	G	L	J	U	O	Q	U	O	U	P	Fol
Antiamoebin I	Ac	F	U	U	U	J	G	L	U	U	O	Q	J	O	U	P	Fol
Samarosporin I	Ac	F	U	U	U	V	G	L	U	U	O	Q	J	O	A	Fol	

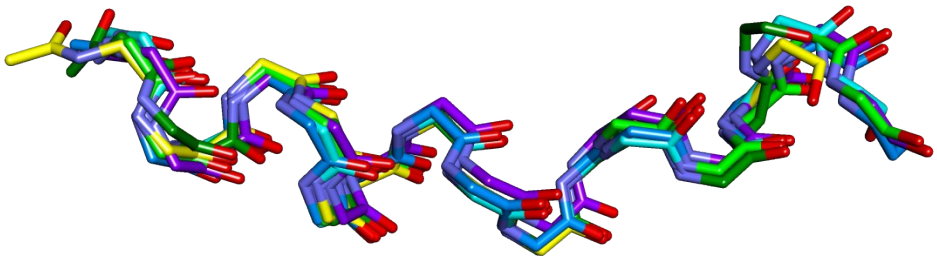

Superimposition of the Cα traces of the crystal structures of BergA (in forest, PDB entry 5mas) and its analogues: cephaibol A (in cyan, PDB entry 1ob4, rmsd: 0.55), cephaibol B (in blue, PDB entry 1ob6, rmsd: 0.71), cephaibol (in magenta, PDB entry 1ob7, rmsd: 1.78), antiamoebin 1 (in cyan, PDB entry 4g14, rmsd: 0.34) and an samatosporin 1 (in yellow, rmsd: 0.75).

Sequence alignement and superimposition of bergofungin A analogues highlighted the well-conserved three-dimensional structures of these medium-length peptaibols despite some amino acids subsitutions.

Figure S2-4: Crystal structures of bergofungin D **5a** (in gray) and its analogues **5b** (in orange) **5d** (in green) and **5f** (in magenta). Superimposition of analogues **5b**, **5d** and **5f** on bergofungin D **5a**. Side chains were omitted for clarity. Tz were couloured yellow. The root mean square deviations (rmsd, Å) on the Cα atoms on various regions were calculated.

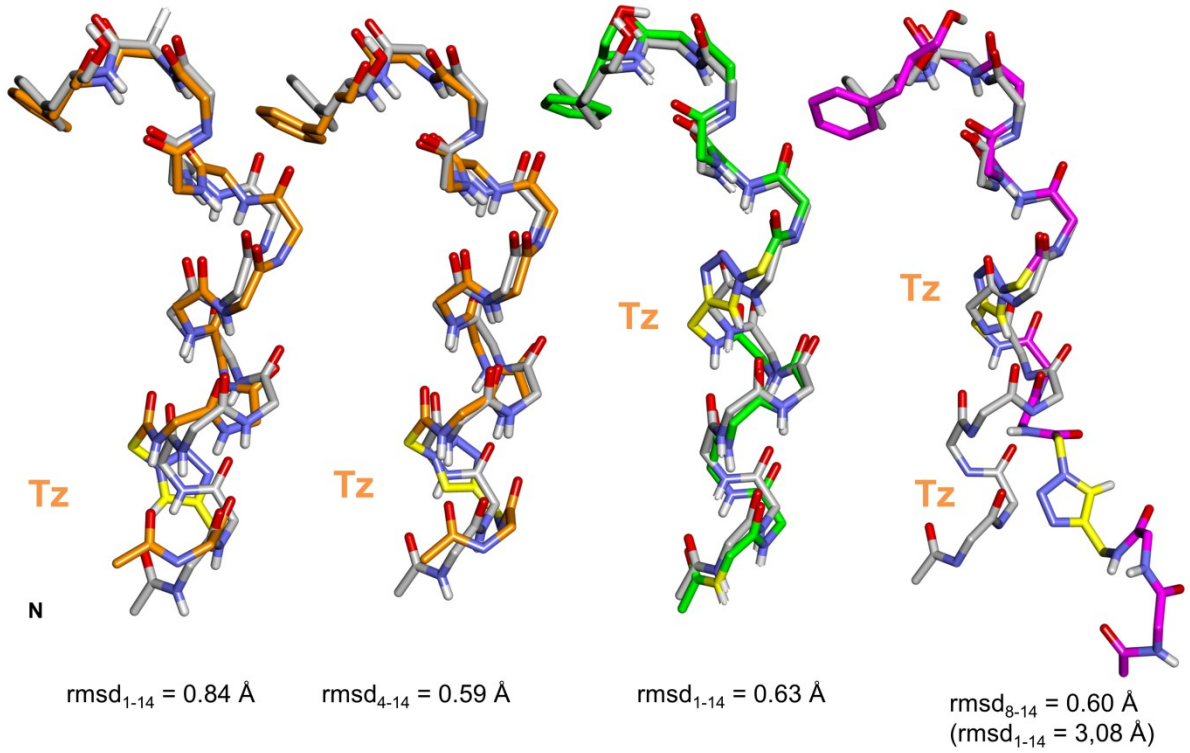

$rmsd_{1-14}$ = 0.84 Å $rmsd_{4-14}$ = 0.59 Å $rmsd_{1-14}$ = 0.63 Å $rmsd_{8-14}$ = 0.60 Å ($rmsd_{1-14}$ = 3,08 Å)

Table S2-4: Characteristic ϕ and ψ dihedral angles values (°) for **5a**, **5b**, **5d** and **5f**. Dihedrals values of the ϕ and ψ torsion angles adjacent to the triazole core were measured using the C^5H_{Tz} and N^2 of the heterocycle, respectively (in bold). The angles values deviating more than 20° from those of the native bergofungin D structure **5a** were highlighted in yellow.

Residue	Torsion angles (°)			
	5a	**5b**	**5d**	**5f**
Val 1	-61,3 ± 12.6	-64.8	-72,7	-80,9
	-30,0 ± 27.8	-43.9	-8,6	140,8
Aib 2	-52,6 ± 4.9	-53.4	-49,8	59,9
	-40,0 ± 7.1	**-46.7**	-39,4	27,2
Aib 3	-55,6 ± 2.1	**-60.5**	-55,2	-62,5
	-41,5 ± 3.0	-67.7	-31,5	**88.0**
Val 4	-57,4 ± 2.1	-63.8	-60,6	**-105,9**
	-45,0 ± 2.3	-37.5	-31,4	101,8
Gly 5	-61,7 ± 1.8	-56.2	-71,2	-66,9
	-40,4 ± 3.5	-42.7	-37,4	163,9
Leu 6	-71,4 ± 0.5	-68,7	-75,7	-66,4
	-37,2 ± 2.8	-46,4	-48,8	-28,1
Aib 7	-67,5 ± 0.4	-66	-60	-56,2
	-38,4 ± 3.5	-36,9	**-51,2**	**-30,1**
Aib 8	-52,8 ± 0.6	-51,8	**-40,1**	**-46**
	-45,2 ± 1.6	-50,9	-51,3	-41,1
Pro 9	-62,7 ± 0.7	-64,7	-56,1	-59,9
	-17,3 ± 1.8	-22,1	-27,3	-22
Gln 10	-83,2 ± 0.1	-91,3	-79,2	-70,9
	-17,1 ± 0.4	-4,6	-15,4	-12,8
Aib 11	-52,0 ± 0.4	-50,3	-51,1	-51,7
	-45,4 ± 2.2	-39,5	-47,5	-38,2
Pro 12	-64,9 ± 1.8	-58,5	-62,7	-60,5
	-27,0 ± 1.6	-30	-29	-14,8
Aib 13	-57,5 ± 1.8	-49,5	-63,3	-50,1
	-29,4 ± 7.4	-42,7	-16,9	-30,7
Phl 14	-104,1 ± 18.5	-99,1	-107,2	-91.0
	56,2 ± 4.7	60,7	52,2	57.0

Table S2-5: Intramolecular hydrogen bonds stabilizing helix for Bergofungin **5a** and analogues **5b**, **5d** and **5f**.

	3_{10} Helix				α-Helix				
	Distance O…HN				Distance O…HN				
	Berg D **5a**	**5b**	**5d**	**5f**		BergD **5a**	**5b**	**5d**	BergD **5a** Hydrogen bond network[b]
Bonded atoms	Mean value				Bonded atoms	Mean value			
$C^5H_{Tz}2_{U..}O_{Ace}$		**2.75**							
$N3_{U...}O_{Ace}$	2.39 ±0.27		2.30	2.49	$N4_{V...}O_{Ace}$	2.26	2.09		
$N4_{V.....}O1_V$	2.40 ±0.27		2.13		$N5_{G...}O1_V$	2.66 ±0.48	2.10		
					$N6_{L...}O2_U$		**2.37 N^2Tz**		
$N5_{G.....}O2_U$	2.48 ±0.15		2.23		$N6_{L...}O2_U$	2.46			
$N6_{L.....}O3_U$	2.72	2.85	2.55		$N7_{U...}O3_U$	2.17	2.14	2.14	
					$C^5H_{Tz}7_{U..}O4_V$		**2.12**		
$N7_{u.....}O4_V$	3.00	2.76			$N8_{U...}O4_V$	2.23 ±0.03	2.11		
$C^5H_{Tz}7_{U..}O5_G$				**2.32**					
$N8_{U.....}O5_G$					$N9_{V...}O5_G$				
					$N10_{Q...}O6_L$				
$N10_{Q...}O7_U$	2.16 ±0.03	2.20	**2.31 N^2Tz**	**2.47 N^2Tz**	$N11_{U...}O7_U$		3.02		
$N11_{U...}O8_U$	2.19 ±0.06	2.26	2.28	2.14	$N12_{L...}O8_U$				
$N12_{U...}O9_O$					$N13_{U...}O9_O$				
$N13_{U.}O10_Q$	2.39 ±0.1	2.12	2.40	2.08	$N14_{Fol}O10_Q$				
$N14_{Fol}O11_U$	2.32 ±0.23	2.38	2.21	2.17					

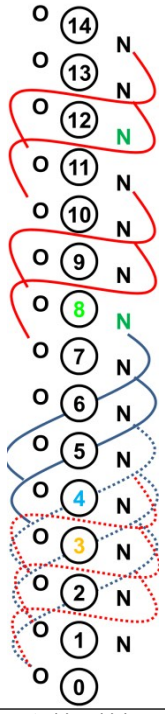

[a] Ace: acetyl ; Fol : Phenylalaninol ; U : Aib ; [b] The mean intramolecular hydrogen bonding pattern for bergofungin D is represented in which residue 0 stand for the acetyl group, N atoms of proline are highlighted in green. i,i+3 H-bonds are represented by red line, i,i+4 H-bonds are represented in blue. Doted lines indicate the presence of the two types of H-Bond in different bergofungin conformers.

Figure S2-5: Superimposition of the $U_{[\psi Tz]}$Xaa with the corresponding native dipeptides in Alm **4a** and bergD **5a**. The dipeptides backbone heavy atoms (N, Cα, C=O) on both side of the considered amide substitution were used for the superimpositions and calculations of the rmsds. Figures show the tetrapeptides sequences.

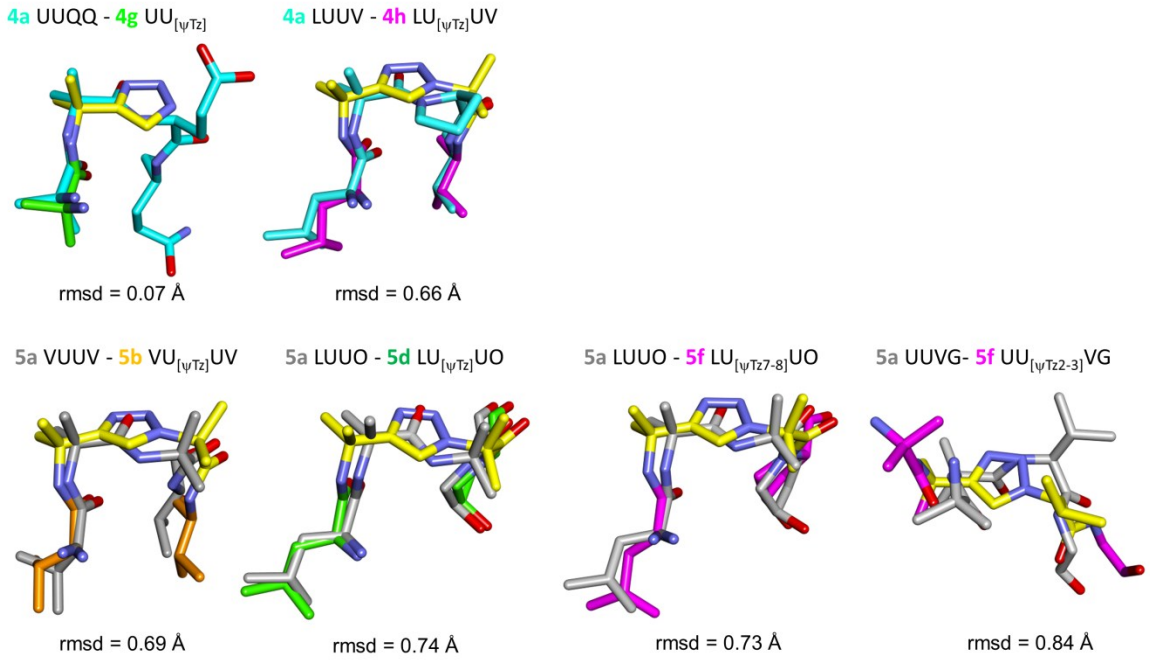

The rmsd value of 0.07 obtained when considering the **4a** to **4g** substitution is very low because sequence following the Tz insertion (17-18) was unfolded and no electron density was observed for this region in the Fourier-difference map.

Figure S2-6. Comparison of induced conformation and dihedral angles around triazoles. Structures and sequences inducing major distortions of the alpha-helix in which they are inserted are red encircled.

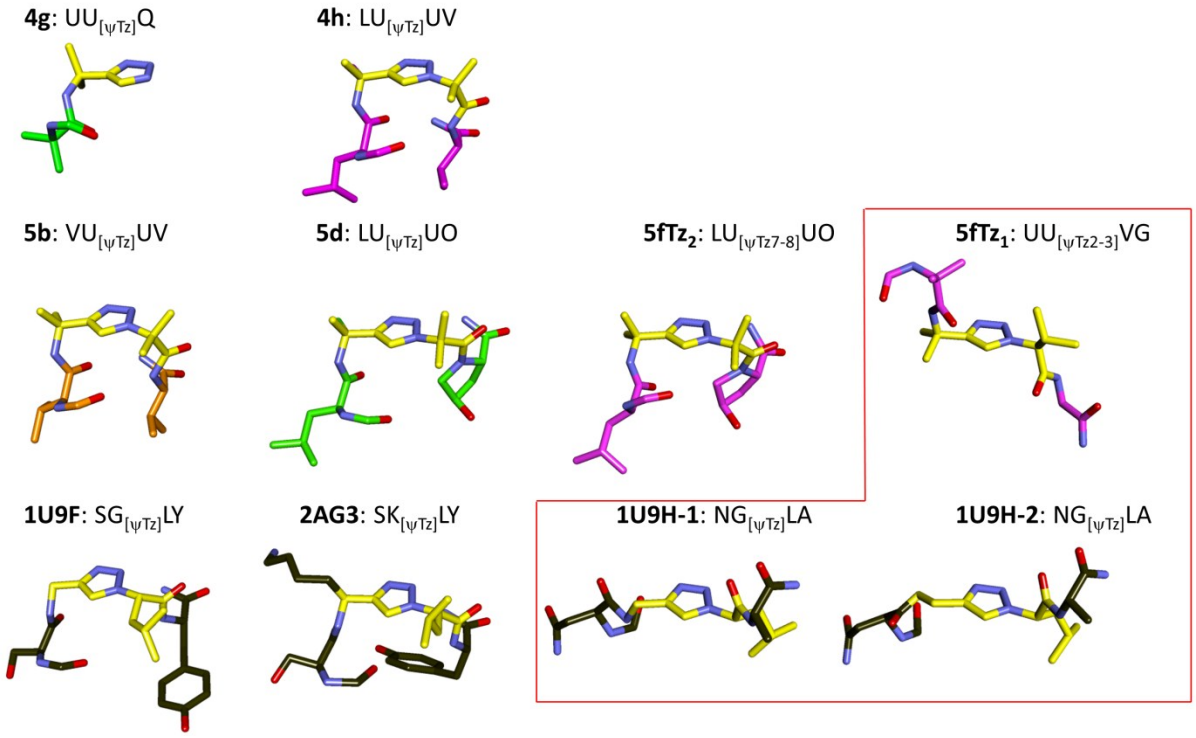

Table S2-6: Comparison of the ϕ and ψ dihedral angles values (°) surrounding the triazole core for **4g**, **4h**, **5a**, **5b**, **5d** and **5f** and in the α-helical coiled coil GCN4 (PDB entry: 1U9F, 2AG3, 1U9H).

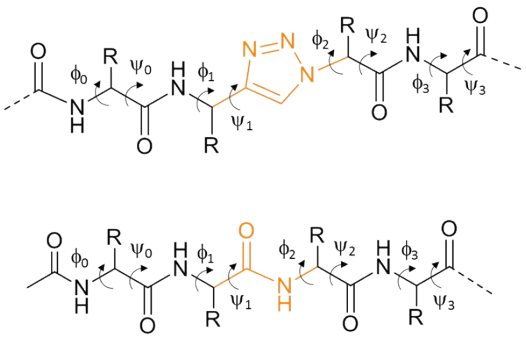

ϕ and ψ dihedral angles aroud triazole were measured using the C^5H and N^2 (labeled with star) of the heterocycle. d: disordered C terminal end. Bold: ϕ and ψ torsion angle surrounding triazole.

	ϕ and ψ torsion angle sets compatible with helix structures							ϕ and ψ torsion angle sets inconsistent with helix structures			
	4g	**4h**	**5b**	**5d**	**5f [ΨTz$_{7-8}$]**	**1U9F**	**2AG3**	**5f [ΨTz$_{3-4}$]**	**1U9H-1**	**1U9H-2**	**1U9G**
ϕ_0	-73.5	-62.9 ± 1.3	-64.8	-75.7	-66.4	-64.8 ± 2.6	-47.2	59.9	-85.7	-113.6	nd
ψ_0	-50.6	-42.9 ± 2.0	-43.9	-48.8	-28.1	-24.8 ± 4.1	-36.3	27.2	-16.9	87.3	nd
ϕ_1	-63.6	-52.0 ± 0.8	-53.4	-60	-56.2	-96.9 ± 1.4	-106.0	-62.5	-129.5	+141.2	nd
ψ_1	**-19.6**	**-49.7 ± 0.6**	**-46.7**	**-51.2**	**-30.1**	**-42.6 ± 5.9**	**-34.2**	**88.0**	**-106.5**	**-156.4**	nd
ϕ_2	**d**	**-60.0 ± 0.2**	**-60.5**	**-40.1**	**-46**	**-41.8 ± 2.8**	**-53.7**	**-105.9**	**109.2**	**101.03**	**94.5 ± 60**
ψ_2	d	-63.8 ± 0.4	-67.7	-51.3	-41.1	-63.3 ± 3.2	-64.7	101.8	144.4	131.7	80.9 ± 3.5
ϕ_3	d	-61,0 ± 0.6	-63.8	-56.1	-59.9	-70.0 ± 5.5	-50.9	-66.9	-62.8	-48.6	-69 ± 4
ψ_3	d	-55,2 ± 0.2	-37.5	-27.3	-22	-39.8 ± 8.2	-44.1	163.9	-50.0	-45.9	-40.5 ± 10

NMR and molecular modeling studies:

NMR experiments. The NMR samples contained 4 mM of **4a-j 5a-f** in CD_3OH. All spectra were recorded on a Bruker Avance 600 AVANCE III spectrometer equipped with a 5 mm quadruple-resonance probe (^1H, ^{13}C, ^{15}N, ^{31}P). Homonuclear 2-D spectra DQF-COSY, TOCSY (DIPSI2) and ROESY were typically recorded in the phase-sensitive mode using the States-TPPI method as data matrices of 256-700 real (t_1) × 2048 (t_2) complex data points; 8-64 scans per t_1 increment with 1.0-1.5 s recovery delay and spectral width of 6009 Hz in both dimensions were used. The mixing times were 60 ms for TOCSY and 350 ms for the ROESY experiments. In addition, 2D heteronuclear spectra ^{15}N, ^{13}C-HSQC and ^{13}C-HMBC were acquired (8-32 scans, 256-512 real (t_1) × 2048 (t_2) complex data points). Spectra were processed with Topspin (Bruker Biospin) and visualized with Topspin or NMRview on a Linux station. The matrices were zero-filled to 1024 (t_1) x 2048 (t_2) points after apodization by shifted sine-square multiplication and linear prediction in the F1 domain. Chemical shifts were referenced to the tetramethylsilane (TMS). ^1H, ^{15}N and ^{13}C chemical shifts were assigned according to classical procedures.[18] NOE cross-peaks were integrated and assigned within the NMRView software.[19] The volumes of NOE peaks between methylene pair protons were used as reference of 1.8 Å. The lower bound for all restraints was fixed at 1.8 Å and upper bounds at 2.7, 3.3 and 5.0 Å, for strong, medium and weak correlations, respectively. Pseudo-atoms corrections of the upper bounds were applied for unresolved aromatic, methylene and methyl protons signals as described previously.[18]

Structure calculations. The force field parameters for the triazolo-dipeptides and phenylalaninol residue were generated using R.E.D. Server Developement (http://upjv.q4md-forcefieldtools.org/REDServer/).[20] Structure calculations were performed with AMBER 11[21] in two stages: cooking, simulated annealing in vacuum. The cooking stage was performed at 1000 K to generate 100 initial random structures. SA calculations were carried during 20 ps (20000 steps, 1 fs long) as described elsewhere. First, the temperature was risen quickly and was maintained at 1000 K for the first 5000 steps, then the system was cooled gradually from 1000 K to 100 K from step 5001 to 18000 and finally the temperature was brought to 0 K during the 2000 remaining steps. For the 3000 first steps, the force constant of the distance restraints was increased gradually from 2.0 kcal.mol^{-1} Å to 20 kcal.mol^{-1}.Å. For the rest of the simulation (step 3001 to 20000), the force constant is kept at 20 kcal.mol^{-1}.Å. The 15 lowest energy structures with no violations > 0.3 Å were considered as representative of the compound structure. The representation and quantitative analysis were carried out using MOLMOL[22] and PyMOL (Delano Scientific).

Figure S3-1: ^{1}H NMR spectra of **4a-e** in CD_3OH at 298 K

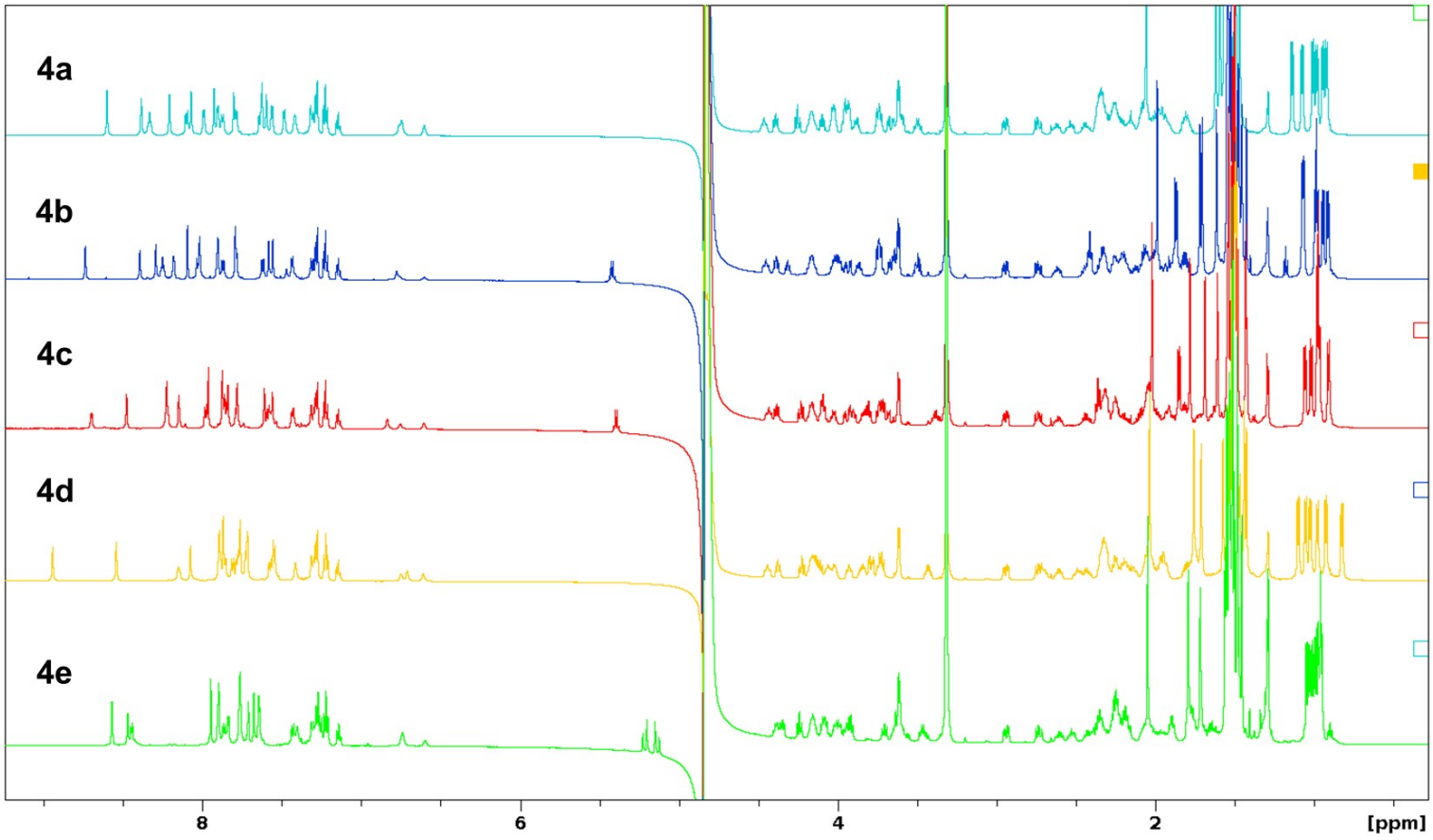

Figure S3-2: ^{1}H NMR spectra of **4f-j** in CD_3OH at 298 K

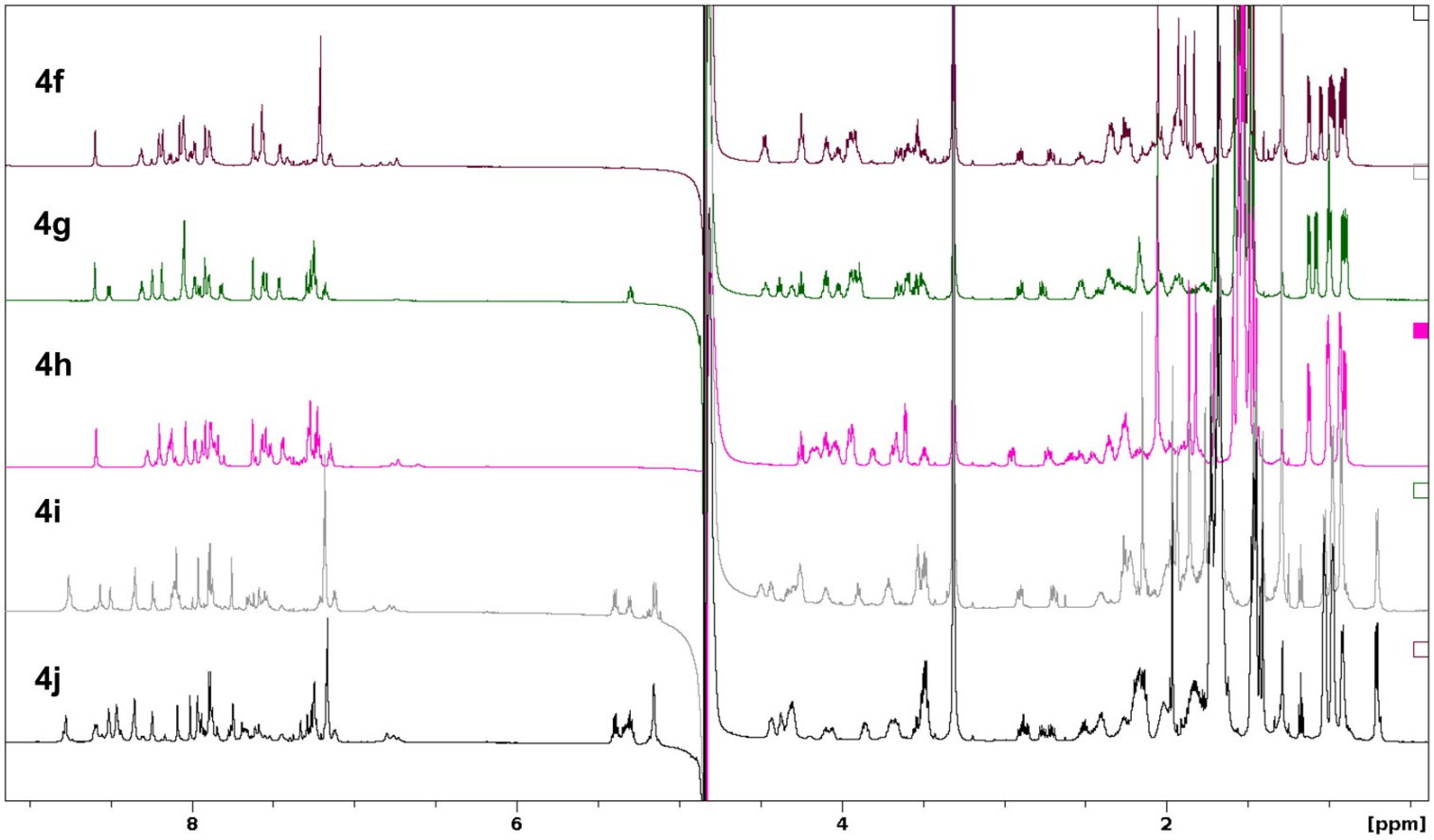

Figure S3-3: ^{1}H NMR spectra of **5a-f** in CD_3OH at 298 K

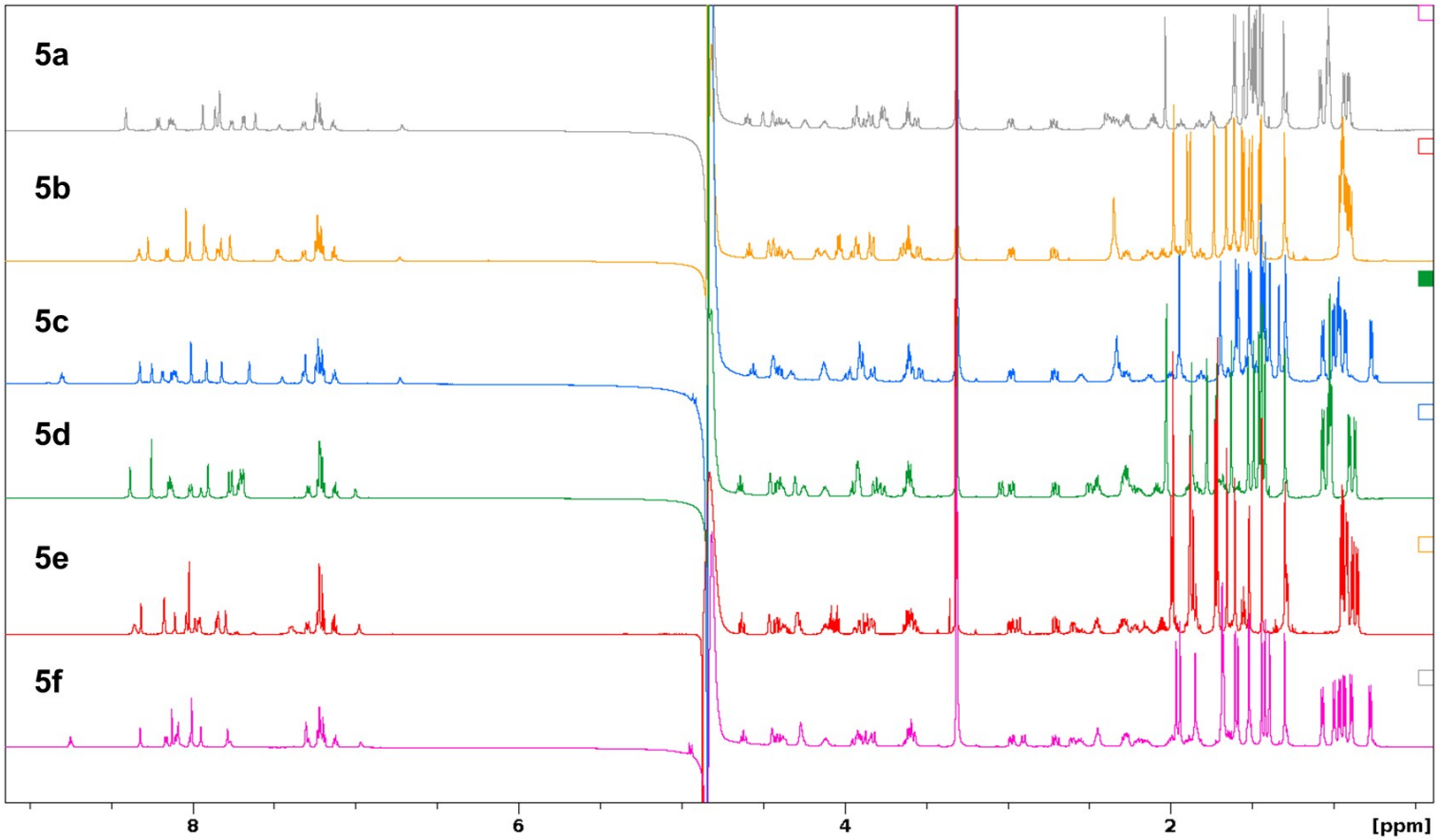

^{1}H, ^{13}C and ^{15}N NMR chemical shifts for **4a-j** and **5a-f** in CD_3OH at 298 K. *nd*: not determined, chemical shifts could not be accurately determined due to strong overlaps broad linewitdhs.

Table S4-1: ^{1}H NMR chemical shifts for **4a** in CD_3OH at 298 K

Residues	*HN*	*Hα*	*Hβ*	**Others**
Aib 1	8.59	-	1.46, 1.54	CH_3 2.05
Pro 2	-	4.25	1.78, 2.34	Hγ 1.96, 2.08; Hδ 3.49, 3.94
Aib 3	7.62	-	1.53	
Ala 4	7.56	4.09	1.49	
Aib 5	7.92	-	1.43, 1.49	
Ala 6	7.89	4.02	1.53	
Gln 7	7.99	3.92	2.15, 2.28	Hγ 2.34, 2.53; NH_2 6.74, 7.41
Aib 8	8.06	-	1.51, 1.58	
Val 9	7.48	3.59	2.23	Hγ 1.00, 1.12
Aib 10	8.20	-	1.56	
Gly 11	8.32	3.67, 3.94		
Leu 12	8.08	4.46	1.58, 1.94	Hγ 1.94; CH_3 0.92
Aib 13	8.38	-	1.54, 1.61	
Pro 14	-	4.38	1.81, 2.32	Hγ 1.99, 2.07; Hδ 3.73, 3.87
Val 15	7.63	3.73	2.33	Hγ 0.98, 1.06
Aib 16	7.59	-	1.54	
Aib 17	7.80	-	1.54	
Gln 18	7.78	4.02	2.25	Hγ 2.42, 2.61; NH_2 6.75, 7.41
Gln 19	7.86	4.16	2.02	Hγ 2.19, 2.33; NH_2 6.59, 7.31
Phl 20	7.30	3.61	4.15	Hγ 2.73, 2.93

Table S4- 2: ^{15}N and ^{13}C NMR chemical shifts for **4a** in CD_3OH at 298 K

Residues	*N*	*Cα*	*Cβ*	**Others**
Aib 1	137.1	56.0	22.0, 25.2	$COCH_3$ 171.1; CH_3 21.0; CO 174.2
Pro 2	-	64.4	28.4	Cγ 25.7; Cδ 48.6; CO 174.2
Aib 3	124.4	56.0	21.8, 25.8	CO 177.2
Ala 4	117.2	52.7	15.7	CO 175.9
Aib 5	127.6	55.9	21.6, 25.6	CO 176.6
Ala 6	115.3	52.5	15.7	CO 176.7
Gln 7	115.3	56.8	25.9	Cγ 31.2; Cδ 176.0; Nε 106.1 ; CO 174.5
Aib 8	127.6	56.2	21.7, 25.9	CO 176.9
Val 9	113.7	64.4	29.2	Cγ 18.2, 19.5; CO 174.0
Aib 10	129.7	56.2	21.8, 25.2	CO 177.7
Gly 11	100.1	43.7		CO 171.7
Leu 12	117.7	52.7	40.3	Cγ 24.3; CH_3 19.9, 22.0; CO 173.7
Aib 13	132.9	56.7	22.0, 22.5	CO 174.6
Pro 14	-	63.3	28.7	Cγ 25.7; Cδ 49.2; CO 175.1
Val 15	115.3	62.9	29.1	Cγ 18.0, 18.8 CO 174.1
Aib 16	129.1	56.1	21.8, 25.9	CO 176.4
Aib 17	124.1	56.2	25.8	CO 177.5
Gln 18	113.2	55.6	26.7	Cγ 31.9; Cδ 176.4; Nε 106.1; CO 174.4
Gln 19	115.2	54.4	26.7	Cγ 31.6; Cδ 176.0; Nε 106.1; CO 172.7
Phl 20	119.2	63.4	53.1	Cγ 36.7

Table S4-3: ^{1}H NMR chemical shifts for **4b** in CD_3OH at 298 K

Residues	*HN*	*Hα*	*Hβ*	**Others**
Aib 1	8.38	-	1.42, 1.46	CH_3 2.05
Pro 2	-	4.30	1.81, 2.18	Hγ 1.86, 2.00; Hδ 3.49, 3.74
Aib 3	7.90	-	1.71	$H_{\psi Tz}$ 8.09
Ala 4	-	5.42	1.86	
Aib 5	8.73	-	1.43, 1.49	
Ala 6	8.17	3.99	1.46	
Gln 7	7.90	3.97	2.11	Hγ 2.40; NH_2 6.73, 7.41
Aib 8	7.56	-	1.53	
Val 9	7.43	3.63	2.21	Hγ 0.96 ,1.10
Aib 10	8.01	-	1.54	
Gly 11	8.25	3.65, 3.92		
Leu 12	8.02	4.44	1.59, 1.93	Hγ 1.93; CH_3 0.92
Aib 13	8.29	-	1.53, 1.60	
Pro 14	-	4.38	1.80, 2.31	Hγ 1.98, 2.06; Hδ 3.72, 3.86
Val 15	7.62	3.72	2.32	Hγ 0.97, 1.06
Aib 16	7.58	-	1.53	
Aib 17	7.78	-	1.54	
Gln 18	7.78	4.01	2.24	Hγ 2.42, 2.60; NH_2 6.77, 7.56
Gln 19	7.86	4.16	2.02	Hγ 2.19, 2.33; NH_2 6.84, 7.59
Phl 20	7.30	3.61	4.15	Hγ 2.73, 2.93

Table S4-4: ^{15}N and ^{13}C NMR chemical shifts for **4b** in CD_3OH at 298 K

Residue	*N*	*Cα*	*Cβ*	**Others**
Aib 1	136.7	56.0	23.3	$COCH_3$ 170.8; CH_3 21.0; CO 173.1
Pro 2	-	63.1	28.6	Cγ 25.4; Cδ 48.3; CO 173.2
Aib 3	128.4	51.1	25.3	C_{Tz} 153.7; $C_{\psi Tz}$ 120.9
Ala 4	-	59.2	16.3	CO 170.1
Aib 5	134.5	56.5	24.7	CO 176.0
Ala 6	114.7	52.5	15.5	CO 176.1
Gln 7	115.3	56.5	25.8	Cγ 31.4; Cδ 175.8; Nε 106.6; CO 174.1
Aib 8	127.4	56.2	25.8	CO 176.8
Val 9	112.6	63.7	29.2	Cγ 18.1, 18.9; CO 173.7
Aib 10	129.8	56.3	25.4	CO 177.5
Gly 11	100.1	43.7		CO 171.7
Leu 12	117.7	52.6	40.1	Cγ 24.3; CH_3 19.9, 22.1; CO 173.6
Aib 13	133.0	56.6	22.0, 22.5	CO 174.4
Pro 14	-	63.3	28.6	Cγ 25.6; Cδ 49.1; CO 175.1
Val 15	115.2	63.0	29.1	Cγ 18.1, 18.9; CO 174.1
Aib 16	129.0	56.1	25.8	CO 176.3
Aib 17	124.1	56.3	25.3	CO 177.5
Gln 18	113.2	55.6	26.7	Cγ 31.8; Cδ 176.3; Nε 106.2; CO 174.2
Gln 19	115.0	54.4	26.7	Cγ 31.8; Cδ 175.9; Nε 105.7; CO 172.7
Phl 20	119.2	63.5	53.1	Cγ 36.7

Table S4-5: ^{1}H NMR chemical shifts for **4c** in CD_3OH at 298 K

Residue	*HN*	*Hα*	*Hβ*	**Others**
Aib 1	8.47	-	1.42, 1.49	CH_3 2.01
Pro 2	-	4.23	1.71, 2.30	Hγ 1.92, 2.03; Hδ 3.38, 3.90
Aib 3	7.83	-	1.48	
Ala 4	7.84	4.08	1.42	
Aib 5	7.60	-	1.52	$H_{\psi Tz}$ 7.96
Ala 6	-	5.39	1.83	
Gln 7	8.69	4.10	2.04	Hγ 2.08, 2.35; NH_2 6.83, 7.56
Aib 8	8.22	-	1.50	
Val 9	7.43	3.79	2.24	Hγ 0.99
Aib 10	7.87	-	1.50	
Gly 11	8.22	3.69, 3.93		
Leu 12	7.97	4.42	1.63, 1.90	Hγ 1.81; CH_3 0.90, 0.97
Aib 13	8.14	-	1.51, 1.60	
Pro 14	-	4.38	1.81, 2.30	Hγ 1.97, 2.04; Hδ 3.72, 3.83
Val 15	7.58	3.73	2.31	Hγ 0.96, 1.05
Aib 16	7.57	-	1.53	
Aib 17	7.77	-	1.52	
Gln 18	7.78	4.02	2.24	Hγ 2.42, 2.60; NH_2 6.75, 7.41
Gln 19	7.86	4.16	2.02	Hγ 2.19, 2.32; NH_2 6.60, 7.31
Phl 20	7.30	3.60	4.15	Hγ 2.73, 2.93

Table S4-6: ^{15}N and ^{13}C NMR chemical shifts for **4c** in CD_3OH at 298 K

Residue	*N*	*Cα*	*Cβ*	**Others**
Aib 1	136.7	56.0	22.6	$COCH_3$ 171.0; CH_3 21.0; CO 174.1
Pro 2	-	64.2	28.3	Cγ 25.7; Cδ 48.3; CO 173.6
Aib 3	122.8	56.4	26.0	CO 176.4
Ala 4	115.7	51.1	16.1	CO 174.0
Aib 5	129.4	51.3	26.1, 28.5	C_{Tz} 153.8; $C_{\psi Tz}$ 120.9
Ala 6	-	59.2	16.2	CO 170.6
Gln 7	121.2	55.9	25.9	Cγ 30.9; Cδ 176.0; Nε 106.8; CO 172.8
Aib 8	128.2	56.5	25.4	CO 176.6
Val 9	111.0	62.0	29.2	Cγ 18.6; CO 173.2
Aib 10	130.9	56.4	25.4	CO 177.4
Gly 11	99.5	43.6		CO 171.4
Leu 12	117.2	52.4	40.0	Cγ 24.3; CH_3 18.2, 19.9; CO 173.4
Aib 13	132.6	56.6	22.2	CO 174.3
Pro 14	-	63.3	28.7	Cγ 26.7; Cδ 49.0; CO 174.9
Val 15	115.0	62.9	29.0	Cγ 18.8, 22.1 CO 174.0
Aib 16	124.3	56.3	25.9	CO 176.2
Aib 17	129.0	56.2	25.9	CO 177.3
Gln 18	113.2	55.6	26.7	Cγ 31.8; Cδ 176.4; Nε 106.2; CO 174.1
Gln 19	115.1	54.4	26.8	Cγ 31.6; Cδ 175.9; Nε 105.9; CO 172.7
Phl 20	119.1	63.5	53.1	Cγ 36.7

Table S4-7: ^{1}H NMR chemical shifts for **4d** in CD_3OH at 298 K

Residue	*HN*	*Hα*	*Hβ*	**Others**
Aib 1	8.53	-	1.43, 1.51	CH_3 2.03
Pro 2	-	4.22	1.74, 2.33	Hγ 1.94, 2.05; Hδ 3.42, 3.92
Aib 3	7.71	-	1.47	
Ala 4	7.72	4.10	1.46	
Aib 5	7.88	-	1.50	
Ala 6	7.76	4.12	1.48	
Gln 7	7.80	4.05	2.13	Hγ 2.33, 2.47; NH_2 6.70, 7.40
Aib 8	7.55	-	1.70, 1.75	$H_{\psi Tz}$ 7.86
Val 9	-	4.81	2.66	Hγ 0.82, 1.09
Aib 10	8.93	-	1.42, 1.49	
Gly 11	8.14	3.78		
Leu 12	7.89	4.43	1.73, 1.95	Hγ 1.72; CH_3 0.91, 1.01
Aib 13	8.07	-	1.56, 1.59	
Pro 14	-	4.37	1.80, 2.30	Hγ 1.95, 2.02; Hδ 3.72, 3.84
Val 15	7.56	3.72	2.31	Hγ 0.96, 1.04
Aib 16	7.54	-	1.53	
Aib 17	7.76	-	1.52	
Gln 18	7.78	4.02	2.24	Hγ 2.42, 2.60; NH_2 6.75, 7.40
Gln 19	7.85	4.16	2.01	Hγ 2.19, 2.32; NH_2 6.60, 7.30
Phl 20	7.30	3.60	4.15	Hγ 2.73, 2.93

Table S4-8: ^{15}N and ^{13}C NMR chemical shifts for **4d** in CD_3OH at 298 K

Residue	*N*	*Cα*	*Cβ*	**Others**
Aib 1	136.8	56.0	22.4	$COCH_3$ 171.1; CH_3 21.1; CO 174.2
Pro 2	-	64.4	28.3	Cγ 25.6; Cδ 48.6; CO 174.0
Aib 3	123.6	56.2	21.8, 25.8	CO 177.3
Ala 4	116.8	52.3	15.7	CO 175.8
Aib 5	127.4	56.2	22.1, 25.6	CO 176.6
Ala 6	114.1	51.2	15.9	CO 174.7
Gln 7	114.5	54.5	26.8	Cγ 31.7; Cδ 176.3; Nε 106.1; CO 172.3
Aib 8	130.0	51.2	26.8, 27.9	C_{Tz} 153.4; $C_{\psi Tz}$ 121.4
Val 9	-	69.8	30.2	Cγ 17.5, 18.5; CO 168.6
Aib 10	137.7	56.7	24.1	CO 176.6
Gly 11	99.5	43.7		CO 171.1
Leu 12	116.4	52.3	40.0	Cγ 28.1; CH_3 20.0, 22.0; CO 173.5
Aib 13	132.5	56.7	22.2	CO 174.2
Pro 14	-	63.3	28.7	Cγ 25.6; Cδ 48.9; CO 175.0
Val 15	115.0	62.9	29.1	Cγ 18.0, 18.9 CO 174.0
Aib 16	129.0	56.1	21.8, 26.0	CO 176.3
Aib 17	124.1	58.3	25.9	CO 177.3
Gln 18	113.2	55.6	26.6	Cγ 31.8; Cδ 176.4; Nε 106.1; CO 174.1
Gln 19	115.3	54.3	26.8	Cγ 31.6; Cδ 175.9; Nε 105.8; CO 172.7
Phl 20	119.1	63.5	53.1	Cγ 36.7

Table S4-9: ^{1}H NMR chemical shifts for **4e** in CD_3OH at 298 K

Residue	*HN*	*Hα*	*Hβ*	**Others**
Aib 1	8.56	-	1.45, 1.54	CH_3 2.04
Pro 2	-	4.23	1.79, 2.35	Hγ 1.96, 2.07; Hδ 3.47, 3.94
Aib 3	7.67	-	1.51	
Ala 4	7.64	4.09	1.47	
Aib 5	7.89	-	1.54	
Ala 6	7.83	4.07	1.50	
Gln 7	7.89	3.98	2.18	Hγ 2.37, 2.52; NH_2 6.73, 7.39
Aib 8	7.70	-	1.55	
Val 9	7.25	3.92	2.24	Hγ 0.97, 1.03
Aib 10	7.76	-	1.54	$H_{\psi Tz}$ 7.94
Gly 11	-	5.14, 5.19		
Leu 12	8.44	4.38	1.67	Hγ 1.67; CH_3 0.94, 0.99
Aib 13	8.46	-	1.50, 1.54	
Pro 14	-	4.34	1.78, 2.24	Hγ 1.88; Hδ 3.60
Val 15	7.42	3.70	2.26	Hγ 0.95, 1.02
Aib 16	7.64	-	1.50	
Aib 17	7.75	-	1.51	
Gln 18	7.76	4.01	2.23	Hγ 2.41, 2.60; NH_2 6.74/7.39
Gln 19	7.86	4.16	2.01	Hγ 2.19, 2.32; NH_2 6.60/7.30
Phl 20	7.30	3.60	4.14	Hγ 2.73, 2.92

Table S4-10: ^{15}N and ^{13}C NMR chemical shifts for **4e** in CD_3OH at 298 K

Residue	*N*	*Cα*	*Cβ*	**Others**
Aib 1	136.9	56.0	22.3	$COCH_3$ 171.2; CH_3 21.0; CO 174.3
Pro 2	-	64.4	28.3	Cγ 25.7; Cδ 48.5; CO 173.2
Aib 3	123.9	56.1	25.7	CO 177.3
Ala 4	117.1	52.5	15.5	CO 175.7
Aib 5	127.7	56.0	25.5	CO 176.7
Ala 6	114.7	52.0	15.4	CO 176.2
Gln 7	115.3	55.6	26.3	Cγ 31.6; Cδ 176.2; Nε 106.4 ; CO 173.3
Aib 8	125.4	56.6	26.1	CO 176.3
Val 9	109.8	61.2	29.6	Cγ 17.7, 18.5; CO 172.1
Aib 10	133.3	51.3	25.9	C_{Tz} 153.7; $C_{\psi Tz}$ 123.7
Gly 11	-	52.0		CO 166.9
Leu 12	119.9	53.2	40.9	Cγ 28.6; CH_3 20.6, 21.6; CO 173.3
Aib 13	132.4	56.6	22.2	CO 173.7
Pro 14	-	63.3	28.5	Cγ 25.4; Cδ 48.7; CO 175.0
Val 15	119.9	63.0	29.0	Cγ 18.0, 19.2; CO 173.9
Aib 16	129.3	56.2	25.9	CO 176.3
Aib 17	124.2	56.2	25.9	CO 177.4
Gln 18	113.2	55.6	26.6	Cγ 31.9; Cδ 176.4; Nε 106.4; CO 174.2
Gln 19	115.3	54.3	26.8	Cγ 31.6; Cδ 176.0; Nε 105.8; CO 172.7
Phl 20	119.1	63.5	53.1	Cγ 36.7

Table S4-11: ^{1}H NMR chemical shifts for **4f** in CD_3OH at 298 K

Residue	*HN*	*Hα*	*Hβ*	**Others**
Aib 1	8.59	-	1.46, 1.54	CH_3 2.05
Pro 2	-	4.24	1.80, 2.35	Hγ 1.95, 2.08; Hδ 3.49, 3.94
Aib 3	7.62	-	1.52	
Ala 4	7.56	4.08	1.49	
Aib 5	7.91	-	1.55	
Ala 6	7.89	4.02	1.52	
Gln 7	7.98	3.93	2.14, 2.27	Hγ 2.35, 2.52; NH_2 6.73, 7.40
Aib 8	8.05	-	1.51, 1.58	
Val 9	7.46	3.59	2.23	Hγ 0.99, 1.11
Aib 10	8.18	-	1.55	
Gly 11	8.30	3.66, 3.92		
Leu 12	8.04	4.48	1.58, 1.92	Hγ 1.90; CH_3 0.91
Aib 13	8.20	-	1.49, 1.56	
Pro 14	-	4.46	1.79, 2.34	Hγ 1.93, 2.03; Hδ 3.56, 3.89
Val 15	7.88	3.96	2.33	Hγ 0.97, 1.04
Aib 16	7.56	-	1.67, 1.82	$H_{\psi Tz}$ 8.07
Aib 17	-	-	1.88, 1.92	
Gln 18	8.00	4.24	1.94, 2.08	Hγ 2.26; NH_2 6.77, 7.56
Gln 19	8.13	4.24	2.04	Hγ 2.19, 2.33; NH_2 6.84, 7.59
Phl 20	7.57	3.53	4.09	Hγ 2.70, 2.90

Table S4-12: ^{15}N and ^{13}C NMR chemical shifts for **4f** in CD_3OH at 298 K

Residue	*N*	*Cα*	*Cβ*	Others
Aib 1	136.9	56.0	22.5, 25.8	$COCH_3$ 171.2; CH_3 21.0; CO 174.0
Pro 2	-	64.3	28.4	Cγ 25.8; Cδ 48.6; CO 174.3
Aib 3	124.3	56.0	25.9	CO 177.1
Ala 4	117.2	53.0	15.7	CO 175.9
Aib 5	127.8	55.8	22.6, 25.6	CO 176.6
Ala 6	115.5	52.5	15.6	CO 176.8
Gln 7	115.3	56.7	26.0	Cγ 31.3; Cδ 176.0; Nε 105.9 ; CO 174.5
Aib 8	127.5	56.3	26.1	CO 176.9
Val 9	113.6	64.3	29.2	Cγ 18.3, 19.4; CO 174.0
Aib 10	129.7	56.2	25.3	CO 177.7
Gly 11	100.0	43.6		CO 171.5
Leu 12	117.9	52.4	40.3	Cγ 24.3; CH_3 19.9, 22.2; CO 173.8
Aib 13	132.9	56.5	22.4	CO 177.7
Pro 14	-	63.1	29.0	Cγ 26.0; Cδ 49.0; CO 174.2
Val 15	111.9	60.8	29.6	Cγ 18.1, 18.5 CO 172.4
Aib 16	132.3	51.3	25.8, 29.2	C_{Tz} 153.4; $C_{\psi Tz}$ 120.5
Aib 17	124.1	56.2	25.8	CO 172.7
Gln 18	115.8	54.5	25.8	Cγ 31.2; Cδ 176.4; Nε 106.9 ; CO 172.3
Gln 19	117.0	53.3	25.7	Cγ 31.2; Cδ 176.4; Nε 107.7 ; CO 172.5
Phl 20	121.1	62.8	52.7	Cγ 36.6

Table S4-13: ^{1}H NMR chemical shifts for **4g** in CD_3OH at 298 K

Residue	*HN*	*Hα*	*Hβ*	**Others**
Aib 1	8.59	-	1.45, 1.54	CH_3 2.05
Pro 2	-	4.25	1.79, 2.35	Hγ 1.96, 2.08; Hδ 3.48, 3.95
Aib 3	7.62	-	1.53	
Ala 4	7.56	4.09	1.50	
Aib 5	7.92	-	1.48, 1.55	
Ala 6	7.89	4.02	1.52	
Gln 7	7.98	3.93	2.14, 2.27	Hγ 2.34, 2.52; NH_2 6.74, 7.41
Aib 8	8.04	-	1.50, 1.58	
Val 9	7.46	3.59	2.22	CH_3 0.99, 1.12
Aib 10	8.18	-	1.55	
Gly 11	8.30	3.66, 3.92		
Leu 12	8.05	4.46	1.57, 1.91	Hγ 1.91; CH_3 0.90
Aib 13	8.24	-	1.53, 1.56	
Pro 14	-	4.38	1.75, 2.30	Hγ 1.94, 2.03; Hδ 3.58, 3.89
Val 15	7.82	3.89	2.36	CH_3 1.00, 1.07
Aib 16	7.53	-	1.48	
Aib 17	7.29	-	1.48, 1.70	$H_{\psi Tz}$ 8.04
Gln 18	-	5.30	2.41, 2.52	Hγ 2.16; NH_2 6.55, 7.24
Gln 19	8.51	4.31	1.83, 2.03	Hγ 2.17; NH_2 6.55, 7.24
Phl 20	7.95	3.59	4.10	Hγ 2.75, 2.89

Table S4-14: ^{15}N and ^{13}C NMR chemical shifts for **4g** in CD_3OH at 298 K

Residue	*N*	*Cα*	*Cβ*	**Others**
Aib 1	136.9	55.9	22.5, 25.2	$COCH_3$ 171.2; CH_3 21.1; CO 174.2
Pro 2	-	64.3	28.4	Cγ 25.8; Cδ 48.7; CO 174.2
Aib 3	124.2	56.0	25.8	CO 177.2
Ala 4	117.3	52.9	15.7	CO 176.0
Aib 5	127.8	56.0	25.5	CO 176.6
Ala 6	115.6	52.5	15.7	CO 176.8
Gln 7	115.3	56.7	25.9	Cγ 31.2; Cδ 176.0; Nε 106.1; CO 174.4
Aib 8	127.6	56.2	25.3	CO 176.8
Val 9	113.5	64.3	29.2	Cγ 18.3, 19.5; CO 174.0
Aib 10	126.7	56.2	25.2	CO 177.6
Gly 11	99.9	43.6		CO 171.5
Leu 12	117.9	52.4	40.3	Cγ 24.3; CH_3 19.9, 22.2; CO 173.7
Aib 13	132.3	56.5	56.5	CO 174.5
Pro 14	-	63.1	28.8	Cγ 25.6; Cδ 49.1; CO 174.6
Val 15	112.6	61.2	29.2	CH_3 18.3, 18.5; CO 172.9
Aib 16	128.5	56.8	25.4	CO 174.9
Aib 17	125.2	51.1	27.2	C_{Tz} 153.4; $C_{\psi Tz}$ 121.8
Gln 18	-	62.6	27.6	Cγ 30.8; Cδ 176.2; Nε 107.4; CO 168.2
Gln 19	121.2	53.2	27.4	Cγ 30.8; Cδ 176.2; Nε 107.4; CO 171.6
Phl 20	122.5	62.7	52.8	Cγ 36.6

Table S4-15: ^{1}H NMR chemical shifts for **4h** in CD_3OH at 298 K

Residue	*HN*	*Hα*	*Hβ*	**Others**
Aib 1	8.58	-	1.46, 1.54	CH_3 2.05
Pro 2	-	4.24	1.78, 2.35	Hγ 1.96, 2.08; Hδ 3.49, 3.95
Aib 3	7.62	-	1.50	
Ala 4	7.56	4.09	1.49	
Aib 5	7.91	-	1.55	
Ala 6	7.88	4.02	1.52	
Gln 7	7.98	3.93	2.14, 2.26	Hγ 2.35, 2.53; NH_2 6.73, 7.40
Aib 8	8.04	-	1.59	
Val 9	7.43	3.67	2.26	CH_3 1.00, 1.13
Aib 10	8.12	-	1.55	
Gly 11	8.27	3.68, 3.94		
Leu 12	8.14	4.10	1.58, 1.90	Hγ 1.58; CH_3 0.91
Aib 13	7.93	-	1.70, 1.82	$H_{\psi Tz}$ 8.19
Aib 14	-	-	1.86	
Val 15	7.51	3.81	2.06	CH_3 0.93, 0.99
Aib 16	7.83	-	1.44, 1.56	
Aib 17	7.54	-	1.53	
Gln 18	7.86	4.05	2.24	Hγ 2.45, 2.59; NH_2 6.77, 7.40
Gln 19	7.88	4.18	2.00	Hγ 2.18, 2.25; NH_2 6.61, 7.28
Phl 20	7.95	3.61	4.15	Hγ 2.72, 2.95

Table S4-16: ^{15}N and ^{13}C NMR chemical shifts for **4h** in CD_3OH at 298 K

Residue	*N*	*Cα*	*Cβ*	**Others**
Aib 1	136.9	56.1	22.6, 25.6	$COCH_3$ 171.2; CH_3 21.0; CO 174.2
Pro 2	-	64.4	28.4	Cγ 25.8; Cδ 48.6; 174.3
Aib 3	124.3	56.0	25.8	CO 177.2
Ala 4	117.3	52.7	15.7	CO 176.0
Aib 5	127.7	55.9	25.6	CO 176.6
Ala 6	115.3	52.6	15.6	CO 176.8
Gln 7	*nd*	56.7	25.9	Cγ 31.3; Cδ 176.0; Nε 105.9 ; CO 174.5
Aib 8	127.2	56.2	26.0	CO 176.9
Val 9	113.3	64.0	29.1	CO 174.0; CH_3 18.3, 19.4
Aib 10	129.6	56.3	25.3	CO 177.7
Gly 11	100.3	43.9		CO 171.5
Leu 12	120.6	54.7	40.3	Cγ 26.2; CH_3 19.9, 22.2; CO 174.1
Aib 13	132.2	51.4	25.3, 29.3	CO 177.7
Aib 14	-	*nd*	24.3	CO 172.4
Val 15	116.5	63.2	25.8	CH_3 18.1, 18.5 CO 173.4
Aib 16	130.2	56.4	25.8, 29.2	C_{Tz} 153.9; $C_{\psi Tz}$ 120.8
Aib 17	123.5	55.4	25.8	CO 172.7
Gln 18	112.7	55.4	26.4	Cγ 31.8; Cδ 176.3; Nε 106.9 ; CO 172.3
Gln 19	115.3	54.2	26.8	Cγ 31.6; Cδ 175.9; Nε 107.7 ; CO 172.5
Phl 20	119.2	63.4	53.1	Cγ 36.6

Table S4-17: ^{1}H NMR chemical shifts for **4i** in CD_3OH at 298 K

Residue	*HN*	*Hα*	*Hβ*	**Others**
Aib 1	8.34	-	1.42	CH_3 1.96
Pro 2	-	4.33	1.77, 2.25	Hγ 1.86; Hδ 3.49, 3.70
Aib 3	7.87	-	1.68	$H_{\psi Tz}$ 7.95
Ala 4	-	5.30	1.72	
Aib 5	8.49	-	1.69	$H_{\psi Tz}$ 7.89
Ala 6	-	5.39	1.70	
Gln 7	8.35	4.29	1.82, 2.01	Hγ 2.14; NH_2 6.75, 7.44
Aib 8	8.24	-	1.67	$H_{\psi Tz}$ 7.88
Val 9	-	4.87	2.40	CH_3 0.69, 1.02
Aib 10	8.76	-	1.71	$H_{\psi Tz}$ 7.75
Gly 11	-	5.16		
Leu 12	8.75	4.49	1.62, 1.67	Hγ 1.67; CH_3 0.92, 0.97
Aib 13	8.56	-	1.46	
Pro 14	-	4.43	1.83, 2.14	Hγ 1.97; Hδ 3.48, 3.71
Val 15	7.65	3.90	2.23	CH_3 0.93, 0.97
Aib 16	7.58	-	1.69, 1.76	$H_{\psi Tz}$ 8.09
Aib 17	-	-	1.69, 1.76	
Gln 18	8.11	4.25	1.98	Hγ 2.22; NH_2 6.88, 7.79
Gln 19	8.07	4.25	1.94, 2.08	Hγ 2.26; NH_2 6.78, 7.54
Phl 20	7.54	3.52	4.12	Hγ 2.68, 2.89

Table S4-18: ^{15}N and ^{13}C NMR chemical shifts for **4i** in CD_3OH at 298 K

Residue	*N*	*Cα*	*Cβ*	**Others**
Aib 1	136.6	56.1	23.5	$COCH_3$ 170.7; CH_3 21.0; CO 173.0
Pro 2	-	62.9	28.7	Cγ 25.5; Cδ 48.4; CO 173.0
Aib 3	128.8	51.1	27.4	C_{Tz} 153.1; $C_{\psi Tz}$ 120.7
Ala 4	-	59.1	16.8	CO 168.7
Aib 5	134.4	51.0	26.7	C_{Tz} 152.8; $C_{\psi Tz}$ 120.3
Ala 6	-	58.8	16.8	CO 169.4
Gln 7	119.8	53.2	27.4	Cγ 30.7; Cδ 176.1; Nε 107.6; CO 170.9
Aib 8	134.2	50.9	26.9	C_{Tz} 153.1; $C_{\psi Tz}$ 120.1
Val 9	-	69.9	31.7	Cγ 17.7, 18.2; CO 166.7
Aib 10	139.5	51.0	26.6	C_{Tz} 152.2; $C_{\psi Tz}$ 123.0
Gly 11	-	51.7		CO 167.5
Leu 12	120.9	52.0	40.3	Cγ 27.7; Cδ 18.5, 18.7; CO 173.8
Aib 13	134.1	56.6	22.7	CO *nd*
Pro 14	-	62.9	28.5	Cγ 25.4; Cδ 48.4; CO 173.9
Val 15	112.8	60.7	29.6	Cγ 18.5, 18.6; CO 172.2
Aib 16	132.5	54.0	26.6	C_{Tz} 153.3; $C_{\psi Tz}$ 120.5
Aib 17	-	*nd*	26.9, 27.1	CO 172.3
Gln 18	116.8	53.5	27.6	Cγ 31.4; Cδ 176.5; Nε 108.3 ; CO 172.6
Gln 19	116.1	54.5	26.2	Cγ 31.1; Cδ 176.3; Nε 106.9 ; CO 171.7
Phl 20	121.2	62.8	53.0	Cγ 36.5

Table S4-19: ^{1}H NMR chemical shifts for **4j** in CD_3OH at 298 K

Residue	*HN*	*Hα*	*Hβ*	**Others**
Aib 1	8.35	-	1.42	CH_3 1.97
Pro 2	-	4.33	1.86, 2.15	Hγ 2.01; Hδ 3.48, 3.70
Aib 3	7.87	-	1.67	$H_{\psi Tz}$ 7.96
Ala 4	-	5.30	1.72	
Aib 5	8.51	-	1.68	$H_{\psi Tz}$ 7.89
Ala 6	-	5.39	1.71	
Gln 7	8.45	4.30	2.87, 2.02	Hγ 2.19; NH_2 6.77, 7.51
Aib 8	8.24	-	1.67	$H_{\psi Tz}$ 7.88
Val 9	-	7.88	2.40	CH_3 0.70, 1.03
Aib 10	8.77	-	1.65, 1.73	$H_{\psi Tz}$ 7.73
Gly 11	-	5.15		
Leu 12	8.58	4.43	1.64	Hγ 1.67; CH_3 0.91, 0.97
Aib 13	8.46	-	1.74, 2.20	
Pro 14	-	4.36	1.74, 2.20	Hγ 1.82; Hδ 3.49, 3.67
Val 15	7.67	3.85	2.26	CH_3 1.00
Aib 16	7.59	-	1.45	
Aib 17	7.29	-	1.68	$H_{\psi Tz}$ 8.01
Gln 18	-	5.29	2.16	Hγ 2.31, 2.51; NH_2 6.74, 7.44
Gln 19	8.51	4.30	1.83, 2.03	Hγ 2.16; NH_2 6.79, 7.55
Phl 20	7.94	3.52	4.10	Hγ 2.76, 2.88

Table S4-20: ^{15}N and ^{13}C NMR chemical shifts for **4j** in CD_3OH at 298 K

Residue	*N*	*Cα*	*Cβ*	**Others**
Aib 1	136.6	56.1	26.9	$COCH_3$ 170.7; CH_3 21.0; CO 173.0
Pro 2	-	62.9	28.7	Cγ 25.5; Cδ 48.4; CO 173.0
Aib 3	128.7	51.0	27.2	C_{Tz} 153.1; $C_{\psi Tz}$ 120.6
Ala 4	-	59.1	16.8	CO 168.7
Aib 5	134.6	51.0	27.2	C_{Tz} 152.8; $C_{\psi Tz}$ 120.2
Ala 6	-	58.8	16.8	CO 173.0
Gln 7	120.0	53.2	27.4	Cγ 30.9; Cδ 176.1; Nε 107.5; CO 168.3
Aib 8	134.0	50.8	27.0	C_{Tz} 153.0; $C_{\psi Tz}$ 120.1
Val 9	-	70.0	31.7	Cγ 17.7, 18.1; CO 167.5
Aib 10	139.5	51.0	26.6	C_{Tz} 152.3 ; $C_{\psi Tz}$ 123.0
Gly 11	-	51.7		CO 171.2
Leu 12	120.8	52.2	40.3	Cγ 26.9; Cδ 18.4, 20.6; CO 174.2
Aib 13	133.0	56.5	22.6	CO *nd*
Pro 14	-	63.0	28.5	Cγ 25.4; Cδ 48.5; CO 174.2
Val 15	113.4	61.2	29.3	Cγ 18.2; CO 172.6
Aib 16	128.8	56.6	25.5	
Aib 17	125.3	51.2	27.3	C_{Tz} 153.4; $C_{\psi Tz}$ 122.1
Gln 18	-	62.5	nd	Cγ 28.0; Cδ 176.9; Nε 107.5 ; CO 168.2
Gln 19	121.5	53.2	27.4	Cγ 30.8; Cδ 177.2; Nε 107.5 ; CO 171.8
Phl 20	121.2	62.7	53.1	Cγ 36.6

Table S4-21: ^{1}H NMR chemical shifts for **5a** in CD_3OH at 298 K

Residue	*HN*	*Hα*	*Hβ*	**Others**
Val 1	8.13	3.92	2.10	Hγ 1.03; CH_3 2.03
Aib 2	8.40	-	1.44	
Aib 3	7.83	-	1.47	
Val 4	7.69	3.76	2.25	H_{γ} 1.02, 1.07
Gly 5	8.12	3.76, 3.87	-	
Leu 6	7.76	4.25	1.63, 1.74	Hγ 1.73; CH_3 0.91
Aib 7	7.61	-	1.52	
Aib 8	7.85	-	1.51, 1.60	
Hyp 9	-	4.59	1.95, 2.35	Hγ 4.49; Hδ 3.74, 3.93
Gln 10	8.21	4.35	2.11	Hγ 2.31, 2.39; NH_2 6.71, 7.46
Aib 11	7.93	-	1.50, 1.60	
Hyp 12	-	4.39	1.83, 2.25	Hγ 4.44; Hδ 3.55, 3.83
Aib 13	7.83	-	1.31	
Phl 14	7.31	3.63	4.11	Hγ 2.70, 2.97

Table S4-22: ^{15}N and ^{13}C NMR chemical shifts for **5a** in CD_3OH at 298 K

Residue	*N*	*Cα*	*Cβ*	**Others**
Val 1	123.1	60.8	29.4	$COCH_3$ 172.5; CH_3 21.0; Cγ 17.8; CO 172.0
Aib 2	134.1	56.3	24.3	CO 175.8
Aib 3	123.6	56.6	22.5	CO 177.5
Val 4	113.4	62.5	26.3	Cγ 17.6, 18.3; CO 172.3
Gly 5	105.8	43.7	-	CO 171.8
Leu 6	117.6	54.2	39.6	Cγ 24.4; Cδ 20.5; CO 173.8
Aib 7	125.6	56.6	25.4	CO 176.5
Aib 8	126.8	56.7	22.5	CO 174.8
Hyp 9	-	61.4	36.5	Cγ 69.9; Cδ 56.8; CO 173.9
Gln 10	110.5	52.8	26.4	Cγ 31.4; Cδ 175.9; Nε 106.3; CO 172.4
Aib 11	130.6	56.3	22.7	CO 174.3
Hyp 12	-	62.4	36.4	Cγ 70.0; Cδ 57.0; CO 173.5
Aib 13	124.8	56.6	26.4	CO 175.8
Phl 14	115.3	63.7	53.1	Cγ 36.6

Table S4-23: ^{1}H NMR chemical shifts for **5b** in CD_3OH at 298 K

Residue	*HN*	*Hα*	*Hβ*	**Others**
Val 1	7.92	4.02	1.98	Hγ 0.95; CH_3 1.98
Aib 2	8.27	-	1.65, 1.73	$H_{\psi Tz}$ 8.04
Aib 3	-	-	1.98	
Val 4	7.47	4.02	2.04	Hγ 0.89, 0.93
Gly 5	8.33	3.84, 3.93	-	
Leu 6	7.84	4.16	1.61	Hγ 1.65; H_{δ} 0.91, 0.94
Aib 7	8.01	-	1.53	
Aib 8	7.76	-	1.55	
Hyp 9	-	4.59	1.93, 2.33	Hγ 4.47; Hδ 3.65, 3.92
Gln 10	8.15	4.34	2.13	Hγ 2.35; NH_2 6.73, 7.46
Aib 11	7.93	-	1.61	
Hyp 12	-	4.40	1.82, 2.27	Hγ 4.40; Hδ 3.55, 3.82
Aib 13	7.82	-	1.30, 1.44	
Phl 14	7.31	3.60	4.12	Hγ 2.70, 2.97

Table S4-24: ^{15}N and ^{13}C NMR chemical shifts for **5b** in CD_3OH at 298 K

Residue	*N*	*Cα*	*Cβ*	**Others**
Val 1	114.7	60.6	29.1	$COCH_3$ 172.5; CH_3 24.8; Cγ 17.8, 18.3; CO 172.0
Aib 2	137.0	50.7	26.6, 27.7	C_{Tz} 153.0 ; $C_{\psi Tz}$ 120.4
Aib 3	-	59.6	21.1	CO 174.3
Val 4	122.8	49.7	30.2	CO 172.3
Gly 5	107.7	42.7	-	CO 170.9
Leu 6	119.0	53.4	39.8	Cγ 24.4; Cδ 20.7, 21.7; CO 173.3
Aib 7	128.4	56.7	24.2	CO 176.4
Aib 8	127.0	56.8	22.7, 26.4	CO 174.7
Hyp 9	-	61.5	36.5	Cγ 70.0; Cδ 56.4; CO 173.8
Gln 10	110.9	52.9	26.5	Cγ 31.7; Cδ 175.9; Nε 106.9; CO 172.4
Aib 11	130.7	56.4	22.9	CO 174.2
Hyp 12	-	62.3	36.4	Cγ 70.0; Cδ 57.0; CO 173.4
Aib 13	123.5	56.7	22.4, 26.4	CO 175.8
Phl 14	115.3	63.7	53.1	Cγ 36.5

Table S4-25: ^{1}H NMR chemical shifts for **5c** in CD_3OH at 298 K

Residue	*HN*	*Hα*	*Hβ*	**Others**
Val 1	8.09	3.90	1.99	Hγ 0.96, 1.00; CH_3 1.95
Aib 2	8.32	-	1.40	
Aib 3	7.30	-	1.58, 1.69	$H_{\psi Tz}$ 8.01
Val 4	-	4.92	2.54	CH_3 0.77, 1.06
Gly 5	8.80	3.93	-	
Leu 6	8.18	4.12	1.57	Hγ 1.68; CH_3 0.92, 0.97
Aib 7	8.25	-	1.45, 1.52	
Aib 8	7.65	-	1.33, 1.43	
Hyp 9	-	4.56	1.94, 2.32	Hγ 4.44; Hδ 3.58, 3.89
Gln 10	8.12	4.32	2.12	Hγ 2.33; NH_2 6.72, 7.44
Aib 11	7.91	-	1.51, 1.60	
Hyp 12	-	4.39	1.81, 2.28	Hγ 4.43; Hδ 3.54, 3.84
Aib 13	7.82	-	1.30, 1.45	
Phl 14	7.31	3.60	4.12	Hγ 2.71, 2.97

Table S4-26: ^{15}N and ^{13}C NMR chemical shifts for **5c** in CD_3OH at 298 K

Residue	*N*	*Cα*	*Cβ*	**Others**
Val 1	124.7	60.2	29.7	$COCH_3$ 169.1; CH_3 23.2; Cγ 18.0; CO 172.6
Aib 2	134.7	56.8	25.5	CO 174.5
Aib 3	124.8	50.9	26.7, 28.0	C_{Tz} 153.4; $C_{\psi Tz}$ 121.3
Val 4	-	69.7	31.7	Cγ 17.8, 18.3; CO 169.1
Gly 5	111.2	42.0	-	CO 170.2
Leu 6	119.5	52.7	39.7	Cγ 26.4; Cδ 20.8, CO 172.5
Aib 7	129.7	56.6	23.8, 25.4	CO 174.6
Aib 8	126.7	56.6	25.3	CO 176.2
Hyp 9	-	61.5	36.5	Cγ 69.9; Cδ 56.2; CO 173.8
Gln 10	111.1	53.0	26.6	C.9 ; γ 31.8; Cδ 175Nε 105.9; CO 172.3
Aib 11	130.8	56.4	22.8, 25.3	CO 174.2
Hyp 12	-	62.3	36.5	Cγ 69.9; Cδ 57.0; CO 173.3
Aib 13	123.5	56.8	23.7, 26.3	CO 175.7
Phl 14	115.4	63.7	53.1	Cγ 36.6

Table S4-27: ^{1}H NMR chemical shifts for **5d** in CD_3OH at 298 K

Residue	*HN*	*Hα*	*Hβ*	**Others**
Val 1	8.14	3.91	2.08	Hγ 1.02; CH_3 2.02
Aib 2	8.38	-	1.43	
Aib 3	7.76	-	1.44, 1.48	
Val 4	-	3.90	2.28	CH_3 1.02, 1.06
Gly 5	8.13	3.77, 3.93	-	
Leu 6	7.71	4.25	1.58, 1.67	Hγ 1.67; CH_3 0.87, 0.90
Aib 7	7.68	-	1.71, 1.77	$H_{\psi Tz}$ 8.25
Aib 8	7.65	-	1.87, 2.02	
Hyp 9	-	4.63	1.88, 2.25	Hγ 4.30; Hδ 2.50, 3.04
Gln 10	8.01	4.38	2.19, 2.27	Hγ 2.44; NH_2 6.99, 7.95
Aib 11	7.90	-	1.52, 1.63	
Hyp 12	-	4.41	1.84, 2.28	Hγ 4.45; Hδ 3.60, 3.81
Aib 13	7.78	-	1.30, 1.44	
Phl 14	7.29	3.60	4.11	Hγ 2.71, 2.98

Table S4-28: ^{15}N and ^{13}C NMR chemical shifts for **5d** in CD_3OH at 298 K

Residue	*N*	*Cα*	*Cβ*	**Others**
Val 1	123.4	61.7	29.4	$COCH_3$ 172.9; CH_3 22.6; Cγ 18.3; CO 172.9
Aib 2	134.1	56.4	24.2	CO 175.7
Aib 3	124.0	56.6	22.4, 25.5	CO 177.2
Val 4	111.5	60.6	29.2	Cγ 18.4; CO 174.0
Gly 5	105.8	43.1	-	CO 171.0
Leu 6	118.0	53.1	40.0	Cγ 24.3; Cδ 20.3, 21.9; CO 172.9
Aib 7	131.9	50.9	26.4, 27.9	C_{Tz} 154.0; $C_{\psi Tz}$ 120.6
Aib 8	-	64.9	22.4, 28.2	CO 171.9
Hyp 9	-	61.7	36.1	Cγ 70.0; Cδ 54.7; CO 173.0
Gln 10	111.1	53.0	27.2	Cγ 31.7; Cδ 176.3 ; Nε 108.3; CO 171.7
Aib 11	131.2	56.4	22.8, 25.5	CO 174.0
Hyp 12	-	62.3	36.4	Cγ 70.0; Cδ 56.9; CO 173.3
Aib 13	123.6	57.0	22.5, 26.4	CO 175.7
Phl 14	115.5	63.7	53.1	Cγ 36.5

Table S4-29: ^{1}H NMR chemical shifts for **5e** in CD_3OH at 298 K

Residue	*HN*	*Hα*	*Hβ*	**Others**
Val 1	7.95	4.04	1.97	Hγ0.94; CH_3 1.98
Aib 2	8.31	-	1.65, 1.72	$H_{\psi Tz}$ 8.02
Aib 3	-	-	1.88	
Val 4	7.39	4.08	2.05	CH_3 0.86, 0.91
Gly 5	8.35	3.86, 3.92	-	
Leu 6	7.84	4.27	1.55	Hγ 1.62; CH_3 0.88, 0.90
Aib 7	8.04	-	1.71	$H_{\psi Tz}$ 8.17
Aib 8	-	-	1.86, 1.99	
Hyp 9	-	4.63	1.88, 2.22	Hγ 4.29; Hδ 2.59, 2.92
Gln 10	8.17	4.37	2.14, 2.28	Hγ 2.45; NH_2 6.98, 7.84
Aib 11	7.98	-	1.60	
Hyp 12	-	4.41	1.84, 2.29	Hγ 4.46; Hδ 3.57, 3.82
Aib 13	7.79	-	1.29	
Phl 14	7.29	3.60	4.12	Hγ 2.70, 2.98

Table S4-30: ^{15}N and ^{13}C NMR chemical shifts for **5e** in CD_3OH at 298 K

Residue	*N*	*Cα*	*Cβ*	**Others**
Val 1	*nd*	59.6	30.1	$COCH_3$ 172.1; Cγ 21.0; Cγ 18.1
Aib 2	137.2	50.9	26.3, 27.4	C_{Tz} 152.9; $C_{\psi Tz}$ 120.3
Aib 3	-	65.1	24.9	CO 172.4
Val 4	114.1	60.0	29.9	Cγ 17.8; CO 172.5
Gly 5	108.4	42.2		CO 170.1
Leu 6	119.1	52.3	40.2	Cγ ; Cδ 18.2, 20.7; CO 172.6
Aib 7	133.3	50.7	27.1	C_{Tz} 152.9; $C_{\psi Tz}$ 120.3
Aib 8	-	65.1	23.1, 27.6	CO 171.7
Hyp 9	-	61.5	36.0	Cγ 69.8; Cδ 54.5; CO 172.9
Gln 10	112.8	52.8	26.9	Cγ 31.4; Cδ 176.5; Nε 108.5; CO 172.7
Aib 11	122.9	56.4	22.7	CO 174.0
Hyp 12	-	62.2	36.3	Cγ 69.8; Cδ 56.7; CO 173.2
Aib 13	123.7	56.9	25.2	CO 175.7
Phl 14	115.6	63.6	53.0	Cγ 36.5

Table S4-31: ^{1}H NMR chemical shifts for **5f** in CD_3OH at 298 K

Residue	*HN*	*Hα*	*Hβ*	**Others**
Val 1	8.09	3.91	2.00	Hγ 0.97; CH_3 1.95
Aib 2	8.32	-	1.41	
Aib 3	7.30	-	1.58, 1.68	$H_{\psi Tz}$ 8.00
Val 4	-	4.93	2.56	CH_3 0.77, 1.07
Gly 5	8.74	3.90	-	
Leu 6	8.01	4.27	1.51, 1.66	Hγ 1.66; CH_3 0.90
Aib 7	8.08	-	1.51, 1.68	$H_{\psi Tz}$ 8.09
Aib 8	-	-	1.67	
Hyp 9	-	4.61	1.88, 2.20	Hγ 4.26; Hδ 2.60, 2.91
Gln 10	8.16	4.37	2.14, 2.27	Hγ 2.44; NH_2 6.96, 7.76
Aib 11	7.95	-	1.51, 1.60	
Hyp 12	-	4.41	1.83, 2.26	Hγ 4.44; Hδ 3.57, 3.81
Aib 13	7.78	-	1.29, 1.44	
Phl 14	7.29	3.60	4.11	Hγ 2.70, 2.97

Table S4-32: ^{15}N and ^{13}C NMR chemical shifts for **5f** in CD_3OH at 298 K

Residue	*N*	*Cα*	*Cβ*	**Others**
Val 1	124.1	60.1	29.7	$COCH_3$ 171.8; CH_3 23.3; Cγ 18.1
Aib 2	134.5	56.7	25.5	CO 174.6
Aib 3	125.0	50.8	26.7, 27.9	C_{Tz} 153.4 ; $C_{\psi Tz}$ 121.2
Val 4	-	69.7	31.5	Cγ 17.8, 18.3; CO 169.1
Gly 5	111.3	42.3	-	CO 169.6
Leu 6	119.4	52.5	40.3	Cγ 24.5; Cδ 20.6; CO 172.7
Aib 7	133.4	50.6	25.5, 26.6	C_{Tz} 153.8 ; $C_{\psi Tz}$ 120.4
Aib 8	-	50.8	27.3	CO 173.9
Hyp 9	-	61.6	36.1	Cγ 69.8; Cδ 54.5; CO 173.0
Gln 10	112.5	53.0	26.9	Cγ 31.5; Cδ 176.6; Nε 107.7; CO 171.7
Aib 11	131.3	56.4	22.9, 25.5	CO 173.9
Hyp 12	-	62.3	36.4	Cγ 69.9; Cδ 56.9; CO 175.7
Aib 13	123.4	56.8	22.5, 26.4	CO 175.7
Phl 14	115.3	63.7	53.1	Cγ 36.6

Perturbations of the ^{1}HN, ^{1}Hα,^{15}N and ^{13}Cα, ^{13}CO chemical shifts of the Alm analogues upon the introduction of triazolo-dipeptides. The variations of chemical shifts (Δδ, in ppm) were calculated as the difference between the analogues and Alm chemical shifts (Δδ = δ**4b-j** - δ**4a**). *nd*: not determined.

0.05 < $\Delta\delta^{1}$H < 0.1 are in yellow, 0.1 < $\Delta\delta^{1}$H < 0.3 are in orange, $\Delta\delta^{1}$H > 0.3 are in red

0.3 < $\Delta\delta^{15}$N, ^{13}C < 1.0 are in yellow, 1.0 < $\Delta\delta^{1}$H < 3.0 are in orange, $\Delta\delta^{1}$H > 3.0 are in red

Table S5-1: Variation of the δ_{HN} chemical shifts in the peptides **4b-j** upon incorporation of Tz.

Residues	Compounds								
	4b	**4c**	**4d**	**4e**	**4f**	**4g**	**4h**	**4i**	**4j**
Aib 1	-0.21	-0.12	-0.06	-0.03	-0.01	0	-0.01	-0.25	-0.24
Pro 2									
Aib 3	0.28	0.21	0.09	0.05	0	0	0	0.25	0.25
Ala 4	Tz	0.28	0.16	0.08	0	0	0	Tz	Tz
Aib 5	0.81	-0.32	-0.04	-0.03	-0.01	0	-0.01	0.57	0.59
Ala 6	0.28	Tz	-0.13	-0.06	0	0	-0.01	Tz	Tz
Gln 7	-0.09	0.7	-0.19	-0.1	-0.01	-0.01	-0.01	0.36	0.46
Aib 8	-0.5	0.16	-0.51	-0.36	-0.01	-0.02	-0.02	0.18	0.18
Val 9	-0.05	-0.05	Tz	-0.23	-0.02	-0.02	-0.05	Tz	Tz
Aib 10	-0.19	-0.33	0.73	-0.44	-0.03	-0.02	-0.08	0.56	0.57
Gly 11	-0.07	-0.1	-0.18	Tz	-0.02	-0.02	-0.05	Tz	Tz
Leu 12	-0.06	-0.11	-0.19	0.36	-0.04	-0.03	0.06	0.67	0.5
Aib 13	-0.09	-0.24	-0.31	0.08	-0.18	-0.14	-0.45	0.18	0.08
Pro 14							Tz		
Val 15	-0.01	-0.05	-0.07	-0.21	0.25	0.19	-0.12	0.02	0.04
Aib 16	-0.01	-0.03	-0.05	0.05	-0.03	-0.06	0.24	-0.01	0
Aib 17	-0.02	-0.03	-0.04	-0.05	Tz	-0.51	-0.26	Tz	-0.51
Gln 18	0	0	0	-0.02	0.24	Tz	0.08	0.33	Tz
Gln 19	0	0	-0.01	0	0.27	0.65	0.02	0.21	0.65
Phl 20	0	0	0	0	0.27	0.65	0.65	0.24	0.64

Table S5-2: Variation of the δ_N chemical shifts in the peptides **4b-j** upon incorporation of 1,2,3-triazole.

Residues	Compounds								
	4b	**4c**	**4d**	**4e**	**4f**	**4g**	**4h**	**4i**	**4j**
Aib 1	-0.4	-0.4	-0.3	-0.2	-0.2	-0.2	-0.2	-0.5	-0.5
Pro 2									
Aib 3	4	-1.6	-0.8	-0.5	-0.1	-0.2	-0.1	4.4	4.3
Ala 4	Tz	-1.5	-0.4	-0.1	0	0.1	0.1	Tz	Tz
Aib 5	6.9	1.8	-0.2	0.1	0.2	0.2	0.1	6.8	7
Ala 6	-0.6	Tz	-1.2	-0.6	0.2	0.3	0	Tz	Tz
Gln 7	0	5.9	-0.8	0	*nd*	0	*nd*	4.5	4.7
Aib 8	-0.2	0.6	2.4	-2.2	-0.1	0	-0.4	6.6	6.4
Val 9	-1.1	-2.7	Tz	-3.9	-0.1	-0.2	-0.4	Tz	Tz
Aib 10	0.1	1.2	8	3.6	0	-3	-0.1	9.8	9.8
Gly 11	0	-0.6	-0.6	Tz	-0.1	-0.2	0.2	Tz	Tz
Leu 12	0	-0.5	-1.3	2.2	0.2	0.2	2.9	3.2	3.1
Aib 13	0.1	-0.3	-0.4	-0.5	-0.7	-0.6	-0.7	1.2	0.1
Pro 14									
Val 15	-0.1	-0.3	-0.3	0.3	-3.4	-2.7	1.2	-2.5	-1.9
Aib 16	-0.1	-0.1	-0.1	0.2	3.2	-0.6	1.1	3.4	-0.3
Aib 17	0	0.2	0	0.1	Tz	1.1	-0.6	Tz	*nd*
Gln 18	0	0	0	0	2.6	Tz	-0.5	3.6	Tz
Gln 19	-0.2	-0.1	0.1	0.1	1.8	6	0.1	0.9	6.3
Phl 20	0	-0.1	-0.1	-0.1	1.9	3.3	0	2	2

Table S5-3: Variation of the $\delta_{H\alpha}$ chemical shifts in the peptides **4b-j** upon incorporation of 1,2,3-triazole.

Residues	Compounds								
	4b	**4c**	**4d**	**4e**	**4f**	**4g**	**4h**	**4i**	**4j**
Aib 1									
Pro 2	0.05	-0.02	-0.03	-0.02	-0.01	0	-0.01	0.08	0.08
Aib 3	Tz							Tz	Tz
Ala 4	1.33	-0.01	0.01	0	-0.01	0	0	1.21	1.21
Aib 5		Tz						Tz	Tz
Ala 6	-0.03	1.37	0.1	0.05	-0.04	0	0	1.37	1.37
Gln 7	0.05	0.18	0.13	0.06	0.01	0.01	0.01	0.37	0.38
Aib 8			Tz					Tz	Tz
Val 9	0.04	0.2	1.22	0.33	0	0	0.08	1.28	1.29
Aib 10				Tz				Tz	Tz
Gly 11									
Leu 12	-0.02	-0.04	-0.03	-0.08	0.02	0	-0.36	0.03	-0.03
Aib 13							Tz		
Pro 14	0	0	-0.01	-0.04	0.08	0	-	0.05	-0.02
Val 15	-0.01	0	-0.01	-0.03	0.23	0.16	0.08	0.17	0.12
Aib 16					Tz			Tz	
Aib 17						Tz			Tz
Gln 18	-0.01	0	0	-0.01	0.22	1.28	0.03	0.2	1.27
Gln 19	0	0	0	0	0.08	0.15	0.02	0.09	0.14
Phl 20	0	0	0	-0.01	-0.06	-0.05	0	-0.03	-0.05

Table S5-4: Variation of the $\delta_{C\alpha}$ chemical shifts in the peptides **4b-j** upon incorporation of 1,2,3-triazole.

Residues	Compounds								
	4b	**4c**	**4d**	**4e**	**4f**	**4g**	**4h**	**4i**	**4j**
Aib 1	0	0	0	0	0	-0.1	0.1	0.1	0.1
Pro 2	-1.3	-0.2	0	0	-0.1	-0.1	0	-1.5	-1.5
Aib 3	-4.9	0.4	0.2	0.1	0	0	0	-4.9	*nd*
Ala 4	6.5	-1.6	-0.4	-0.2	0.3	0.2	0	6.4	6.4
Aib 5	0.6	-4.6	0.3	0.1	-0.1	*nd*	0	-4.9	-4.8
Ala 6	0	6.7	-1.3	-0.5	0	0	0.1	6.3	6.3
Gln 7	-0.3	-0.9	-2.3	-1.2	-0.1	-0.1	-0.1	-3.6	-3.6
Aib 8	0	0.3	-5	0.4	0.1	0	0	-5.3	0.3
Val 9	-0.7	-2.4	5.4	-3.2	-0.1	-0.1	-0.4	5.5	5.6
Aib 10	0.1	0.2	0.5	-4.9	0	0	0.1	-5.2	-5.1
Gly 11	0	-0.1	0	8.3	-0.1	-0.1	0.2	8	8
Leu 12	-0.1	-0.3	-0.4	0.5	-0.3	-0.3	2	-0.7	-0.5
Aib 13	-0.1	-0.1	0	-0.1	-0.2	-0.2	-5.3	-0.1	-0.2
Pro 14	0	0	0	0	-0.2	-0.2	*nd*	-0.4	-0.3
Val 15	0.1	0	0	0.1	-2.1	-1.7	0.3	-2.2	-1.7
Aib 16	0	0.1	0	0.1	-4.8	0.7	0.3	-2.1	0.5
Aib 17	0.1	0.1	0.1	0	8.8	-5.1	-0.8	*nd*	-5
Gln 18	0	0	0	0	-1.1	7	-0.2	-2.1	6.9
Gln 19	0	0	-0.1	-0.1	*nd*	-1.2	-0.2	0.1	-1.2
Phl 20	0	0	0	0	-0.2	-0.3	0	-0.1	0

Table S5-5: Variation of the δ_{CO} chemical shifts in the peptides **4b-j** upon incorporation of 1,2,3-triazole.

Residue	Compounds								
	4b	**4c**	**4d**	**4e**	**4f**	**4g**	**4h**	**4i**	**4j**
Aib 1	-1.1	-0.1	0	0.1	0	0	0	-1.2	-1.2
Pro 2	-1	-0.6	-0.2	0	0.1	0	0.1	-1.2	-1.2
Aib 3	Tz	-0.8	0.1	0.1	0	0	0	Tz	Tz
Ala 4	-5.8	-1.9	-0.1	-0.2	0	0.1	0.1	-7.2	-7.2
Aib 5	-0.6	Tz	0	0.1	0	0	-0.1	Tz	Tz
Ala 6	-0.6	-6.1	-2	-0.5	0.1	0.1	0.1	-7.3	-3.7
Gln 7	-0.4	-2.3	-2.2	-1.2	0	-0.1	0	-3.6	-6.2
Aib 8	-0.1	-0.3	Tz	-0.6	0	-0.1	0	Tz	Tz
Val 9	-0.3	-0.8	-5.4	-1.9	0	0	-0.4	-7.3	-6.5
Aib 10	-0.2	-0.3	-1.1	Tz	0	-0.1	0	Tz	Tz
Gly 11	0	-0.3	-0.6	-4.8	-0.2	-0.2	-0.2	-4.2	-0.5
Leu 12	-0.2	-1.2	-1.1	-1.3	-0.8	-0.9	-0.5	-1.6	-0.4
Aib 13	-0.1	0.6	0.5	0	4	0.8	Tz	*nd*	*nd*
Pro 14	0	-0.2	-0.1	-0.1	-0.9	-0.6	-2.7	-1.2	-0.9
Val 15	0	-0.1	-0.1	-0.2	-1.7	-1.2	-0.7	-1.9	-1.5
Aib 16	-0.1	-0.2	-0.1	-0.1	Tz	-1.4	-0.4	Tz	-1.5
Aib 17	0	-0.2	-0.2	-0.1	-4.8	Tz	0	-5.2	Tz
Gln 18	-0.2	-0.3	-0.3	-0.1	-2.1	-6.2	-2.1	-1.8	-6.2
Gln 19	0	0	0	0	-0.2	-1.1	-0.2	-1	-0.9
Phl 20	0	0	0	0	0	0	0	0	0

Table S5-6: Variation of the δ_{HN} chemical shifts in the peptides **5b-f** upon incorporation of 1,2,3-triazole

Residue	Compounds				
	5b	**5c**	**5d**	**5e**	**5f**
Val 1	-0.21	-0.04	0.01	-0.18	-0.04
Aib 2	-0.13	-0.08	-0.02	-0.09	-0.08
Aib 3	Tz	-0.53	-0.07	Tz	-0.53
Val 4	0.23	Tz	0.01	-0.3	Tz
Gly 5	0.21	0.68	0.01	0.23	0.62
Leu 6	0.08	0.42	-0.05	0.08	0.25
Aib 7	0.4	0.64	0.07	0.43	0.47
Aib 8	-0.09	-0.2	Tz	Tz	Tz
Hyp 9					
Gln 10	-0.06	-0.09	-0.2	-0.04	-0.05
Aib 11	0	-0.02	-0.03	0.05	0.02
Hyp 12					
Aib 13	-0.01	-0.01	-0.05	-0.04	-0.05
Phl 14	0	0	-0.02	-0.02	-0.02

Table S5-7: Variation of the δ_{N} chemical shifts in the peptides **5b-f** upon incorporation of 1,2,3-triazole

Residue	Compounds				
	5b	**5c**	**5d**	**5e**	**5f**
Val 1	-8.4	1.6	0.3	*nd*	1
Aib 2	2.9	0.6	0	3.1	0.4
Aib 3	Tz	1.2	0.4	Tz	1.4
Val 4	9.4	Tz	-1.9	0.7	Tz
Gly 5	1.9	5.4	0	2.6	5.5
Leu 6	1.4	1.9	0.4	1.5	1.8
Aib 7	2.8	4.1	6.3	7.7	7.8
Aib 8	0.2	-0.1	Tz	Tz	Tz
Hyp 9					
Gln 10	0.4	0.6	0.6	2.3	2
Aib 11	0.1	0.2	0.6	0.6	0.7
Hyp 12					
Aib 13	0.1	0.1	0.2	0.3	0
Phl 14	0	0.1	0.2	0.3	0

Table S5-8: Variation of the $\delta_{H\alpha}$ chemical shifts in the peptides **5b-f** upon incorporation of 1,2,3-triazole

Residue	Compounds				
	5b	**5c**	**5d**	**5e**	**5f**
Val 1	0.1	-0.02	-0.01	0.12	-0.01
Aib 2					
Aib 3					
Val 4	0.27	1.16	0.14	0.32	1.17
Gly 5					
Leu 6	-0.09	-0.13	0	0.02	0.02
Aib 7					
Aib 8					
Hyp 9	0	-0.03	0.04	0.04	0.02
Gln 10	-0.01	-0.03	0.03	0.02	0.02
Aib 11					
Hyp 12	0.01	0	0.02	0.02	0.02
Aib 13					
Phl 14	-0.03	-0.03	-0.03	-0.03	-0.03

Table S5-9: Variation of the $\delta_{C\alpha}$ chemical shifts in the peptides **5b-f** upon incorporation of 1,2,3-triazole

Residue	Compounds				
	5b	**5c**	**5d**	**5e**	**5f**
Val 1	-0.2	-0.6	0.9	-1.2	-0.5
Aib 2	-5.6	0.5	0.1	-5.4	6
Aib 3	3	-5.7	0	8.5	-8.8
Val 4	-12.8	7.2	-1.9	-2.5	20
Gly 5	-1	-1.7	-0.6	-1.5	-0.4
Leu 6	-0.8	-1.5	-1.1	-1.9	-0.9
Aib 7	0.1	0	-5.7	-5.9	-6.1
Aib 8	0.1	-0.1	8.2	8.4	-6
Hyp 9	0.1	0.1	0.3	0.1	0.1
Gln 10	0.1	0.2	0.2	0	0.1
Aib 11	0.1	0.1	0.1	0.1	0
Hyp 12	-0.1	-0.1	-0.1	-0.2	0
Aib 13	0.1	0.2	0.4	0.3	0.1
Phl 14	0	0	0	-0.1	0

Table S5-10: Variation of the δ_{CO} chemical shifts in the peptides **5b-f** upon incorporation of 1,2,3-triazole

Residue	Compounds				
	5b	**5c**	**5d**	**5e**	**5f**
Val 1	0	0.6	0.9	0.1	0.5
Aib 2	Tz	-1.3	-0.1	Tz	-1.3
Aib 3	-3.2	Tz	-0.3	-5.1	Tz
Val 4	0	-3.2	1.7	0.2	-3.2
Gly 5	-0.9	-1.6	-0.8	-1.7	-2.2
Leu 6	-0.5	-1.3	-0.9	-1.2	-1.1
Aib 7	-0.1	-1.9	Tz	Tz	Tz
Aib 8	-0.1	1.4	-2.9	-3.1	-3.1
Hyp 9	-0.1	-0.1	-0.9	-1	-0.9
Gln 10	0	-0.1	-0.7	0.3	-0.7
Aib 11	-0.1	-0.1	-0.3	-0.3	-0.4
Hyp 12	-0.1	-0.2	-0.2	-0.3	-0.2
Aib 13	0	-0.1	-0.1	-0.1	-0.1
Phl 14					

Table S6-1: $^{3}J(HNH_{\alpha})$ coupling constants of the Alamethicin and analogues in CD_3OH at 298K (in Hz).

	Compounds									
Residue	**4a**	**4b**	**4c**	**4d**	**4e**	**4f**	**4g**	**4h**	**4i**	**4j**
Aib 1										
Pro 2										
Aib 3										
Ala 4	5.6	Tz	5.3	5.5	5.8	5.7	5.7	5.7	Tz	Tz
Aib 5										
Ala 6	4.4	3.2	Tz	5.6	4.8	4.3	4.4	*nd*	Tz	Tz
Gln 7	4.9	5.1	4.6	7.3	5.6	4.9	5.0	5.0		
Aib 8										
Val 9	5.4	5.8	5.9	Tz	7.5	5.6	5.5	5.8	Tz	Tz
Aib 10										
Gly 11					Tz					
Leu 12	7.7	7.8	7.9	7.8	6.7	7.4	*nd*	6	*nd*	6.7
Aib 13										
Pro 14								Tz		
Val 15	7.9	7.7	7.8	7.6	7.5	nd	7.6	6.2	8.2	*nd*
Aib 16										
Aib 17						Tz			Tz	
Gln 18	5.5	5.2	5.6	5.6	5.5	6.2	Tz	6.1	6.0	Tz
Gln 19	7.2	7.4	7.3	7.3	7.4	7.7	7.7	*nd*	6.5	6.5
Phl 20	9.1	9.1	9.3	8.9	9.0	9.0	8.5	9.0	8.7	9.1

Table S6-2: $^{3}J(HNH_{\alpha})$ coupling constants of the Bergofungin D and analogues in CD_3OH at 298K (in Hz).

	Compounds					
Residue	**5a**	**5b**	**5c**	**5d**	**5e**	**5f**
Val 1	6.2	6.2	6.7	nd		6.9
Aib 2						
Aib 3		Tz			Tz	
Val 4	7.7	nd	Tz	nd		Tz
Gly 5						
Leu 6	6.3	5.6	5.1	nd		7.1
Aib 7						
Aib 8				Tz	Tz	Tz
Hyp 9						
Gln 10	8.8	8.8	8.9	7.1		7.6
Aib 11						
Hyp 12						
Aib 13						
Phl 14	9.1	9.1	nd	9.2		nd

Assessment of the helical structure of Alm and BergD analogues: NOE correlations.

Table S7-1: Expected backbone NOE correlations around the 1,2,3 triazole in helical secondary structures based on the crystal structure of modified GCN4-pLI coiled coils (pdbID: 1U9F). Measured distances were averaged on the four chains (A, B, C and D) in the crystal lattice. Close distance values were measured around the 1,2,3 triazole in the crystal structure of the BergD analogues **5b** and **5d**. Values in brackets are the characteristic distances measured for the canonical α-helix in peptides and proteins.[18]

NOE summary	*Distances (Å)*	**Intensity**
$H_{\psi Tz}(i)$-$H_N(i-1)$	2.3 ± 0.1	Strong
$H_{\psi Tz}(i)$-$H_N(i+1)$	4.0 ± 0.1	Weak
$H_{\psi Tz}(i)$-$H_N(i-2)$	4.3 ± 0.1	Weak
$H_{\psi Tz}(i)$-$H_\alpha(i-2)$	4.9 ± 0.1	Weak
$H_{\psi Tz}(i)$-$H_\alpha(i-3)$	3.3 ± 0.2	Medium
$H_{\psi Tz}(i)$-$H_\alpha(i-4)$	4.1 ± 0.2	Weak
$H_N(i+1)$-$H_N(i-1)$ $[H_N(i)$-$H_N(i-2)]$	5.3 ±0.2 [4.4]	Absent
$H_N(i+1)$-$H_\alpha(i-1)$ $[H_N(i)$-$H_\alpha(i-2)]$	5.6 ± 0.1 [3.7]	-
$H_N(i+1)$-$H_\alpha(i-2)$ $[H_N(i)$-$H_\alpha(i-3)]$	5.0 ±0.2 [3.7]	Absent
$H_\alpha(i-2)$-$H_\beta(i)$ $[H_\alpha(i)$-$H_\beta(i+2)]$	6.0 ± 0.3 [~4]	Absent
$H_\alpha(i-2)$-$H_\beta(i+1)$ $[H_\alpha(i)$-$H_\beta(i+3)]$	6.8 ± 1.0 [~4]	Absent
Hα(i-3)-Hβ(i) [Hα(i)-Hβ(i+2)]	3.3 ± 0.3 [~4]	Medium

Table S8-1: Root mean square deviations (rmsd, Å) of the 15 lowest energy NMR structures of **4a**, **4c**, **4g**, **4h**, **5a**, **5d**, **5e** and **5f**.

Compounds	4a	4c	4g	4h	5a	5d	5e	5f
All atoms	1.30	1.98	2.20	2.26	1.34	1.55	2.03	3.67
All heavy atoms	1.07	1.75	2.05	2.11	1.04	1.27	1.81	3.21
Backbone heavy atoms	0.45	1.05	1.12	1.09	0.42	0.86	0.63	2.33

References :

1 K. Ben Haj Salah, B. Legrand, S. Das, J. Martinez and N. Inguimbert, *Pept. Sci.*, 2015, **104**, 611–621.
2 S. Das, K. Ben Haj Salah, E. Wenger, J. Martinez, J. Kotarba, V. Andreu, N. Ruiz, F. Savini, L. Stella, C. Didierjean, B. Legrand and N. Inguimbert, *Chem. – Eur. J.*, 2017, **23**, 17964–17972.
3 F. Denizot and R. Lang, *J. Immunol. Methods*, 1986, **89**, 271–277.
4 T. Mosmann, *J. Immunol. Methods*, 1983, **65**, 55–63.
5 H. S. Thippeswamy, S. K. Sood, R. Venkateswarlu and I. Raj, *Ann. Microbiol.*, 2009, **59**, 593–601.
6 M. Roth, P. Carpentier, O. Kaïkati, J. Joly, P. Charrault, M. Pirocchi, R. Kahn, E. Fanchon, L. Jacquamet, F. Borel, A. Bertoni, P. Israel-Gouy and J.-L. Ferrer, *Acta Crystallogr. D Biol. Crystallogr.*, 2002, **58**, 805–814.
7 W. Kabsch, *Acta Crystallogr. D Biol. Crystallogr.*, 2010, **66**, 125–132.
8 Z. Dauter and A. Wlodawer, *Acta Crystallogr. D Biol. Crystallogr.*, 2015, **71**, 2217–2226.
9 M. C. Burla, R. Caliandro, M. Camalli, B. Carrozzini, G. L. Cascarano, L. De Caro, C. Giacovazzo, G. Polidori and R. Spagna, *J. Appl. Crystallogr.*, 2005, **38**, 381–388.
10 G. M. Sheldrick, *Acta Crystallogr. Sect. Found. Adv.*, 2015, **71**, 3–8.
11 G. M. Sheldrick, *Acta Crystallogr. D Biol. Crystallogr.*, 2010, **66**, 479–485.
12 L. Palatinus and G. Chapuis, *J. Appl. Crystallogr.*, 2007, **40**, 786–790.
13 G. M. Sheldrick, *Acta Crystallogr. A*, 2008, **64**, 112–122.
14 A. L. Spek, *Acta Crystallogr. D Biol. Crystallogr.*, 2009, **65**, 148–155.
15 R. E. Hubbard and M. Kamran Haider, in *eLS*, John Wiley & Sons, Ltd, 2001.
16 S. Aravinda, S. Datta, N. Shamala and P. Balaram, *Angew. Chem. Int. Ed.*, 2004, **43**, 6728–6731.
17 J. K. Chugh, H. Brückner and B. A. Wallace, *Biochemistry (Mosc.)*, 2002, **41**, 12934–12941.
18 K. Wüthrich, *NMR of Proteins and Nucleic acids*, Wiley-Interscience: New York, 1986.
19 B. A. Johnson and R. A. Blevins, *J. Biomol. NMR*, 1994, **4**, 603–614.
20 E. Vanquelef, S. Simon, G. Marquant, E. Garcia, G. Klimerak, J. C. Delepine, P. Cieplak and F.-Y. Dupradeau, *Nucleic Acids Res.*, 2011, **39**, W511-517.
21 D. A. Case, T. A. Darden, T. E. Cheatham, C. L. Simmerling, J. Wang, R. E. Duke, R. Luo, R. C. Walker, W. Zhang, K. M. Merz, B. Wang, S. Hayik, A. Roitberg, G. Seabra, I. Kolossvary, K. F. Wong, F. Paesani, J. Vanicek, J. Liu, X. Wu, S. R. Brozell, T. Steinbrecher, H. Gohlke, Q. Cai, X. Ye, M.-J. Hsieh, V. Hornak, G. Cui, D. R. Roe, D. H. Mathews, M. G. Seetin, C. Sagui, V. Babin, T. Luchko, S. Gusarov, A. Kovalenko, P. A. Kollman and B. P. Roberts, .
22 R. Koradi, M. Billeter and K. Wüthrich, *J. Mol. Graph.*, 1996, **14**, 51–55.

Author Contributions

K. Ben Haj Salah, S. Das, E. Wenger: investigation, equal.

N. Ruiz, V. Andreu : investigation, supporting.

J. Martinez, M Amblard : writing of original draft, supporting.

C. Didierjean B. Legrand, N. Inguimbert : formal analysis, validation, writing of original draft, funding acquisition, equal.